

DOCTORAL SCHOOL SPI
SCIENCES PHYSIQUES ET DE L'INGENIEUR

H D R T H E S I S

of Université de Bordeaux
Specialty : MECHANICAL ENGINEERING

Defended by
Dr. Stéphane CHEVALIER

THERMAL TOMOGRAPHY FOR MICROSCALE ENERGY CONVERSION DEVICES

prepared at Institute of Mechanical Engineering of Bordeaux
(I2M, UMR 5295)

defended on April 11, 2024

Jury :

<i>Reviewers :</i>	Thierry DUVAUT	- Professor, Université de Reims
	Annie COLIN	- Professor, ESPCI
	Helcio ORLANDE	- Professor, Federal University of Rio
<i>Examinators :</i>	Jean-Christophe BATSALE	- Professor, ENSAM
	Ivan IORDANOFF	- Professor, ENSAM
	Cathy CASTELAIN	- Research Director, CNRS
	Farid BAKIR	- Professor, ENSAM
<i>Guest :</i>	Jean-Noël TOURVIEILLE	- PhD, SYENSQO

"La science n'est pas le domaine des héros : c'est le domaine des anonymes, qui contribuent les uns après les autres à un même résultat."

Anonyme.

Acknowledgments

Par ces quelques lignes, je voudrais témoigner de ma gratitude aux personnes qui ont contribué à ces travaux.

Tout d'abord aux membres du jury qui ont chaleureusement accepté d'expertiser mon manuscrit et permis une riche discussion à l'issue de la soutenance. J'ai vraiment pu apprécier ce moment en votre compagnie.

Un grand merci à mes collègues du quotidien qui rendent ces recherches agréables, l'équipe TIFC, et surtout aux jeunes scientifiques avec qui j'ai eu la chance de travailler (Marine, Coline, Hamza, Kevin pour ne citer que les derniers docteurs). Une part importante de leur énergie a permis les avancées décrites dans ce document et a nourri mes réflexions durant la construction de ce projet de recherche.

Enfin, à mes filles du quotidien, à qui ce mémoire doit beaucoup. Merci d'être là tous les jours.

A Flo, Daph et Andréa.

Contents

List of Acronyms	vii
1 General Introduction	1
1.1 My research activities at a glance	1
1.2 Objectives and organization of the manuscript	2
I Research records & project	5
2 Toward three-dimensional imaging of heat and mass transfers	7
2.1 IR spectroscopic imaging methods	7
2.1.1 Main technologies for IR transmission spectroscopy	8
2.1.2 Concentration fields measurements	13
2.1.3 Temperature fields measurements	15
2.1.4 Summary of heat and mass transfer measurements	16
2.2 From 2D to 3D mass transfer field reconstruction	17
2.2.1 Concentration field measurements in microfluidic reactors	17
2.2.2 Qualitative 3D absorbance fields in a capillary tube	22
2.3 From 2D to 3D temperature field reconstruction	24
2.3.1 Main working principles in source reconstruction in opaque media	25
2.3.2 Qualitative laminography in semi-transparent media based on thermotransmittance	28
2.4 Conclusions	34
3 Energy transfer imaging in electrochemical systems: from X-rays to infrareds	35
3.1 Elucidating the two-phase flow transport in fuel cell GDLs	35
3.1.1 Fuel cell and electrolyzers working principles	35
3.1.2 X-ray synchrotron imaging	38
3.1.3 Two-phase flow modelling	40
3.2 Operando mass transport imaging in microfluidic electrochemical systems	43
3.2.1 Working principle of flow based electrochemical energy conversion devices	43
3.2.2 Characterizing the kinetics at the electrode/electrolyte interface in MFC	46
3.2.3 Probing the PEM hydration in microfluidic electrolyzers	50
3.3 Conclusions	53

4	Research project	55
4.1	Thermal tomography in solid heterogeneous media	56
4.1.1	Optothermal models in multilayer materials	56
4.1.2	Improved SNR by using laser sources	58
4.1.3	3D temperature measurements in heterogeneous media	58
4.2	Thermal super-resolution imaging	60
4.2.1	Temporal approach	61
4.2.2	Spatial approach	61
4.3	Applications	63
4.3.1	OptUseH2 project: PEM degradation assessment in microfluidic electrolyzers	63
4.3.2	SMARTBAT project: heat and mass transfer characterization in microfluidic redox flow batteries	64
4.4	Timeline	67
5	General conclusion & perspectives	69
II	Personal records	73
6	Curriculum vitae	75
6.1	Professional experience	75
6.2	Education and training	76
6.3	Pedagogic and administrative charges	76
6.4	International & national reputation	76
6.4.1	Scientific and organizing committees membership of national conferences	76
6.4.2	Seminars at foreign Universities	77
6.4.3	International mobility	77
6.5	Scientific collaborations	78
6.6	Ph.D. thesis committees	79
6.6.1	Ph.D. monitoring thesis committee membership	79
6.6.2	Ph.D. thesis defence committee membership	79
6.7	Peer review activity	79
6.8	Scientific production	79
7	Students' supervision and research project granted	81
7.1	Undergraduated students	81
7.2	Master Students	82
7.3	PhD Students	82
7.4	Post-doctoral fellow	83
7.5	Research project granted	83
7.5.1	Project coordination	83
7.5.2	Work package leader	84
7.5.3	Industrial contracts	84

8	Teaching activities at Arts et Métiers Institute of Technology (EN-SAM)	87
8.1	Advanced energetic course	87
8.2	Heat transfer lab class	88
8.3	Hydrogen fundamental and technology course	88
8.4	Undergraduate student projects	89
9	List of publications	91
9.1	Paper published in international peer reviewed journals	91
9.2	Paper submitted to international peer reviewed journal	96
9.3	Plenary Lecture (as invited speaker)	96
9.4	International referenced conference proceedings	97
9.5	National referenced conference proceedings	99
9.6	National and international conference without proceedings	99
	Bibliography	103

List of Acronyms

ACC Automotive Cells Company	69
ANR Agence Nationale de la Recherche	43
ATR Attenuated Total Reflection	8
CFD Computed Fluid Dynamic	40
CNRS Centre National de la Recherche Scientifique	43
DLaTGS Deuterated L-alanine doped Triglycine Sulfate	9
EIS Electrochemical Impedance Spectroscopy	40
FAM Fédération de Microfluidique en Aquitaine	70
FPA Focal Plane Array	8
FTIR Fourier Transform Infrared	8
GDL Gas Diffusion Layer	36
ICMCB Institut de Chimie de la Matière Condensée de Bordeaux	64
InGaAs Indium Gallium Arsenide	9
InSb Indium Antimonide	9
IR Infrared	2
I2M Institut de Mécanique et d'Ingénierie	38
LIFSE Laboratoire d'Ingénierie des Fluides Système Energétique	63
LIMMS Laboratory for Integrated Micro-Mechatronic Systems	64
LOF Laboratoire du Futur	64
LOMA Laboratoire Onde Matière d'Aquitaine	70
MCT Mercury Cadmium Telluride	9
MFC Microfluidic Fuel cell	2
NIR Near Infrared	9
NDT Non Destructive Testing	25
PEM Polymer Electrolyte Membrane	35

PEMFC Polymer Electrolyte Membrane Fuel cell	1
PDMS Polydimethylsiloxane	14
PIMM Procédés et Ingénierie en Mécanique et Matériaux	63
PNM Pore Network Modelling	40
SNR Signal to Noise Ratio	11
TIFC Thermal & Imaging Field Characterization	2

Nomenclature

The main notations used in the manuscript are summarised here. Few exceptions can be found in the text, but a thorough definition of their meaning will be given in these cases.

Symbols	Units	Definition
<i>Roman Alphabet</i>		
A	-	Absorbance
a	m^2/s	Thermal diffusivity
b	V	Tafel slope
c	M	Molar concentration
C_{DL}	F/m^2	Double capacity layer
d	m	Distance
D	m^2/s	Mass (Fickian) diffusivity
f	Hz	Frequency
h	$\text{K}/\text{m}/\text{W}$	Impulse response
I	a.u.	Light intensity
$i = \sqrt{-1}$	-	Complex unity
i_0	A/cm^2	Exchange current
j	A/m^2	Current density
k	$\text{W}/\text{m}/\text{K}$	Thermal conductivity
L	m	Length
l	m	Width or thickness
q	m^3/s	Flow rate
T	K	Temperature
t	s	Time
v	m/s	Velocity
x	m	Coordinate
y	m	Coordinate
z	m	Coordinate
<i>Grec Alphabet</i>		
α	-	Charge transfert coefficient
δ	-	Complex writing
Γ	-	Light transmission
κ	K^{-1}	Thermotransmittance coefficient
η	V	Overpotential
θ	-	Temperature transform
λ	m	Light wavelength
σ	S/m	Electrical conductivity

μ	M^{-1}	Absorptivity coefficient
Φ	rad	Phase
ω	rad/s	Angular frequency
$\vec{\nabla}$	-	Gradient

General Introduction

The past few decades have shown a rapid and continuous exhaustion of the available energy resources which may lead to serious energy global crises. Researchers have been focusing on developing new and renewable energy resources to meet the increasing fuel demand and reduce greenhouse gas emissions. A surge of research effort is also being directed towards replacing fossil fuel-based vehicles with hybrid and electric alternatives. In this context, energy storage and conversion is now seen as a critical element in future "smart grid and electrical vehicle" applications. Thus, microscale energy conversion devices offer one of the best combination of efficiency, cost, flexibility, and power density, with microfluidic technologies [Modestino *et al.* 2016] leading the way in this aspect. To accompany these technological developments and their miniaturisation to microscale and beyond, advanced characterization methods need to be continuously improved. My past works and the proposed research project fall within these objectives with a particular focus in developing field-based measurements and analytical data processing for heat and mass transfers.

1.1 My research activities at a glance

The present thesis reports the works done within the last 10 years, i.e. 2013-2023, after my PhD thesis. This decade corresponds to my two postdoctoral fellowships, done from 2013 to 2018, and my appointment as Associate Professor at ENSAM Bordeaux since 2018.

In order to present an overview of the main research gaps tackled and the main achievements done in the last 10 years, my research background is summarized in Figure 1.1. Each color corresponds to a specific topic. Most of my early works were dedicated to Polymer Electrolyte Membrane Fuel cell (PEMFC) diagnostic techniques with the development of experimental setups and inverse methods to measure their state-of-life. This topic started during my PhD and has been pursued during my second post-doctorate fellowship in Nantes. The first image-based characterization were performed during my first post-doctorate fellowship in Canada using X-ray to image the two-phase flow in microscale porous media. I did not continue any works on porous materials later on, but I kept developing imaging techniques since then.

My research activities in Thermal & Imaging Field Characterization (TIFC) group in Bordeaux were dedicated to the development of Infrared (IR) imaging setup dedicated to energy conversion systems at the microscale and their associated methods. In addition, with the creation of the "Hydrogen Program" at Arts et Métiers (in which I am involved), my past expertise in PEMFC and hydrogen systems are being transferred toward my teaching activities and industrial contact. This illustrates how my past experience greatly fed my current research and teaching activities.

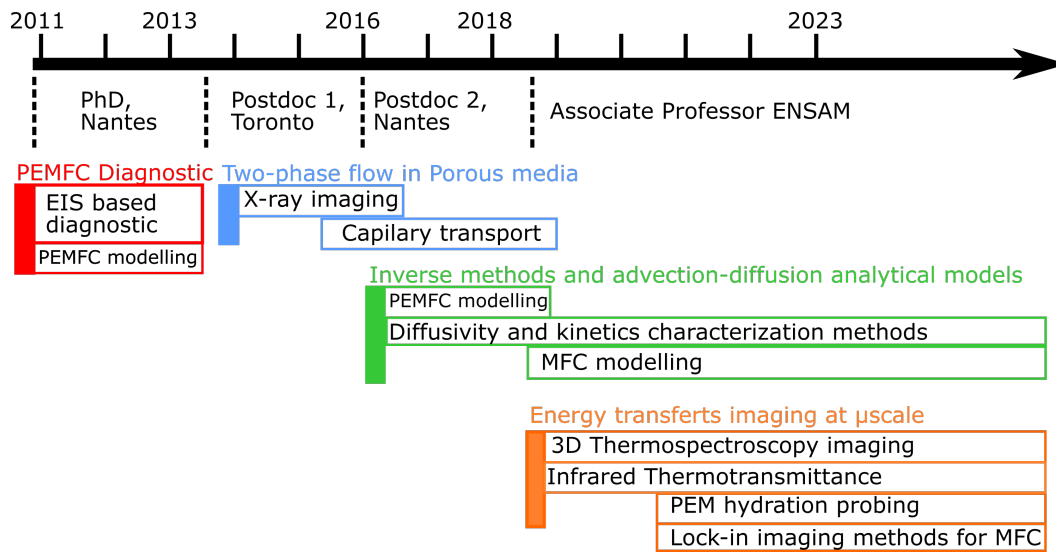


Figure 1.1: Research background at a glance

1.2 Objectives and organization of the manuscript

The first part of the present manuscript aims at summarizing the main outcomes of my past research from which a research project has emerged for the next 5 to 10 years. These works can be found in two main chapters where I first summarised the fundamental methods developed in term of imaging techniques and inverse methods (chapter 2). The first attempts to develop three-dimensional (3D) methods are described, and will feed the proposed research project. The following chapter (i.e. chapter 3), is dedicated to the application of the imaging and inverse methods on several microsystems. In particular, novel characterization techniques applied to microfluidic energy conversion devices including Microfluidic Fuel cell (MFC) and electrolyzers are described. Technological locks solved to apply the imaging methods were stressed to demonstrate how fundamental developments made in chapter 2 were transferred toward their applications on energy conversion devices.

Following this summary of my past works, the proposed research project is described in chapter 4. The definition of the objectives and the methodology to answer them is described and evaluated regarding the current state-of-the-art. As

in my past research, the proposed project describes as well as the fundamental work to developed 3D tomography at the microscale and its application for energy conversion devices. A general conclusion in chapter 5 will close the first part of this thesis.

The second part of the thesis is focused on all my academic indicators (student supervision, h index, citations, number of papers...) and curriculum vitae. An exhaustive list of all my publications, communications, seminars, conferences and research projects can be found in chapter 9. My involvement in teaching and administrative activities is also detailed in chapter 6. All the chapters in this part can be read independently, before or after part I. The purpose of part II is to give to the reader an exhaustive overview of all my achievements since my PhD thesis in 2013.

Part I

Research records & project

Toward three-dimensional imaging of heat and mass transfers

Contents

2.1 IR spectroscopic imaging methods	7
2.1.1 Main technologies for IR transmission spectroscopy	8
2.1.2 Concentration fields measurements	13
2.1.3 Temperature fields measurements	15
2.1.4 Summary of heat and mass transfer measurements	16
2.2 From 2D to 3D mass transfer field reconstruction	17
2.2.1 Concentration field measurements in microfluidic reactors . .	17
2.2.2 Qualitative 3D absorbance fields in a capillary tube	22
2.3 From 2D to 3D temperature field reconstruction	24
2.3.1 Main working principles in source reconstruction in opaque media	25
2.3.2 Qualitative laminography in semi-transparent media based on thermotransmittance	28
2.4 Conclusions	34

To study energy transfer in electrochemical systems, an important fundamental works concerning the development of contactless methods was carried out. Both experimental and mathematical (or modelling) aspects are discussed. Among the large panel of imaging techniques I used over the last ten years, a particular focus on IR imaging methods is done since such wavelength range (2 - 15 μm), is well suited to measure most of concentration and temperature fields. The main working principles of these methods are exposed to frame their use and limitations before to summarise my contributions toward 3D imaging and the main advances to this field since my arrival in the TIFC team in September 2018.

2.1 IR spectroscopic imaging methods

IR methods have the great advantages to give access to the measurements of heat and mass transfers, two out of three phenomena involved in the energy transfers (last one is the charge transfer). To do so, active methods where an IR beam is shed through a semi-transparent medium (assuming there is no scattering) are usually

used. In particular, this section presents Fourier Transform Infrared (FTIR) spectroscopy and tunable band pass filter spectroscopy which are well suited to measure the transmitted IR spectrum within a relatively short time (importance of time resolution will be discussed). However, in order to not overwhelm the reading, the interest of IR imaging methods compared to Raman mapping is not discussed here, but an in-depth analysis can be found in the following paper [Krafft *et al.* 2008].

2.1.1 Main technologies for IR transmission spectroscopy

Working principles of FTIR spectroscopy

A brief history of the development of the FTIR spectroscopic imaging setup is described in [Steiner & Koch 2009] comprehensive review. Although the FTIR spectrometers exist since the 50's, it is the seminal paper published by [Lewis *et al.* 1995] which opens the era of transmission imaging spectroscopy using a Focal Plane Array (FPA) to produce multispectral images. The development of more powerful IR sources (usually a globar of few hundred mW) and more sensitive IR detectors made possible to switch from the classical Attenuated Total Reflection (ATR) spectroscopy to transmission imaging spectroscopy. This latter has the great advantage to give a quantitative measurement of the transmitted light (usually associated with the absorbance). These quantitative measurements led to chemical concentration imaging in microfluidic reactors as depicted in Figure 2.1.

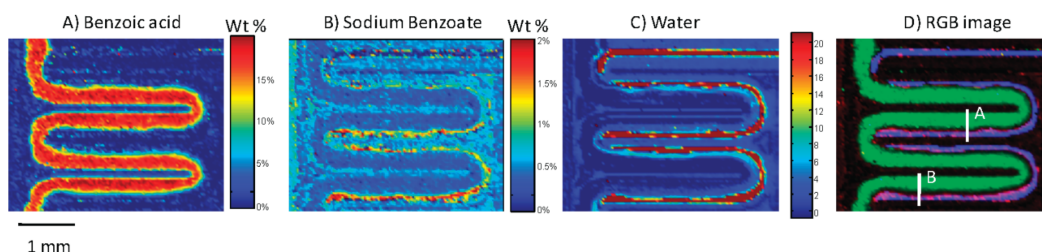


Figure 2.1: Concentration fields measured by FTIR spectroscopic imaging through a microfluidic reactor, from [Chan & Kazarian 2012]

There exists several technologies and setups reported in the literature to image IR spectra, though they all rely on the same working principles with the use of Michelson interferometers to produce light interferogram (see for example the following references [Bhargava *et al.* 2003, Schleegeer *et al.* 2009, Steiner & Koch 2009]). Interferograms are processed through a Fourier transform algorithm to obtain IR spectra (see Figure 2.2(b)). A schematic of one of the first bench proposed by [Lewis *et al.* 1995] can be found in Figure 2.2(a) with the Michelson interferometer comprising a fixed and a moving mirror (also called step-scan mirror). To understand how the performance of the FTIR spectrometers are governed and which

improvements can be made, let us define three main parameters controlling the Fourier transform, the quality of the IR spectrum and the time-resolution of this technology:

- the displacement step of the moving mirror;
- the total travel of the moving mirror;
- the moving mirror velocity.

The displacement step of the moving mirror actually governs the interferogram sampling frequency. This step is controlled using an alignment laser embedded in the interferometer. Typically HeNe lasers with a fundamental wavelength of $\lambda_{HeNe} = 632.8$ nm in air are used. The moving mirror is moved between two HeNe laser zero crossings and therefore travels over a distance of exactly 632.8 nm. Such value leads to a maximum spectral range of

$$\lambda_{max} = 2\lambda_{HeNe} = 1.26 \text{ } \mu\text{m}. \quad (2.1)$$

The factor 2 comes from the Nyquist-Shanon's theorem used in signal processing. This value is also expressed in wavenumbers as $\nu_{max} = 7898 \text{ cm}^{-1}$. In addition to this physical limit induced by the sampling frequency, the spectral range is also constrained by the material used in the FPA. For imaging purposes, most of the large range FPA reported in the literature are made of Mercury Cadmium Telluride (MCT) material with a spectral range from 2 to 13 μm . Imaging setups based on IR camera usually use Indium Antimonide (InSb) material in their detector, limiting the spectral range from 2 to 6 μm . Indium Gallium Arsenide (InGaAs) cameras in the Near Infrared (NIR) region have a spectral range from 1 to 2.5 μm . A quite old, but exhaustive list of the main detector technologies is proposed by [Kempfert *et al.* 2001] from ThermoFisher. It is worth noting that monodetectors are usually based on Deuterated L-alanine doped Triglycine Sulfate (DLaTGS) material allowing a wider spectral range (from 1 to 20 μm) compared to FPA.

The spectral resolution of the measurements, $\Delta\nu$, is completely controlled by the size of the interferometer. It is given by the second parameter: the distance travelled by the moving mirror, d , expressed as

$$\Delta\nu = \frac{1}{d}. \quad (2.2)$$

In practice, the moving mirror travels between 0.25 and 4 cm, corresponding to a spectral resolution ranging from 4 to 0.25 cm^{-1} . Note that, several spectrometers used for gases or far IR measurements can have travel distances up to several meters [Dawadi *et al.* 2015].

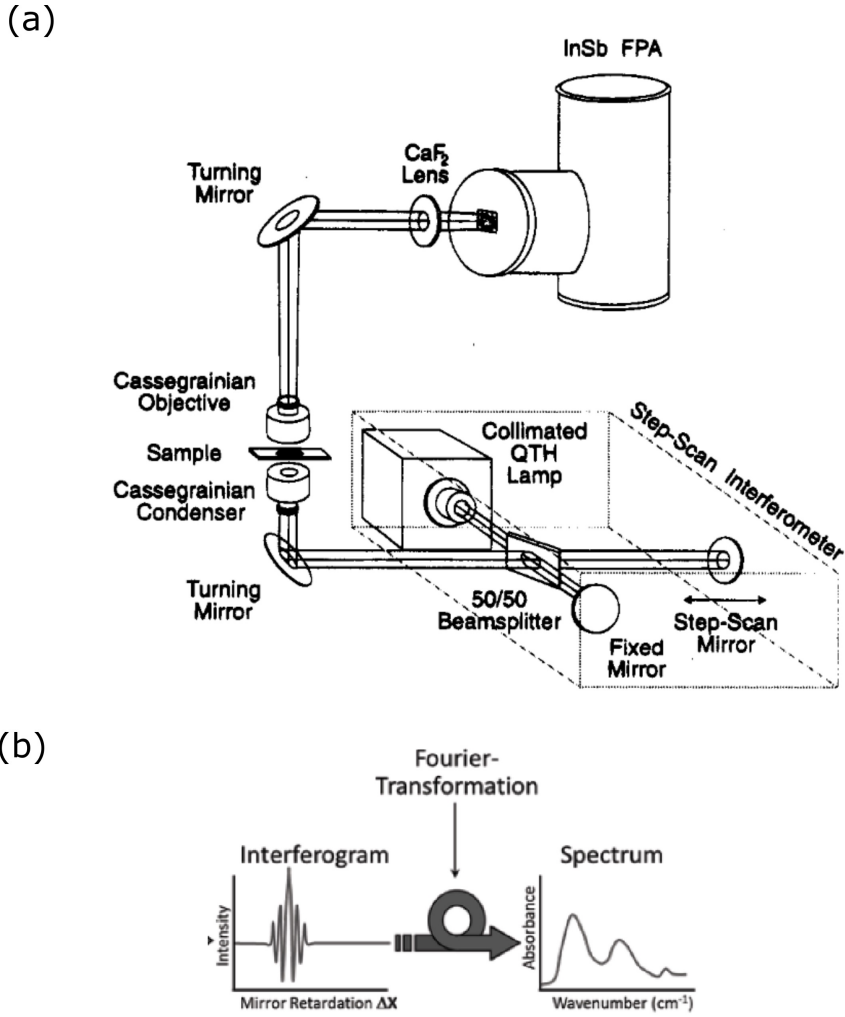


Figure 2.2: Principle of the FTIR imaging spectroscopy. (a) Experimental setup proposed by [Lewis *et al.* 1995]. (b) Signal processing to obtain an IR spectrum (right) from the interferogram (left), figure extracted from [Huck *et al.* 2016].

The third important feature, is the time needed to measure one spectrum, and it is governed by the moving mirror velocity, v_M . This value is in practice limited by the the FPA frame rate, f_{FPA} , since an image of the sample is snapped each time a laser zero crossing produced by the moving mirror is detected. Thus, the time requires to perform one interferogram measurement is

$$t = \frac{d}{v_M} = \frac{d}{f_{FPA} \lambda_{HeNe}}. \quad (2.3)$$

Commercially available state of the art FPA are 128 by 128 px, over a spectral range from 750 to 5000 cm^{-1} and a frame rate of few thousands of Hz [Ghosh *et al.* 2016]. It constrains the mirror velocity roughly from 0.0633 to 0.633 cm/s, leading to a 1 s measurement for a complete spectrum (with a

spectral resolution of 4 cm^{-1} =). In most cases, the measurement needs to be repeated several times (between 10 and 100 times) to increase the Signal to Noise Ratio (SNR), significantly increasing the measurement time. Thus, time resolved FTIR spectroscopy is quite limited to transient phenomena with a time constant of few tens seconds or minutes [Chevalier 2021]. Alternative techniques based on time-resolved step-scan measurements can be used though, but only in the case of fast and periodic transient regimes, see [Schleeger *et al.* 2009]. This particular techniques ensures a time resolution in the order of few ms currently.

To conclude, FTIR transmission spectroscopy is commonly used in microfluidic, biology or food science, as well-resolved IR spectra can be recorded to identify a large number of molecules leading to quantitative measurements of concentration fields. However, as it was discussed, this technique suffers from quite slow measurements (few seconds) due to the relatively low frame rate of the FPA and the necessity to repeat the measurements to increase the SNR. This limitation constrains the use of FTIR spectroscopy for steady state analysis of heat and mass transfers through thin sample ($< 100 \text{ }\mu\text{m}$) ensuring a rather good SNR (10 or higher). To balance these drawbacks, tunable band pass filter imaging spectroscopy has emerged in the recent years.

Working principles of tunable band pass filter imaging spectroscopy

Tunable band pass filters are mainly based on diffraction grating to extract a narrow wavelength range from an IR polychromatic source [Ryu *et al.* 2017]. Such apparatus is often called as *monochromater* in reference to the almost monochromatic light, but without any comparison to an IR laser [Rosas *et al.* 2023] which produce monochromatic and coherent light. The quality and spectral bandwidth of the light depends on the setup, and it is generally not better than $\pm 20 \text{ nm}$ in the IR range. This corresponds to a spectral resolution ranging from $50 - 10 \text{ cm}^{-1}$, compared to the 4 cm^{-1} or even less than 1 cm^{-1} obtained classically using FTIR spectroscopy, the spectral resolution of the light using a monochromater is coarser.

In comparison to transmission FTIR spectroscopy, less setups using monochromaters as light source are reported in literature. The main groups well identified are located in Japan (Kakuta's [Kakuta *et al.* 2016, Uema *et al.* 2021] & Morikawa's [Ryu *et al.* 2017] groups), in UK with Kazarian's group ([Ryu *et al.* 2017]), in France with the TIFC team [Romano *et al.* 2015, Kirchner *et al.* 2018] where the oldest works were published in 2010's. They all proposed a setup similar to the one depicted in Figure 2.3. The detector is, in most cases, an IR camera which, compared to FPA has a limited spectral range but increased detectivity. Such particularity enables the simultaneous measurement of the monochromatic transmitted light from the source and the sample proper emission. This latter can be linked to its local temperature. Most of the applications were focused on the thermo-spectroscopic studies of chemical reaction in microfluidic where the main goal is the simultaneous

measurements of their heat and mass transfer properties, and eventually the reaction enthalpy. This thermo-spectroscopic technique applied to microfluidic can be viewed as contactless calorimetry.

The main parameters governing the performance of the tunable band pass filter imaging spectroscopy are the following:

- the monochromater slit width;
- the chopper chopping frequency (see Figure 2.3).

A very thin slit (see Figure 2.3) enables to select only the first order harmonic of the diffracted light from the grating. Closer the slit is, more monochromatic the light, but with a significant reduction in signal intensity. There is a trade-off between signal and spectral resolution, which is usually established around ± 20 nm as mentioned earlier.

The second important feature, controlling the time resolution of the setup, is the chopping frequency of the mechanical chopper embedded in the light source (see Figure 2.3). The signal, S , recorded by the IR camera is

$$S = E + I \tag{2.4}$$

where E is the proper emission from the sample and the environment, and I is the transmitted signal through the sample (from the IR source). The presence of the chopper, synced with the camera, enables to successively snap one image containing $E + I$ (chopper open) and another one containing only E (chopper close). By making the difference between them, the contribution of E and I can be separated. Such mechanism has two advantages: (i) extract a temperature information from E and (ii) filter the low frequency noise from I . The use of the chopper can be viewed as a zero order lock-in methods with the chopping frequency acting as the cutoff frequency of a high pass filter. Thus, the time resolution of the setup is not limited by the frame rate of the camera, but by the chopping frequency. Time resolution in the order of hundreds Hz are generally achieved [Chevalier 2021].

To conclude, this technique is well adapted when monochromatic light is enough to characterize the chemistry of the system (like in binary solution for example). It enables the measurement of: (i) transient phenomena with time constant in the order of few ms, (ii) phenomena with a poor SNR since a large amount of data can be averaged in a relatively short time, and (iii) information concerning the temperature of the sample, extracted from E , due to the higher detectivity of IR cameras. Several upgrades of the method can even be brought using high speed heterodyne technique to significantly increase the time resolution (down to the μ s), but only in the case of repeatable short periodic phenomena [Pradere *et al.* 2011]. These characteristics make the tunable band pass filter imaging spectroscopy complementary to the transmission FTIR spectroscopy, extended the range of application and measurements to

fast and non isothermal phenomena. My contributions in their development will be developed in section 2.2 of this chapter. Finally, the link between the transmitted signal measured by these techniques and the temperature and concentration fields needs now to be established.

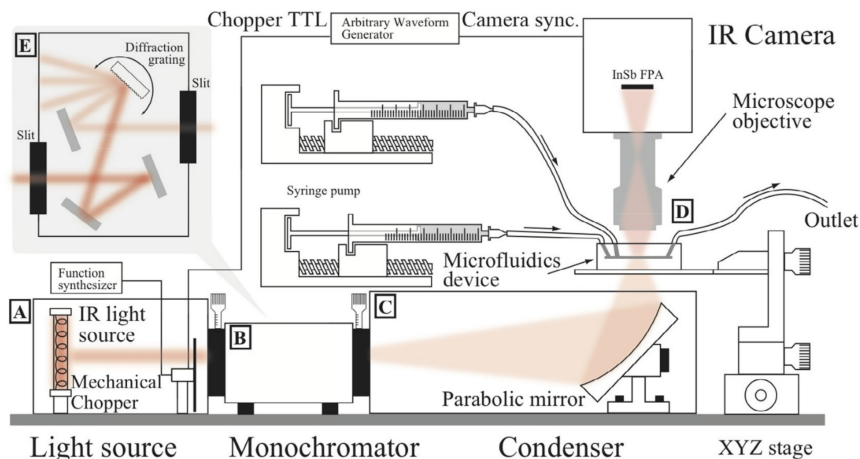


Figure 2.3: Principle of the transmission imaging spectroscopy based on a monochromator, figure from [Ryu *et al.* 2017]

2.1.2 Concentration fields measurements

The fundamental relationship linking light absorption through a medium to its compound concentration is the Beer-Lambert law, expressed as

$$A(\lambda, T, c) = \sum_i \mu_i(\lambda, T, c_i) \bar{c}_i l \quad (2.5)$$

where A is the absorbance of the light through the sample, T and \bar{c} are the average temperature and concentration, respectively, μ is the absorptivity coefficient ($\text{M}^{-1} \cdot \text{m}^{-1}$), l is the optical path and the subscript i is the i th species in the medium. Beyond the apparent simplicity of equation 2.5, several assumptions need to be done to ensure its validity:

- the absorbance is considered equal to the logarithm of the transmission (the effect of light reflection is neglected);
- the compounds are considered diluted in the solvent, i.e. aqueous solution;
- the concentration is constant along the optical path, i.e. $\bar{c} \approx c$;
- the light scattering is neglected.

These four assumptions are generally valid in most of the chemical reactions based on diluted aqueous solutions, without any solid micro particles, in a microfluidic channel, and when the reflection of the light is assumed constant during the

measurement. In the case of an unique compound diluted in water with isothermal conditions, the absorptivity coefficient does not depend on concentration and temperature, and equation 2.5 reads

$$-\log_{10} \left(\frac{I(\lambda)}{I_0(\lambda)} \right) = \mu(\lambda)cl \quad (2.6)$$

where I is the transmitted light at a given concentration and I_0 is the reference transmitted light (generally taken at $c = 0$). Equation 2.6 is the most common one used in literature to measure concentration fields according to the following review [Perro *et al.* 2016] reporting works using microfluidic applications. Counter-examples where equation 2.6 is not valid can be found here: non constant absorptivity coefficient in highly concentrated solutions [Kakuta *et al.* 2016], and in colloidal dispersions [Lehtihet *et al.* 2021].

Currently, two major locks limit the quality of the concentration field measurements. The first one comes from the SNR. Before to reach the studied medium, the light must pass through different materials holding or containing the sample (see Figure 2.3). In this case, the choice of the materials used to build the sample holder is critical [Lehmkuhl *et al.* 2015]. In IR, the light absorption is usually minimized by choosing material like silicon (50% transmission through 1.5 - 20 μm), CaF_2 glass (90% transmission up to 10 μm), or sapphire (90% transmission up to 7 μm)... In microfluidic applications, Polydimethylsiloxane (PDMS) can be considered relatively transparent outside its absorbance peaks [Polshin *et al.* 2014] as long as it is not thicker than 2 mm. Another SNR limitation stems from the solvent itself which is usually highly absorbent. In the case of water, large bands of the IR spectrum can not be selected for concentration measurement as the transmitted signal is completely attenuated [Hale & Querry 1973]. In this case, the only solution is to reduce the optical path in the solvent to few μm (100 μm maximum with water), explaining the necessity to use microchannels for such concentration probing.

The second lock concerns the concentration measurements in multicomponent media, which are encountered in the majority of chemical reactions and biological processes. In these cases, uncertainty in the concentration measurements may arise not only from poor transmitted light SNR, but also from the mathematical correlation of the IR spectra of the different species used in equation 2.5 to compute c_i . An extensive literature in the chemical engineering community has been focused on such aspect of the problem, by developing multivariate inverse techniques [Brereton 2000] and data-based IR spectrum recognition [Butler *et al.* 2019]. Although this aspect remains a key issue for concentration measurements, my contributions to the image-based methods are focused on processing the concentration fields to extract the main transfer properties, not on improving the multivariate analysis.

2.1.3 Temperature fields measurements

In this section, the concept is to use the IR imaging-based setup to simultaneously measure the temperature along with the concentration fields. It has been shown that the previous concentration measurements based on transmission spectroscopy can only be performed through semi-transparent media. The drawback of choosing this material, it is that the use of classical methods based on thermography is not straightforward [Maldague 2012]. In particular, important uncertainties and noise is brought by parasitic light from the environment through the medium. The effect of the focal plane position and the fields of view of the camera optics on temperature measurements is not well understood. Finally, the impact of the medium absorption on the light emitted by the heat source is quite complex to describe [Bourges 2023].

One solution to these problems can be found by carrying temperature measurements based on thermotransmittance of the medium. This technique relies on the change of transmitted light intensity as a function of the medium average temperature [Kakuta *et al.* 2011], see this effect in Figure 2.4 for the water IR spectrum. The thermotransmittance can be described mathematically by writing the absorptivity coefficient as

$$d\mu = \left(\frac{\partial \mu}{\partial T} \right)_c dT. \quad (2.7)$$

Usually, at the first order, the link between μ and the temperature is considered linear such as $\left(\frac{\partial \mu}{\partial T} \right)_c \approx cte$ [Kittel 1986]. Introducing equation 2.7 in equation 2.6 leads to the following relationship, assuming a constant concentration in the medium:

$$-\log_{10} \left(\frac{I(\lambda)}{I_0(\lambda)} \right) = \kappa(\lambda) \Delta \bar{T}, \quad (2.8)$$

where $\kappa = \left(\frac{\partial \mu}{\partial T} \right)_c cl$ is the thermotransmittance coefficient (K^{-1}), and $\Delta \bar{T}$ is the temperature averaged in the direction of the optical path. I_0 is the transmitted light generally measured at a reference temperature T_0 , and I at a temperature different from T_0 . In the case where the reflection does not change with temperature, the logarithm of the transmitted light is equal to the absorbance.

Although such optical methods to measure the temperature have been widely known and used since the eighties (see the works on thermorefectance methods using visible or NIR light), the IR imaging-based thermotransmittance methods were only developed over the last ten years with the development of more sensitive IR FPA. Several works from the main groups developing IR imaging setups have been reported in the literature, see [Kakuta *et al.* 2011, Nguyen & Kakuta 2023, Kakuta *et al.* 2016, Pradere *et al.* 2017].

The major drawback of this method is its poor sensitivity. The coefficient κ is usually in the order of $[10^{-5} - 10^{-3}] \text{ K}^{-1}$. It means that to be able to measure a temperature variation of 1 K, one needs to detect light intensity variation lower than 0.1% in . Thus, an important effort needs to be done concerning the metrology and the data processing to make possible such measurements. Modulated or impulse thermal excitations must be used to increase the SNR and filter the experimental noise. My contributions to the development of such methods are described in the last section of this chapter.

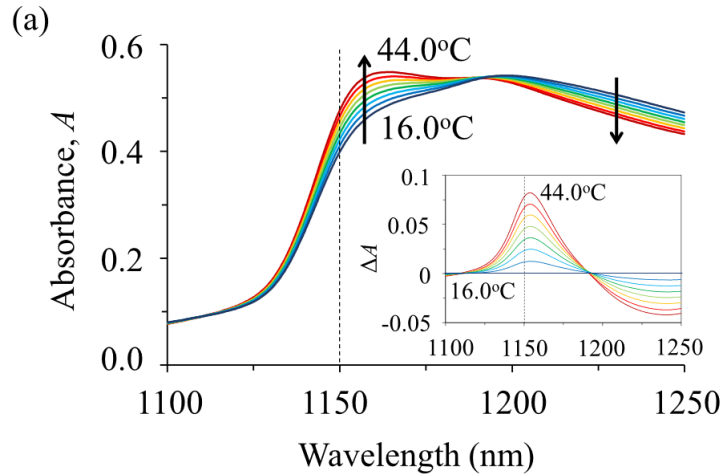


Figure 2.4: Effect of the temperature on the transmitted light intensity (here equal to the absorbance) in the case of pure water in the NIR range. Figure extracted from [Nguyen & Kakuta 2023]

2.1.4 Summary of heat and mass transfer measurements

This section has summarized the main experimental techniques used to measure the concentration and temperature fields in semi-transparent media. The main challenges in term of SNR, time resolution, spectral ranges, and spectral resolution were presented along with the main works reported in the literature. As it was shown, the development of these imaging methods is relatively recent (within the last 20 years) and numerous challenges remain to be solved, in particular :

- the temporal resolution down to the ms;
- the spatial resolution, currently limited to the diffraction limits (5 - 10 $\mu\text{m}/\text{px}$);
- the signal detection limit.

The two first points are a part of my research project for the next 5 years since they require an important development in terms of experimental setup and data processing. The last point however was tackled through the recent work I carried out in the framework of 3 PhD thesis. More specifically, the detection

limit of the average concentration and temperature measurements performed in semi-transparent media was pushed forward to open the path toward 3D imaging methods for microfluidic energy conversion devices.

In the following sections, the development of imaging setup for 2D imaging are first summarised. The proof-of-concepts to use these 2D imaging measurements to produce 3D images are then presented.

2.2 From 2D to 3D mass transfer field reconstruction

These works were carried out during the PhD thesis of A. Aouali (defended in January 2022), M. Garcia and K. Krause (both defended in early 2024). The objectives were to measure concentration fields in microfluidic chip and to develop a reconstruction algorithm based on Radon transform for 3D imaging. Once again, the success of these measurements relies on the combination of the following key concepts:

- an original setup combining FTIR transmission spectroscopy and IR camera to image in 2D both heat and concentration fields in microfluidic reactor;
- an analytical description of the advection-diffusion equations in a 2D microchannel to estimate the diffusivity and kinetic parameters of a chemical reaction;
- an inverse Radon transform algorithm to produce 3D imaging.

2.2.1 Concentration field measurements in microfluidic reactors

The combination of FTIR transmission spectroscopy and IR camera was one of my first experimental development since my arrival in 2018 [Chevalier 2021]. In this framework, I developed a strong collaboration with Solvay (now Syensqo) and the LOF on Bordeaux Campus for the fabrication of microfluidic chips dedicated to the concentration imaging. Three main studies were published using this collaboration [Krause *et al.* 2023, Garcia *et al.* 2023a, Garcia *et al.* 2023b], several works are still undergoing.

Concentration measurements in a binary solution

The first study aims at extend a well-known technique to measure the mass diffusivity in microfluidic chip [Salmon *et al.* 2005] to IR based imaging setup. It consists in measuring the interdiffusion of two fluids in a T-shape channel. It was achieved in the literature using Raman mapping or visible imaging, but never using IR light. Such wavelengths have the great advantage to be selective from the chemical point of view, the measurement is quite fast (few seconds to

produce a multispectral absorbance image), and also carry out information about the temperature. A summary of this experiment can be found in Figure 2.5.

It is based on custom made FTIR setup described in [Chevalier 2021], and depicted in Figure 2.5(a). The microfabrication of the microfluidic channel was adapted to ensure the highest possible transmission of the IR light. Silicon wafer were chosen, a 22 μm -height microchannel and a thin PDMS stamp was used. The advantages of silicon as wafer are two fold: (i) IR transmission is constant over the whole IR domain (50% transmission regardless its thickness), (ii) high thermal conductivity ($k_{Si} \sim 150 \text{ W/m/K}$) ensuring a good thermal control of the chip and the mass transfer. A local thermistor/heating source is embedded in the holding stage for thermal management of the chip, see Figure 2.5(b) and (c).

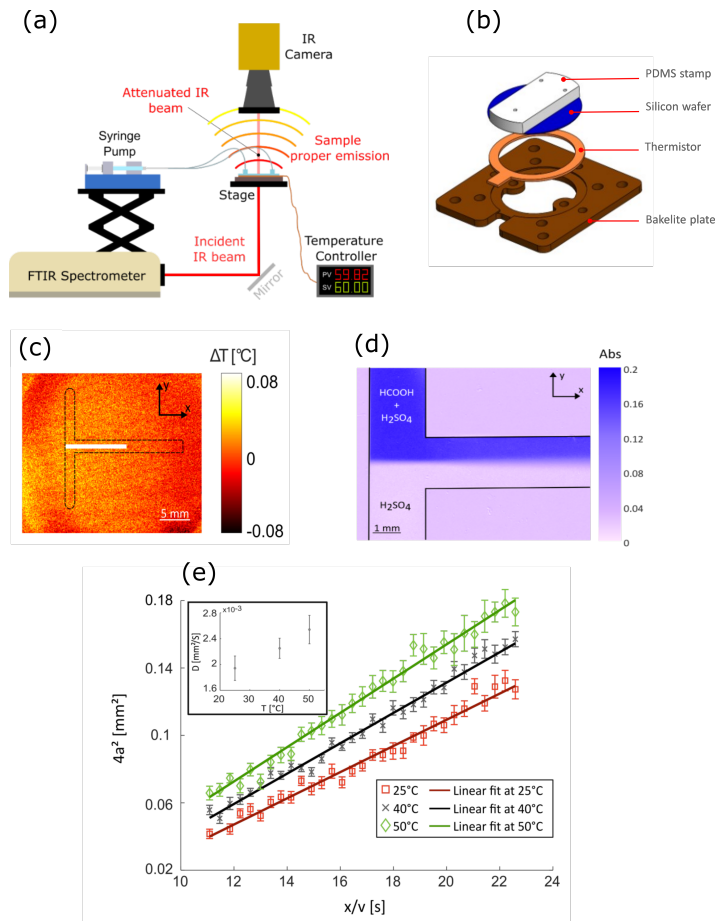


Figure 2.5: Measurement of mass diffusivity in microchannels as a function of temperature. (a) The transmission FTIR imaging setup. (b) the T-shape microchannel. (c) Temperature control of the microchannel. (d) Interdiffusion measurement and (e) Estimation of the mass diffusivity for a range of operating temperature. Figures from [Garcia *et al.* 2023a]

The absorbance images are then obtained for the two fluids, and a clear interdiffusion can be seen in Figure 2.5(d). This measurement is repeated for a range of temperature to study the effect of this latter on the mass transfer. In order to obtain quantitative data, an analytical model, similar to [Salmon *et al.* 2005] was used, where the width of the diffusion cone is plotted versus the channel length. The slope of this function gives a direct access to the mass diffusivity, see Figure 2.5(e). Once again, the analytical inverse method used here enabled a very efficient process of the data to carry out quantitative mass transfer characterization under thermally controlled environment.

Kinetic parameter measurements in acid-base reaction

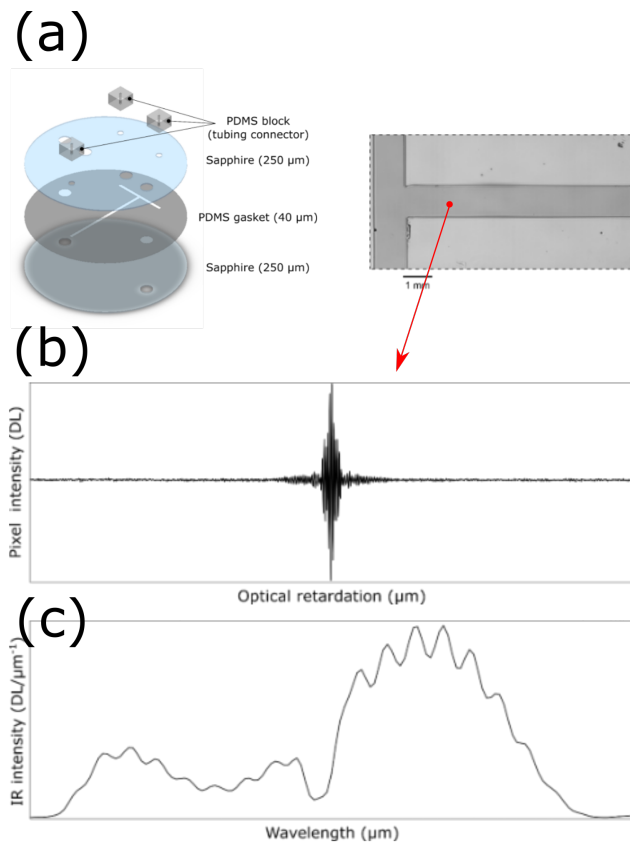


Figure 2.6: Measurement of concentration fields from the absorbance spectra. (a) The IR-transparent microchannel used for the acid/base reaction and the associated IR image. (b) A typical interferogram recorded in the channel and (c) the IR spectrum obtained after processing the interferogram.

After this first success, the idea was to push further the quantitative analysis using a more complex system made of three species: acid, base and resulting salt, i.e.

$HCL + NaOH \rightarrow NaCl + H_2O$. A similar T-shape channel was built with the help of the LOF, to make sure it will be fully transparent through the whole IR range (2 - 6 μm) of our imaging system. Compared to the previous study, an improvement in the design was made by capping the channel with a sapphire wafer instead of PDMS making this chip twice more IR-transparent, see Figure 2.6(b).

The first difficulty to be lifted in this work was the conversion of the IR camera interferogram (typically the one in Figure 2.6(c) for one pixel) to IR spectra. Once again, a demodulation algorithm based on FFT was written to get the IR spectrum in Figure 2.6(d). The information concerning the concentration of each species in each pixel of the channel was then obtained by an inverse methods, based on the multicomponent Beer-Lambert law introduced earlier (section 2.5) as

$$\mathbf{c} = [\boldsymbol{\mu}^T \boldsymbol{\mu}]^{-1} \boldsymbol{\mu} \mathbf{A}, \quad (2.9)$$

where $\mathbf{c} = [c_1 c_2 c_3]^T$ is a vector containing all the species concentration (acid, base and salt), $\boldsymbol{\mu}$ is a matrix containing the species absorptivity coefficient spectra and \mathbf{A} is a vector containing the spectrum measured in each pixel (Figure 2.6(d)). Again, the use of an analytical inverse methods based on least squares ensure a fast processing (around 1 GB of data processed in 10 s). It is important to note that such method is well adapted as long as the absorptivity coefficient spectra of each compound are not correlated. In such case, more complex algorithms must be employed to convert the absorbance spectrum into concentration [Brereton 2000].

One of the main results of this study was to get the simultaneous measurement of the concentration fields and the temperature fields generated by the chemical reaction. They can be seen in Figures 2.7(b) and (c). A schematic of the reaction is given in Figure 2.7(a) to help the understanding. The last step of this work, was to compare this raw data to a mathematical model governing the advection-reaction-diffusion of the chemical in microfluidic chip, such as:

$$\nabla \cdot (-D \vec{\nabla} c + \vec{v} c) = \pm \dot{R}, \quad (2.10)$$

where \dot{R} is a chemical rate which is a function of the kinetic coefficient k_r . The particular geometry used in microchannel makes possible to derive several analytical solutions to equation 2.10 depending of the flow rate regime. The details to get these solutions can be found in [Chevalier *et al.* 2021]. At the end, the mass diffusivity coefficient D for acid and base in salt were obtained as well as the kinetics reaction rate k_r . It is the first time that these values were obtained simultaneously, based on analytical process of the spectra and concentration fields, opening the door to almost on-line chemical analysis. To verify the good agreement of the value estimated, the comparison between the salt concentration distribution and equation 2.10 is made in Figure 2.7(d).

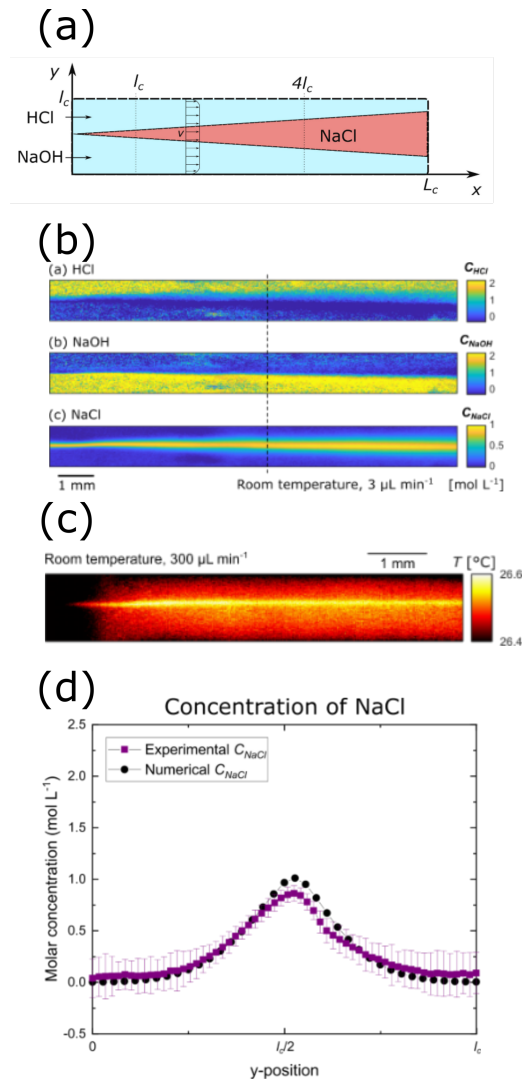


Figure 2.7: Measurement of multicomponent concentration fields. (a) A schematic of the acid/base reaction. (b) Concentration fields measured for the 3 species. (c) The associated temperature fields obtained during the chemical reaction and (d) the validation of the model using the mass estimated transfer parameters.

Finally, associated with the temperature fields measured during the reaction, our thermospectroscopic setup has a ability to make contactless microcalorimetry to measure reaction enthalpy coefficient. However, the temperature signal is still quite weak and the direct measurements of temperature in semi-transparent media remain inaccurate due to the numerous source of noise (as discussed earlier). Thus, there is still a large amount of work to push this methods toward such kind of calorimetry measurement. An association of lock-in method introduced by pulsating flow maybe a path to follow to transpose the thermal techniques develop in solid body to the mass transfer characterization. Such ideas to improve temperature measurements in fluid will be developed in the short term perspective of my research project.

2.2.2 Qualitative 3D absorbance fields in a capillary tube

From the development of the FTIR spectroscopic setup for 2D images in M. Garcia and K. Krause PhD, a step forward was followed through the PhD work of A. Aouali. The idea was to image a sample with different angle positions on a rotating stage to create a sinogram and process it through inverse Radon transform. Working principles of 3D image reconstruction are briefly summarised hereafter before to evaluate the proof-of-concept of 3D multispectral absorbance fields in a capillary tube.

Radon transform working principles

The absorbance defined in equation 2.5 is rewritten in 3D as:

$$A(x, z, \theta, \lambda, C, T) = -\log_{10}[\Gamma(x, z, \theta, \lambda, C, T)] = \int_0^{L_y} \mu(x, z, y, \lambda, C, T) dy, \quad (2.11)$$

where Γ is the light transmission. In equation 2.11, it appears that the absorbance measured along the optical path of the light is the sum of the local absorptivity coefficient. By changing the optical path using a rotating stage (see Figure 2.8), it is possible to deconvolute equation 2.11 to get the local absorptivity coefficient and identify the local material and its concentration.

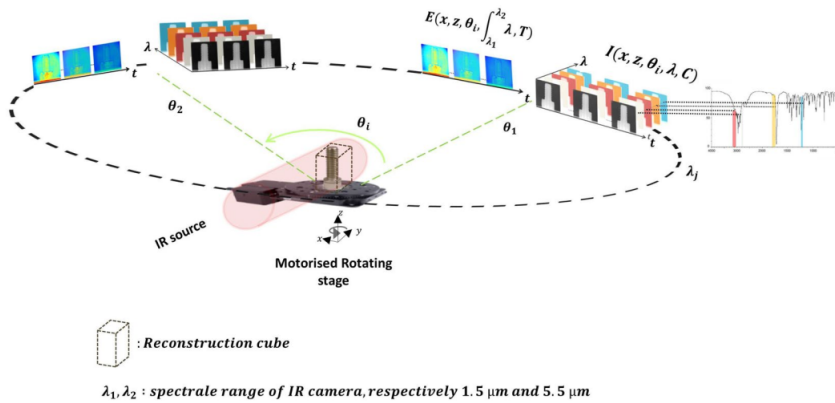


Figure 2.8: Working principle of the Radon transform.

The acquisition sets of each line of the Radon transform (angular projections) obtained for rotations between 0 and 2π is called a sinogram. Figure 2.8 shows the representation of sinogram acquisitions as a function of the rotation angles. Absorbance slices are reconstructed from sinograms calculated previously using the filtered back-projection method. This method allows us to perform inverse Radon transform which is essentially based on the application of an operator defined as follows:

$$\mathcal{B}[\mu(x, z, y, \lambda, C)] = \int_0^\pi \tilde{A}(x \cos \theta + z \sin \theta, \theta, \lambda, C) d\theta, \quad (2.12)$$

where \tilde{A} designates the Fourier transform in the polar coordinate of absorbance A . Finally, the 3D absorptivity field is reconstructed using the following equation:

$$\mu(x, z, y, \lambda, C, T) = \mathcal{B}\{\mathcal{F}^{-1}[\mathcal{F}[\tilde{A}(x, z, \theta, \lambda, C, T)] \cdot |W|]\}, \quad (2.13)$$

where B represents the back-projection filter, \mathcal{F} represents the Fourier transform, and W represents the ramp filter. By analyzing equation 2.13, it can be determined that the sections reconstructed using the back-projection method physically represent the normalized absorption coefficient of the vial. This method allows access to the intrinsic absorption coefficient and therefore to the qualitative chemical information with a phase separation of each compound in the sample. The previous methods is detailed in the following article [Aouali *et al.* 2020].

Absorbance 3D fields

The proof-of-concept of the 3D absorptivity fields was done through a semi-transparent capillary tube filled with water, air and ethanol. An air bubble was introduced between water and ethanol to separate them, avoiding any mixing.

These three fluids has a significant IR spectrum, see Figure 2.9(a), allowing for discrimination of each component. The 3D absorbance was reconstructed for 2 specific wavelengths (3.5 and 4.6 μm) to illustrate the segmentation between the compounds. As shown in Figure 2.9(b) to (d) it was possible to retrieve the position of air, water and ethanol in the capillary tube.

These first results were very promising since they validate both our ability to measure a multispectral sinogram using a rotating stage, and deconvolute it using an inverse Radon transform algorithm to obtain the 3D absorbance fields. However, the results were only qualitative at this stage (only phase separation of the compounds). The quantitative aspect of the absorbance was lost during the inverse method. Further works will pursue this effort, in the fundamental point of view, to develop a quantitative inverse method and makes possible to obtain 3D concentration fields in microfluidic reactor. The forthcoming actions to achieve this goal are detailed in the research project at the end of this part.

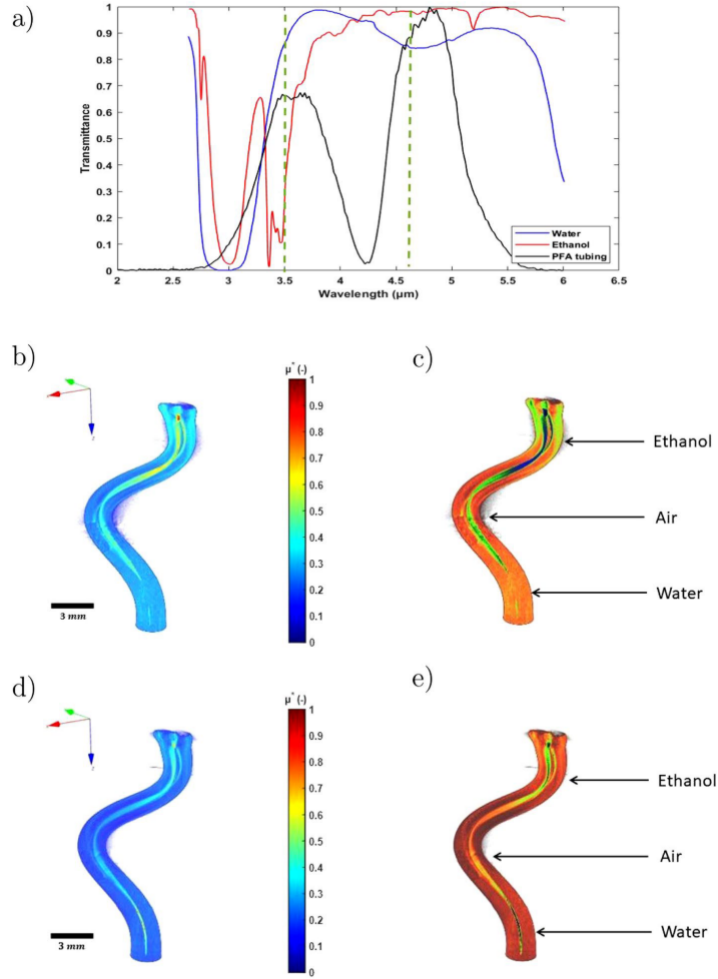


Figure 2.9: (a) Transmittance of water, ethanol and PFA tubing. Dimensionless reconstructed 3D absorptivities maps of the PFA tubing: (b) 3D absorptivity map at $\lambda = 3.5 \mu\text{m}$, (c) 3D absorptivity map at $\lambda = 3.5 \mu\text{m}$ with coloured segmentation for each media, (d) 3D absorptivity map at $\lambda = 4.6 \mu\text{m}$, (e) 3D absorptivity map at $\lambda = 4.6 \mu\text{m}$ with coloured segmentation for each media.

2.3 From 2D to 3D temperature field reconstruction

The works done through A. Aouali and C. Bourgès PhD thesis to achieve 3D measurements of the thermal fields are exposed in this section. They both rely on contactless method using IR cameras and inverse methods to reconstruct the 3D field. Two techniques were investigated: the first one was based on source reconstructions in opaque media from thermographic measurements, and the second one was based on thermal field reconstructions from lock-in thermotransmittance.

2.3.1 Main working principles in source reconstruction in opaque media

Sources in heat and mass transfer can have multiple origins: from Joule effect or molar flux at the electrode/electrolyte interface to heat release during an exothermic reaction. In most systems, reconstructing the sources means that a lot of information concerning the kinetics, the heat losses, the transport properties must be known.

An extensive literature exists on this topic, see for example the works from [Burgholzer *et al.* 2017b], or [Maldague 1993] in Non Destructive Testing (NDT). This topic is also an important part of the work developed in TIFC team in Bordeaux, with a lot of works concerning the source reconstruction in the bulk of opaque material based on thermography, see for example the recent work from [Groz *et al.* 2021] where heat source reconstruction were used to obtain the profilometry profile of buried interfaces.

In order to understand the main working principles and challenges of such source reconstruction, inverse method used in heat transfers are briefly recalled. The recent achievements on this topic done during A. Aouali PhD are then reported.

Inverse method challenges in heat transfers

A common formalism to describe the transfers through a system is to use a convolution product. The system is modelled by its transfer function (in Laplace transform space) or its impulse response in time domain. The response of the system, i.e. a temperature or concentration field, is then obtained by convoluting the impulse response to a source or a boundary condition. Mathematically, this can be written as

$$T(\vec{x}, t) = u(t) \otimes h(\vec{x}, t) \quad (2.14)$$

where $T(\vec{x}, t)$ is a transient temperature fields, $u(t)$ is a source or boundary condition, $h(\vec{x}, t)$ is the impulse response, and \otimes designates the convolution product¹.

The use of pulsed sources, i.e. $u(t) = \delta(t)$, where $\delta(t)$ is the Dirac distribution, is one of the most common techniques to have an analytical description of the field $T(\vec{x}, t)$. In heat transfers, pulsed lasers are generally employed to produce short heat source from ns to ms. This is the case for the flying spot thermography [Salazar *et al.* 2020, Rashed *et al.* 2007], used in NDT and heat diffusivity measurements. The great advantages of this techniques is (i) to ensure a very high SNR since lasers enable a high heat flux (several mW) on a very small area (few mm²), (ii) to compute an analytical description of the heat transfer diffusion after the Dirac excitation [Gaverina *et al.* 2017], i.e. the heat transfer impulse response

¹In this example only the temporal convolution is considered, but the method can be extended to the spatial convolution, i.e. such as in the case of heat diffusion in periodic regime.

$$T(x, y, z = 0, t) = \frac{Q}{\rho c_p} \frac{\exp\left(-\frac{(x-x_0)^2}{4a_x t} - \frac{(y-y_0)^2}{4a_y t}\right)}{\sqrt{\pi^3 t^3 a_x a_y a_z}}. \quad (2.15)$$

The word reconstruction is synonym of deconvolution when used in inverse methods. It is different from the previous parameter estimation in a sense that a function needs to be estimated, not a scalar. In other words, the solution $u(t)$ must be found in equation 2.14, knowing $T(\vec{x}, t)$ and $h(t)$. Usually, equation 2.14 is written in discrete form (as the measure is discrete by definition) using a matrix formalism. At a position \vec{x}_0 we have

$$(\mathbf{T}) = [\mathbf{h}](\mathbf{u}), \quad (2.16)$$

where $[\mathbf{h}]$ is the Toeplitz matrix of the impulse response at x_0 , (\mathbf{T}) and (\mathbf{u}) vectors of the temperature and source, respectively. This latter is in theory obtained by inverting equation 2.16, or deconvoluting [Woodbury *et al.* 2023] as

$$(\mathbf{u}) = [\mathbf{h}]^{-1}(\mathbf{T}). \quad (2.17)$$

But in practice this method does not work due to the experimental noise and model bias. It is the so called "ill-posed" problem, as defined by [Hadamard 1902]. Because of this, numerous deconvolution methods were developed over the past century to ensure a stable solution to equation 2.14.

The least squares and Tikhonov regularization are one of the main regularization methods. One can cite the sequential and future time methods developed by Woodbury and Beck [Woodbury 1999] which are also widely used in heat flux estimation. Those methods are today well understood and has been employed in many applications, even if the choice of the Tikhonov parameter or the time step r in the future time is still somewhat arbitrary. The main challenges remain in the efficiency of these method to treat a large quantity of data and the numerical cost in the matrix inversion of $[\mathbf{h}]^{-1}$. Thus, in the recent years, inverse methods developed directly in Fourier spaces or using modal decomposition based on singular values were particularly suited for these applications [Ayvazyan 2012]. Source reconstruction inspired by acoustic methods has also started to emerge [Burgholzer *et al.* 2017b]. All these recent approaches are presented as one of the best solutions to reconstruct heat and mass sources from a large set of images at a reasonable computational cost (few minutes or less).

Source reconstruction in thin carbon film

In the framework of A. Aouali PhD thesis, these challenges were addressed to reconstruct heat sources from a laser on a thin carbon film. Such work was motivated by the development of a new THz to thermal converter [Aouali *et al.* 2023a]. An important work on direct modelling and inverse methods was done to achieve this task.

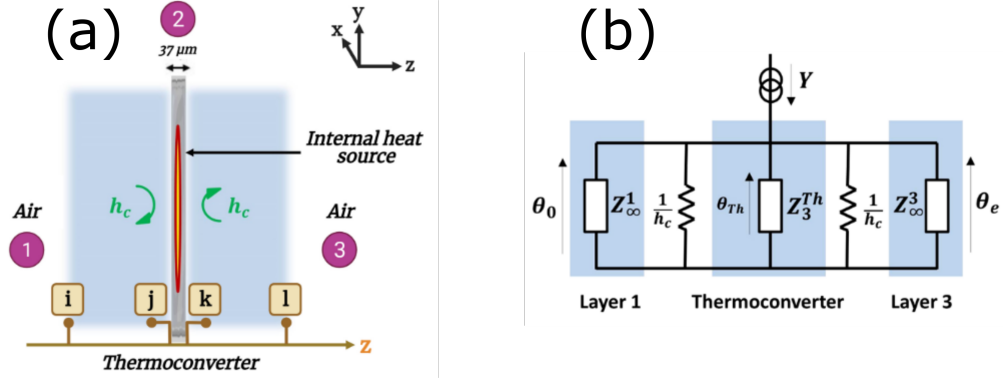


Figure 2.10: Schematic of the direct modelling of the heat transfers in thin carbon film. (a) Geometry used. (b) Electrical equivalent impedance network.

The geometry of the thin carbon film in air can be schemed as in Figure 2.10(a) with three layers (air/carbon film/air) and an internal heat sources. In such case, an impedance network of the transient heat transfers was derived based on the Fourier/Laplace integral transforms [Maillet *et al.* 2000]. It can be modelled using an equivalent electrical circuit as the one depicted in Figure 2.10(b). Such formalism is really convenient since the 3D transient heat transfers simply write:

$$\theta_{Th} = \left(\frac{1}{Z_{eq}^1} + \frac{1}{Z_3^{Th}} + \frac{1}{Z_{eq}^3} \right)^{-1} \times Y, \quad (2.18)$$

where θ_{Th} is the transforms temperature fields (see all the details in [Aouali *et al.* 2021]). The great advantage of equation 2.18, aside from the analytical solution, is its formalism similar to equation 2.16. Thus, classical inversion methods with Tykhonov regularisation was used in combination with a Wiener filter in Fourier space to speed up the inversion and filter the signal. Such methodology was one of the main achievement obtained during A. Aouali PhD thesis with a lot of outcomes both concerning the direct modelling (impedance formalism) and inversion method (Wiener filter).

To illustrate the source reconstruction done, the experimental measurements done using thermography and short laser pulse is presented in Figure 2.11(a). The source reconstruction (energy deposited by the laser) is presented in Figure 2.11(b) and (c). One can note the quantitative data obtained in this work [Aouali *et al.* 2021]. Extensions of this method was also done through 3D imaging of semi transparent samples from visible to THz range [Aouali *et al.* 2023a], or in the development of high intensity power meter [Aouali *et al.* 2023b]. This fundamental work was also at the onset of the Radon method presented in section 2.2.2 where similar inverse methods in Fourier spaces were done.

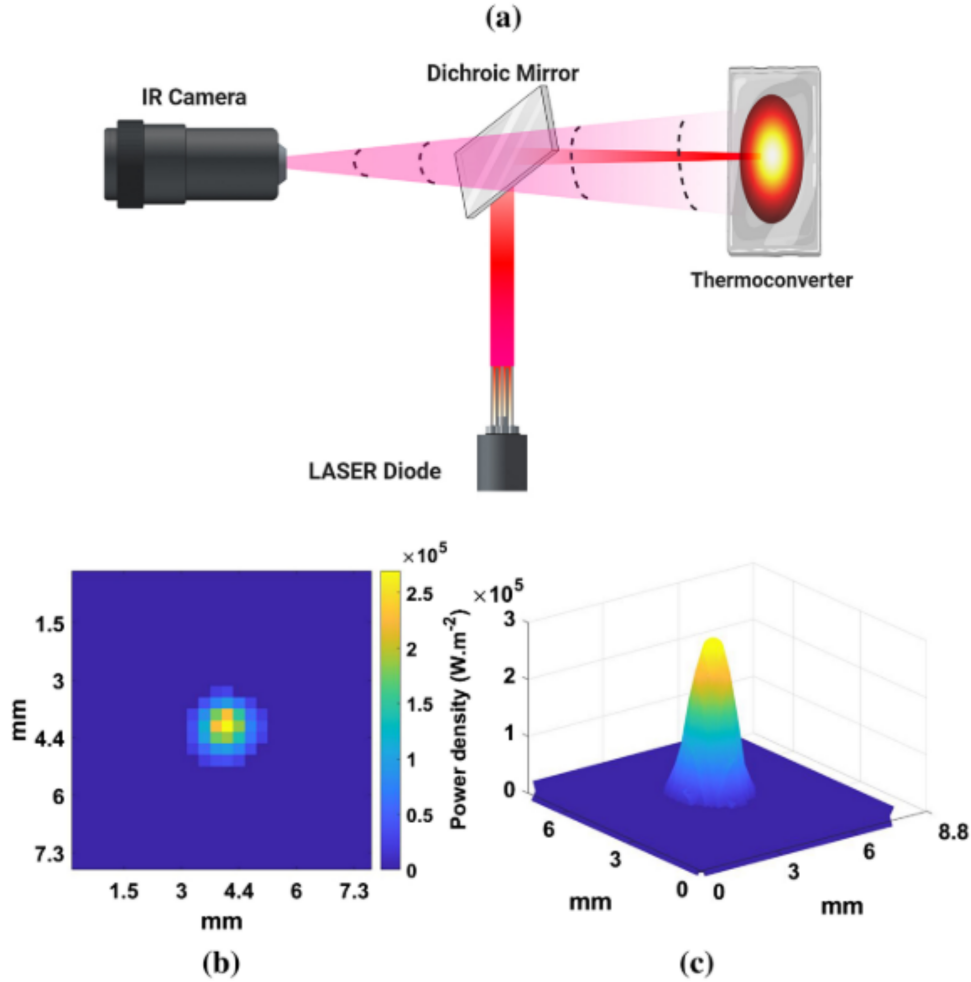


Figure 2.11: (a) Experimental setup. (b) Image of the reconstruction source, and (c) spatial distribution of the power density of the source

2.3.2 Qualitative laminography in semi-transparent media based on thermotransmittance

Lock-in thermotransmittance setup

One of the recent outcome these last three years was the development of a thermal field imaging method dedicated to semi-transparent media. As it was said in section 2.1.3, classical thermography techniques used for opaque media cannot be transposed with semi-transparent ones. An alternative is to use a method based on the thermotransmittance property of the IR light. This work was mainly done during the C. Bourgès PhD [Bourgès *et al.* 2023] in collaboration with the physics laboratory of Bordeaux (LOMA with S. Dilhaire).

To compensate the weakness of this signal (see equation 2.8, a lock-in method was

developed as schemed in Figure 2.12(a). It is an adaptation of the well known lock-in thermography [Busse *et al.* 1992] to thermotransmittance. Using this method, it was possible for the first time to detect less than 1% of IR signal variation though a semi-transparent body at the microscale. The success of this measurement relies on the combination of two things:

- an original setup combining contactless imaging system, and local thermometer/heating source which can be easily modulated;
- an inverse methods based on efficient demodulation algorithm (FFT) associated with an analytical model to process the thermal fields and to measure the thermophysical properties of the material.

The setup described in Figure 2.12 is similar to one depicted earlier in Figure 2.3, including a chopper to separate the transmitted signal from the proper emission, see the section 2.1.1. In this study, the transmitted signal is modulated by the temperature of the sample, heated by Joule effect using a thin gold resistance (see Figure 2.12(b)). The resulting temperature variation of the transmitted signal can be seen in Figure 2.12(c) for one pixel of the camera. As it was mentioned, the signal is weak, less than 1% of variation for a temperature modulation of about 10-20° C. This illustrates the need for lock-in methods in order to increase the SNR.

The other great advantage of the setup designed during C. Bourges PhD, is the use of the gold resistance as local thermometer: the voltage measured at the resistance edges is used as a probe to estimate the temperature variation. This methods relies on the well-know 3ω technique [Cahill 1990], and it was implemented on this setup so the resistance temperature of the surface of the sample is known.

The demodulation of the signal presented in Figure 2.12(c) was done using a classical FFT algorithm which is particularly efficient to process images. A 1 GB images containing 128 x 128 pixels over 10 min (roughly 20,000 images) can be processed on few seconds on a classical laptop using Matlab. The results for one pixel is presented in Figure 2.12(d).

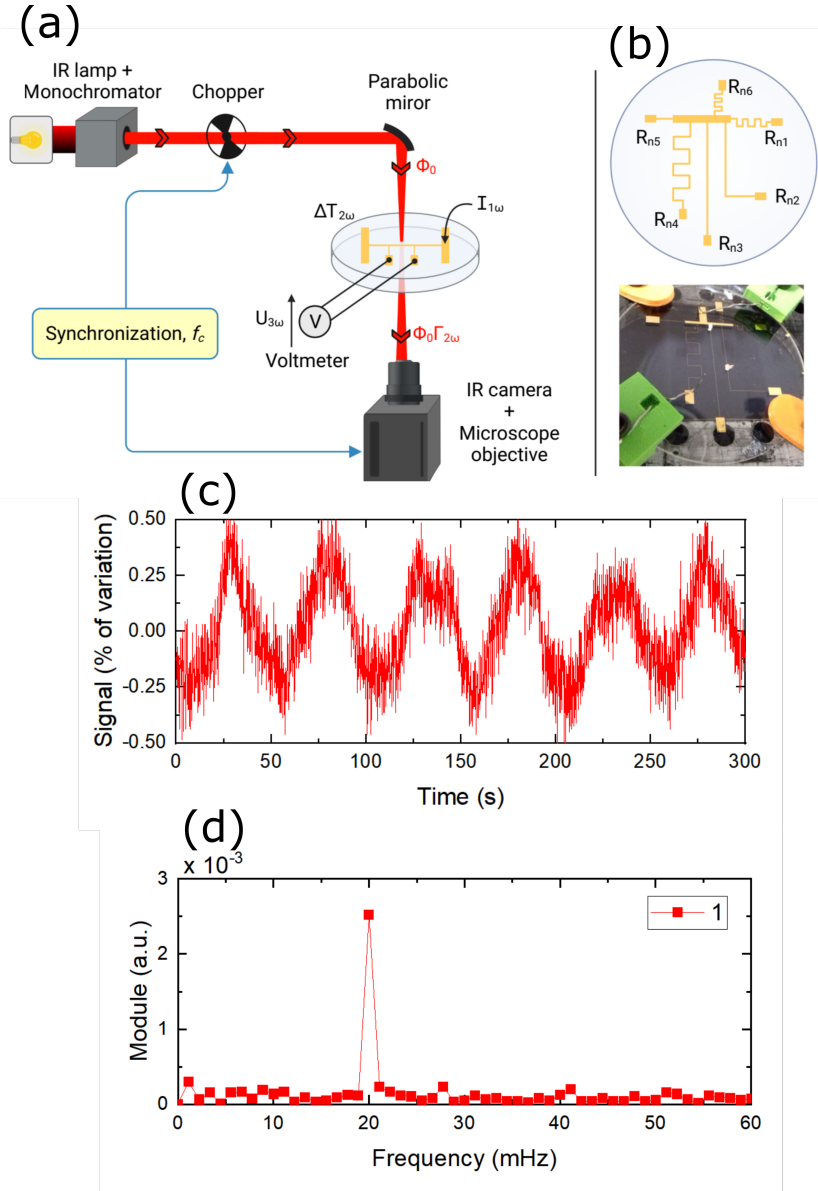


Figure 2.12: Thermotransmittance measurement principle. (a) Experimental setup. (b) The glass wafer with the coated heating resistance in gold. (c) Typically recorded modulation in the transmitted light. (d) Results of the demodulation.

Average temperature and thermal properties measurements

As reported previously, the images are processed through an inverse method relying on an analytical model for improving time efficiency and accuracy. Once again, lock-in measurements are very convenient as they enable direct solving of the heat transfer equation in 2D in Fourier space by adopting the following complex decomposition:

$$\underline{T}(x, z, t) = T_0(x, z) + \delta \underline{T}(x, z, \omega_T) e^{i\omega_T t} \quad (2.19)$$

where \underline{T} designates the complex solution of the temperature fields, T_0 is the steady state field and $\underline{T}(x, z, \omega_T)$ is the complex temperature field solution in the Fourier space. Such kind of decomposition can also be viewed as a Fourier transform to move from the time space to the frequency space.

The semi-transparent material geometry is schemed in Figure 2.13(a) with the axis and the beam path. It needs to be recalled that the measured signal is the average temperature, $T_z(x, t)$, in the beam path direction. Therefore, it was shown that the heat equation to be solved is only the 1D diffusion as

$$\frac{\partial^2 T_z(x, t)}{\partial x^2} = \frac{1}{a} \frac{\partial T_z(x, t)}{\partial t}. \quad (2.20)$$

Solving this equation in Fourier space using the decomposition 2.19 and in the semi-infinity space in x leads to the well-known complex solution²

$$\delta \underline{T}_z(x, \omega) = \delta T_z^0 \exp\left(-x \sqrt{i\omega_T/a}\right). \quad (2.21)$$

The modulus of $\underline{T}_z(x, \omega)$ measured experimentally is presented at a frequency of 80 mHz in Figure 2.13(b). It varies between 5 and 0.1 K in average and decay rapidly over 1 mm validating the semi-infinity assumption in x direction.

Beyond the prediction of the average temperature variation in semi-transparent media such technique is a convenient contactless method to measure the thermal diffusivity. A frequency study in Figure 2.13(c) and (d) have shown that thermal modulation higher than 50 mHz needs to be used in order to assume no heat losses by convection and to ensure the validity of Equation 2.21.

Finally, the monochromatic thermotransmittance coefficient (see equation 2.8) was also estimated using this method. This value gives valuable insights of the light matter interactions when a sample is heated. Such measurements have a great impact in physics to better understand this behaviour in the mid-IR range, a domain which was poorly studied. A recent publication from the group brought new insight on such behaviour ??.

²This proposed 1D solution does not give the value of δT_z^0 since only the heat flux is known. The full complete 2D solution needs to be solved for this. It has been done and can be found in [Bourges 2023].

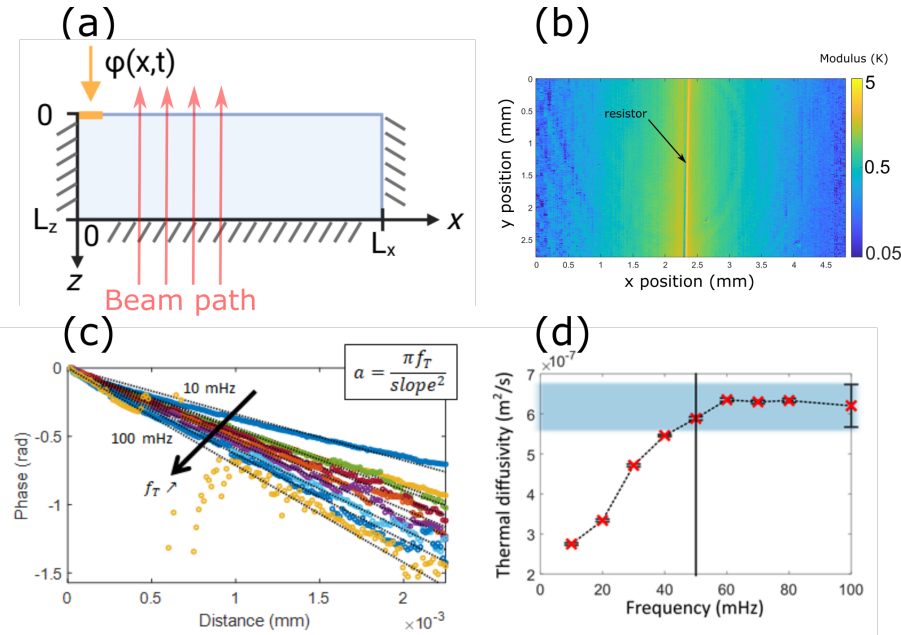


Figure 2.13: Processing the thermotransmittance signal. (a) Geometry used to model the heat transfers in 2D. (b) Average temperature modulus measured. (c) Phase shift measured for a range of temperature modulation (d) Heat diffusivity estimation from the phase for a range of temperature modulation.

Proof-of-concept of the thermotransmittance laminography

Once the principles of the temperature measurement based on thermotransmittance was mastered in 2D, it was translated to 3D cases. To do so, we use the property of average temperature measurements along the optical path and a thick sample with a thermal gradient in the depth.

The mathematical principles of the laminography are not recalled here, but can be found in detailed in C. Bourgès manuscript. Basically, laminography is an extension of Radon tomography where the sample is rotated and tilted on an axis not perpendicular to the beam path, as schemed in Figure 2.14(a) and (b). The thermal modulus is then measured for each position and a reconstruction algorithm is used to extract the 3D temperature fields from each 2D projection.

The first results of the 3D reconstruction of the thermal modulus are presented in Figure 2.14(c). Three different planes and slices show the temperature distribution. At this stage the data are still qualitative; only the distribution was reconstructed, not the magnitude. In addition, several artefacts, due to the presence of the resistor, are visible on the images. An important work on the inverse methods, and filtering techniques still need to be done to remove such artefact during the reconstruction. Last but not the least, a fundamental understanding of the laminography recon-

struction needs to be achieved to switch from the qualitative data presented here to a quantitative temperature distribution in the bulk of semi-transparent materials.

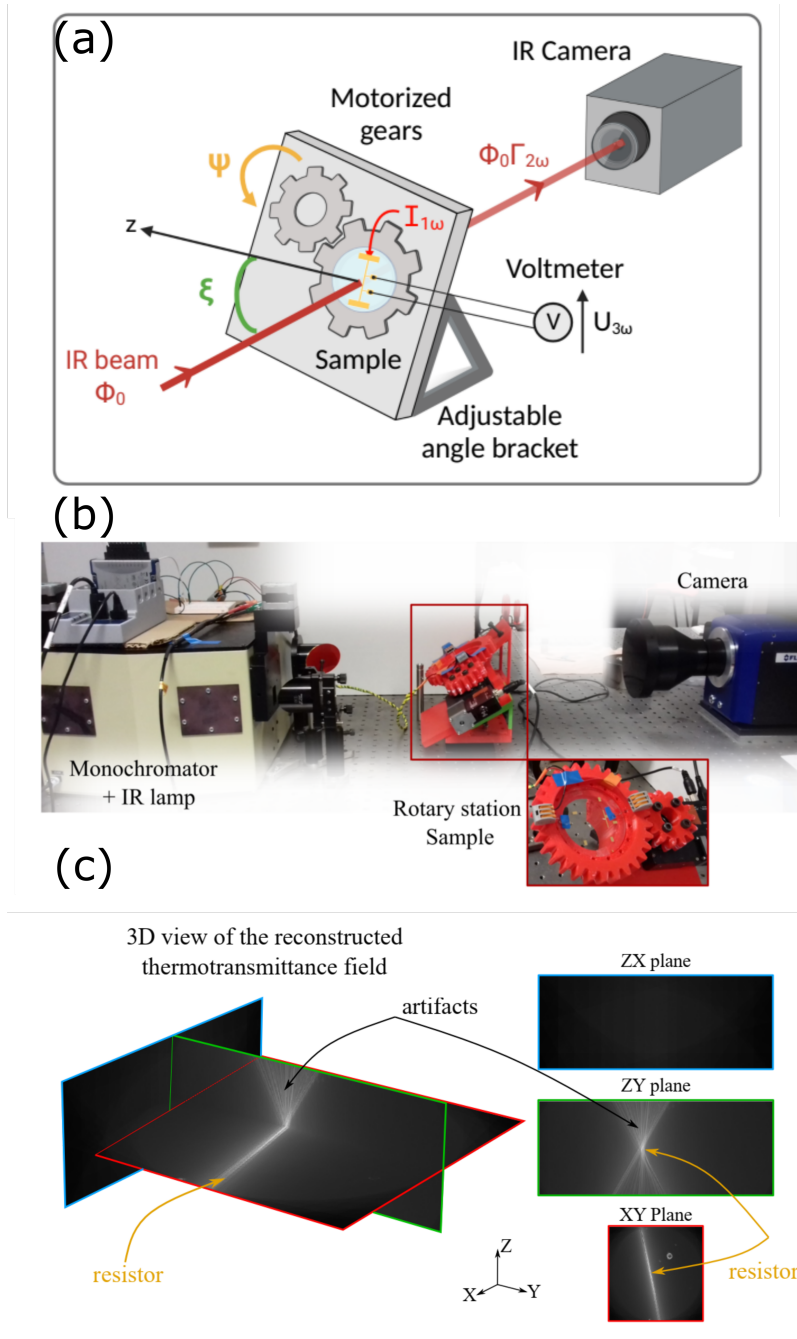


Figure 2.14: Reconstruction of 3D temperature fields based on laminography. (a) Schematic of the setup. (b) Photograph of the bench including the prototype of the rotation stage. (c) First results of the reconstructed thermotransmittance modulus.

2.4 Conclusions

This chapter has reviewed the main achievements made during the last 5 years in the domain of contactless methods to measure the heat and mass transfers. The state-of-art IR-based method were exposed and the main remaining challenges were addressed. In particular a need toward quantitative 3D imaging was pointed out since such goal was never achieve in my previous works. Temporal and spatial resolution were also limited to few seconds and few tens of $\mu\text{m}/\text{px}$ with our current setups. Nonetheless, since my arrival in 2018 and with the work of 4 PhD candidates from 2019 to early 2024, the following advances were made.

On the technological (or instrumentation) point of view, a microfluidic imaging platform has emerged to characterise both the concentration fields and the main transport/transfer properties. Two fully open and multispectral microscopes (one IR and one visible) were built and are now used routinely in the lab. The development of these tools was accompanied with an advanced data processing inherited from the TIFC team inverse method expertise. Strong collaborations with the chemistry laboratories (LOF and ICMCB) in Bordeaux were also tightened through these projects and are still undergoing.

On the fundamental side, a new methodology has emerged from these last five years was the development of a lock-in thermotransmittance imaging technique to measure both temperature and thermophysical properties in semi-transparent media. This work is quite original in the community and has a great potential to develop 3D imaging methods for semi-transparent media as demonstrated in proof of concept of thermotransmittance laminography. The development of this tool was also done in collaboration with the physics laboratory in Bordeaux (LOMA), and is now routinely used to measure the thermal property in semi-transparent in the TIFC team. Finally, to understand how these new developments can be transferred toward microfluidic energy conversion devices, a second chapter dedicated to my past works will summarise my main achievements to characterize these devices.

Energy transfer imaging in electrochemical systems: from X-rays to infrareds

Contents

3.1	Elucidating the two-phase flow transport in fuel cell GDLs	35
3.1.1	Fuel cell and electrolyzers working principles	35
3.1.2	X-ray synchrotron imaging	38
3.1.3	Two-phase flow modelling	40
3.2	Operando mass transport imaging in microfluidic electrochemical systems	43
3.2.1	Working principle of flow based electrochemical energy conversion devices	43
3.2.2	Characterizing the kinetics at the electrode/electrolyte interface in MFC	46
3.2.3	Probing the PEM hydration in microfluidic electrolyzers	50
3.3	Conclusions	53

This chapter describes my research applied to electrochemical energy systems, i.e. fuel cells & electrolyzers from the macro to the microscale. They were mainly focused on imaging transfers in such systems through the study of two phase flow transport in porous layers and the estimation of the main thermophysical parameters in microfluidic fuel cells and electrolyzers. IR imaging methods presented in chapter 2 and X-rays spectroscopy were applied to these electrochemical systems to make operando measurements of concentration and temperature fields.

3.1 Elucidating the two-phase flow transport in fuel cell GDLs

3.1.1 Fuel cell and electrolyzers working principles

PEMFCs are the main technology used in the fuel cell market. They include a Polymer Electrolyte Membrane (PEM) as electrolyte and separator between anode

and cathode. On each side of it, one can find the Gas Diffusion Layer (GDL) with a coated catalyst layer where the electrochemical reaction takes place. Finally, two channels on each side of the system feed the fuel cell with air and hydrogen (or water in the case of electrolysis). A schematic of these systems is proposed in Figure 3.1.

The particularity of these electrochemical systems is that there are multiples phenomena or transfers occurring at multiscales: from the sub-micrometer scale in the catalyst layer and membrane for the proton transport to the millimetre scale for the liquid water transport in the channel. Characterization methods used in my past works were adapted to these different scales.

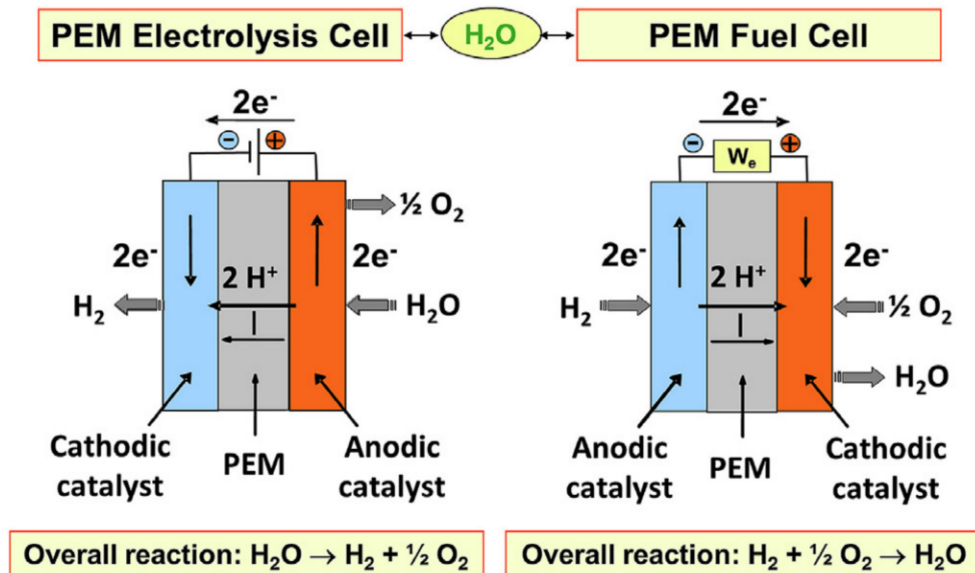


Figure 3.1: Schematic representation of PEM electrolyzer and fuel cell ([Lamy 2016])

In order to get the big picture of the impact of such transfers on the PEMFCs performances and thermophysical properties, a schematic of the main fuel cell component is depicted in Figure 3.2. The liquid water produced by the electrochemical reaction in the catalyst layer is used to humidify the PEM, but needs to be evacuated from the system in order to not clog the channel nor the GDL pores. An exhaustive list of the different phenomena affecting the fuel cell performances due to the liquid water is proposed in Table 3.1.

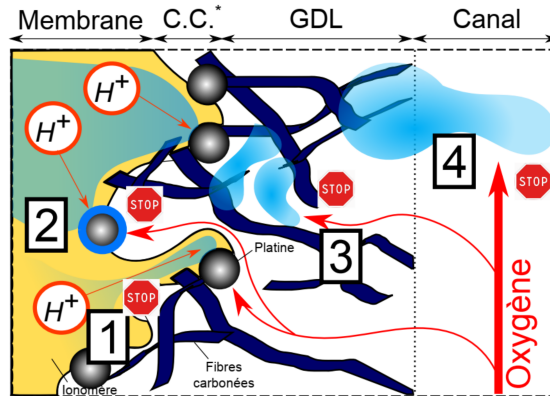


Figure 3.2: Schematic representation the impact of liquid water in fuel cells porous layers.

Num.	Description	Main parameters	References
1	Electrode drying leading to ionic conductivity decreasing. Proton transport is hindered.	Decrease of the electrolyte conductivity σ_e .	[Springer <i>et al.</i> 1991, Bernardi & Verbrugge 1991, Zawodzinski <i>et al.</i> 1993, Zawodzinski 1993, Weber & Newman 2004a, Weber & Newman 2004b, Colinart 2008]
2	Liquid water covers the catalyst, decrease the active surface.	Increase of the Tafel slope b , and decreasing of the exchange current i_0 .	[Bazylak 2009, Eikerling 2006, Siegel <i>et al.</i> 2004, Rao <i>et al.</i> 2007]
3	Liquid water fills the GDL pores, blocking the reactant access to the catalyst.	Decrease of the GDL porosity ε and mass diffusivity D .	[Pharoah <i>et al.</i> 2006, Litster <i>et al.</i> 2006, Chapuis <i>et al.</i> 2008, Liu <i>et al.</i> 2006]
4	Channel flooding blocking the reactant access to the catalyst.	Decrease of the effective channel cross section S_c , increase of the pressure drop ΔP , and decrease of the reactant velocity v .	[Bazylak 2009, Lee & Bae 2012, Barbir <i>et al.</i> 2005, Ding <i>et al.</i> 2013]

Table 3.1: Description of the different phenomena affecting the fuel cell performances (see the corresponding numbers in Figure 3.2).

From Figure 3.2 and Table 3.1, it can be understood that the two-phase flow transport (liquid water and gas - air or hydrogen) occurring in the GDLs, channels, catalyst layers and PEMs has one of the greatest impact on fuel cell performance. It can be a beneficial or a limiting factor for the system. In this context, operando imaging of the liquid water in all these layers was one of the main challenges I tackled during my research in Canada and my Marie Currie fellowship in Nantes University. The goal was to provide both a deep understanding of the two-phase flow mechanisms to optimize the fuel cell performances, and to provide operando diagnostic tools to help the liquid water mitigation. To do this, I was able to develop an experiment based on X-rays imaging, pore network modelling, and analytical modelling of fuel cell impedance [Chevalier *et al.* 2016b].

3.1.2 X-ray synchrotron imaging

Imaging methods based on X-rays were almost routinely used by several groups in the research community to probe the liquid water at the microscale in the different layers comprising a PEMFC [Shrestha & Bazylak 2023]. The working principles of this method is straightforward and it is schemed in Figure 3.3(a). A first X-ray image is taken before to start operating the fuel cell. This image is called background I_0 , see the grayscale image in Figure 3.3(b). Then, the fuel cell is operated and the current production results in liquid water production in the catalyst layer (i.e. by mass and charge conservation - given by Faraday law). This liquid water is then transported to the GDL and channels where it makes X-ray beam to be attenuated. Finally, this attenuation is linked to a liquid water thickness in the beam path, as modelled by the Beer-Lambert law 2.6. An example of the liquid water thickness measured during the fuel cell operation can be seen in Figure 3.3(b).

It has to be noted that such X-ray spectroscopy is similar to the IR spectroscopy developed at Institut de Mécanique et d'Ingénierie (I2M). Nevertheless, X-rays are high energy lights which are able to penetrate through thicker material and enable a better spatial resolution, down to the micrometer in the experiments I performed. The downside of this technique is the confined environment required to use X-ray: these experiments were only conducted at synchrotron facilities, for a limited beam time and in a close hutch, meaning that all the fuel cell operation needed to be done remotely.

Despite the great beam penetration of X-rays, fuel cell design needs to be specifically thought to perform successful imaging. The material thickness in the beam path were minimised to enhance the SNR, but also ensuring the leak proof of the cells. All the operating condition (flow rate, temperature, pressure, humidity) were also thoroughly controlled [Chevalier *et al.* 2016a]. Once all these technological challenges were lifted, many studies were performed to improve the fuel cell performance by controlling the two-phase flow transport.

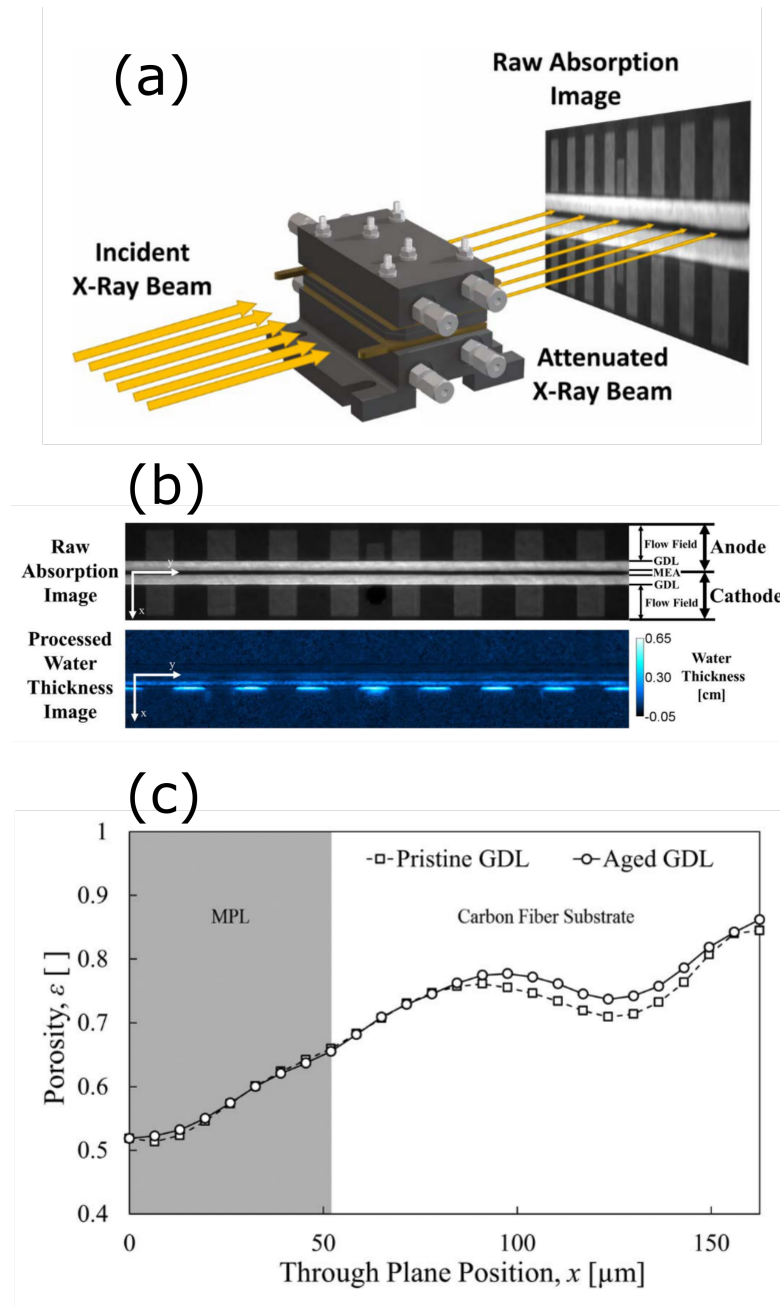


Figure 3.3: X-ray imaging method: in operando visualization of liquid water in PEMFC GDLs. (a) Fuel cells developed for X-ray imaging. (b) Background and liquid water images in the GDL. (c) Effective porosity measured in two GDLs after ageing.

Among all the works I carried out on this topic, one can cite the role of fibres size and orientation of the GDL. It was found that the ohmic resistance of the fuel cell is significantly increased with increasing inter-fiber distance.

It was also observed that the addition of a hydrophobic treatment enhances membrane hydration, and fibres perpendicularly aligned to the channel direction may enhance the contact area between the catalyst layer and the GDL [Chevalier *et al.* 2017a, Chevalier *et al.* 2017b]. The effect of GDL aging on porosity distribution was also conducted, see Figure 3.3(c), where micropore degradation were observed for the first time during fuel cell ageing. In total, during my two-year postdoc in Canada, I was able to perform more than ten studies to elucidate the role of the different fuel cell layers in the liquid water transport. The complete list of these publications can be found in chapter 9.

3.1.3 Two-phase flow modelling

Along with the images collected using X-ray, I have developed two main tools to study/understand the effect of two-phase flow transport on fuel cell performance. The first one, already developed in A. Bazylak's group is called Pore Network Modelling (PNM). Briefly, it consists in discretizing a 3D geometry of a porous media, i.e. a fuel cell GDL in Figure 3.4(a), into an equivalent 3D pores network. I participated to the development of this code during my postdoc, see [Chevalier *et al.* 2019]. The liquid water transport is then solved using basic invasion percolation algorithm to find the main liquid water pathways. The main advantage of such technique is the low computational cost: the liquid water breakthrough in a large scale (few mm³) 3D geometry can be solved in few minutes. It is far more efficient compared to the classical Computed Fluid Dynamic (CFD) technique which required high performance calculations. But such method provides only a global information (pore filling or not).

Applied to a GDL from a high temperature fuel cell, this methods enable to get a better understanding of the role of the microporous layers at the catalyst/GDL interface. The cracks in microporous layers act as preferential pathways for the liquid and enable to keep the catalyst layer hydrated (see the pink phase in Figure 3.4(c)). Such behaviour was clearly observed in the simulations performed using PNM and the ex-situ performance tests carried out on such high-temperature fuel cells.

At the macroscale, I developed a lot of methods to predict and understand the role of the two-phase flow transport on fuel cell performances. These works were done through the use of Electrochemical Impedance Spectroscopy (EIS) combined with a physical modelling of the fuel cell performance. These methods were developed during my PhD and applied all along my two postdocs, and for microfluidic electrolyzers testing during K. Krause PhD.

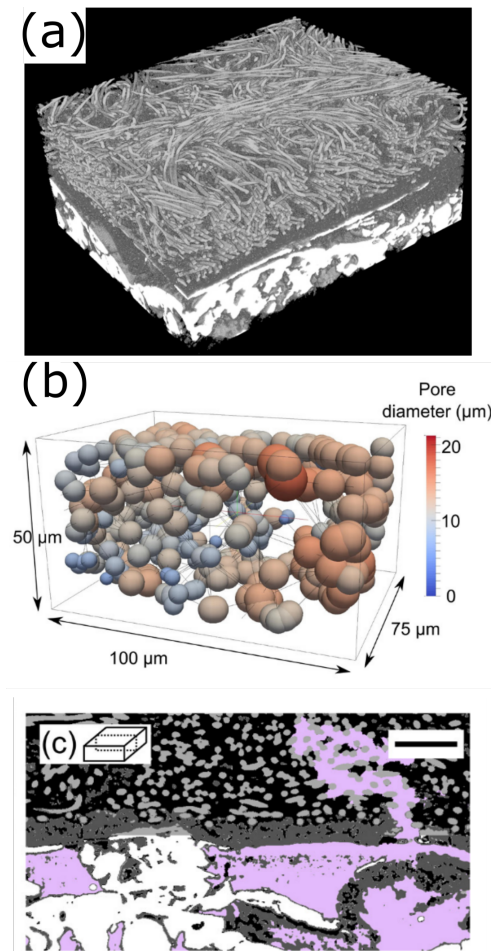


Figure 3.4: PNM of the two-phase flow transport at the pore scale. (a) GDL tomography of the fibers. (b) Equivalent pore network generated from the tomography. (c) Electrolyte invasion in the microporous layer and GDL in a high temperature PEMFC

The key element in the success of this methods was to be able to derive an analytical equation of the fuel cell frequency behavior which can be used in an inverse method algorithm. Such approach combining impedance and analytical models was at the onset of my research works, and it is very similar to what was developed in C. Bourgès PhD thesis to solve the modulated heat transfer in semi transparent media (see section 2.3.2).

The first steps to develop this analytical model was to identify the representation fuel cell geometry from the 3D structure to the 2D geometry (see Figure 3.5(a) and (b)). Then the transient transport equations: advection in the channel, diffusion in the GDL and electrochemical reaction in the catalyst layer were solved in Fourier

transform spaces using the following complex decomposition:

$$\underline{j}(\vec{x}, t) = j(\vec{x})^0 + \delta j(\vec{x}, \omega)e^{i\omega t} \quad (3.1)$$

$$\underline{c}(\vec{x}, t) = c(\vec{x})^0 + \delta c(\vec{x}, \omega)e^{i\omega t} \quad (3.2)$$

where \underline{j} and \underline{c} are the complex current density and concentration fields, respectively. Such fields are decomposed in a steady part, $j(\vec{x})^0$, and a modulated part, $\delta j(\vec{x}, \omega)$, to model the fuel cell frequency behaviour. By using this formalism, an analytical description of the low frequency impedance of the fuel cell was obtained by solving the advection-diffusion-reaction problem in fuel cell:

$$\tan \Phi = \frac{(1 - \lambda)(\omega + \lambda^* \tan(\omega/2)) + \omega^2/\lambda^* \csc \omega}{(1 - \lambda)(\lambda^* - \omega \tan(\omega/2)) - \omega^3/\lambda^{*2} \csc \omega} \quad (3.3)$$

where Φ is the impedance phase of the fuel cell measured by EIS and λ is the oxygen stoichiometry defined as the ratio between the air flow rate and the oxygen needed to produce the fuel cell current.

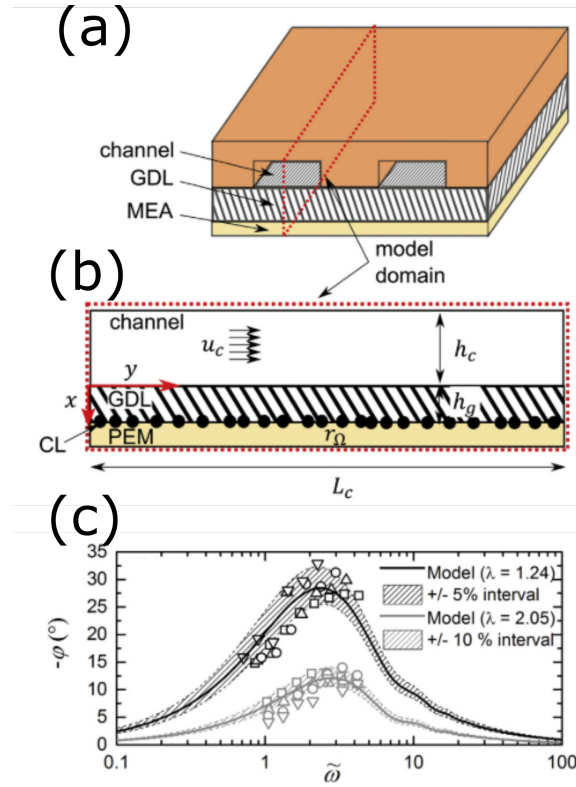


Figure 3.5: Macroscale characterization of the two-phase flow transport in PEMFC. (a) 3D Fuel cell geometry used to model the impedance. (b) 2D schematic of the transport phenomena. (c) Low frequency impedance used to detect channel flooding.

The details to obtain Equation 3.3 can be found in [Chevalier *et al.* 2018] and [Chevalier *et al.* 2016b]. Despite of the apparent complexity of equation 3.3, we

were able to show that a change of oxygen stoichiometry λ produces a phase shift on the EIS response. Therefore, when a liquid water flooding or drying in the GDLs and/or fuel cell channels occur, the oxygen stoichiometry is impacted and quantified by measuring the low frequency phase shift. Such scenario was successfully applied experimentally and the results are shown in Figure 3.5(c) for two oxygen stoichiometries.

To conclude, the multi-scale modelling of the effect of the two-phase flow transport in fuel cells was thoroughly investigated in my past research. At the micro-scale to elucidate the transport mechanism and the role of the different fuel cell materials. At the macro-scale to build diagnostic tool in order to prevent non optimized liquid water transport. The main outcomes of these research were modelling and imaging tools developed which are now used in several research groups in Canada, Germany, France... This is from these strong basis that I transposed the X-ray imaging methods and fuel cell modelling to IR-based imaging experiments applied to microfluidic fuel cells and electrolyzers.

3.2 Operando mass transport imaging in microfluidic electrochemical systems

The second important activity carried out at I2M since my arrival has been focused in elucidating the mass and charge transfer in microfluidic electrochemical systems. I was able to fund these activities through three main projects: an Agence Nationale de la Recherche (ANR) "Jeune Chercheuse, Jeune Chercheur" project, and two Centre National de la Recherche Scientifique (CNRS) Joint PhD program with the University of Toronto and more recently with Tokyo University.

Two main outcomes were achieved in the framework of these research. During M. Garcia PhD, a novel image-based method and model was developed to estimate the mass transfer in microfluidic fuel cell by measuring few μM concentration changes [Garcia *et al.* 2023b]. In parallel, in K. Krause PhD, and following my expertise of liquid water imaging using X-ray, a new liquid water electrolyzer designed for IR-based imaging was developed [Krause *et al.* 2023]. It has enabled to probe the liquid water content in PEM.

3.2.1 Working principle of flow based electrochemical energy conversion devices

Before to go in details concerning my main contributions to the fields, the main physical phenomena governing these flow based electrochemical energy conversion devices are described. Optimal designs of these devices depend strongly on the trade-off between the losses associated with multiple transport processes: advection and diffusion of reactants and products, migration of ionic species, and electrical

charge transport. A balanced assessment of the compromise between these losses is provided for a broad range of electrochemical reactors.

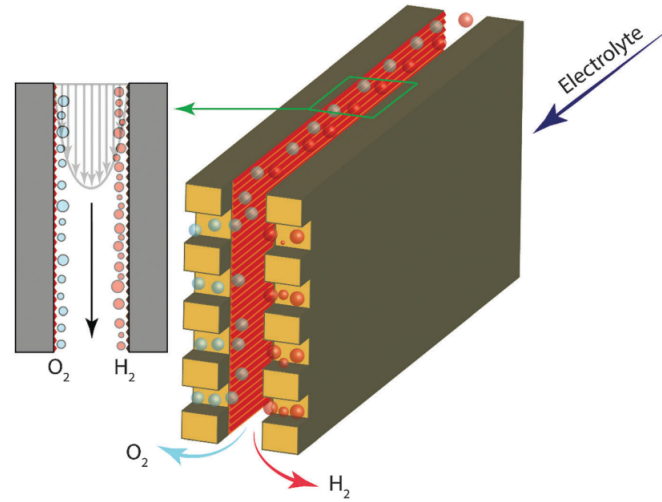


Figure 3.6: Schematic representation a membraneless microfluidic electrolyzers from [H. Hashemi *et al.* 2015]

Among several technologies, MFCs or electrolyzers have the advantage to be fabricated using microfluidic facilities and without any PEM as separator, reducing the complexity of these systems. MFCs are microscale systems used to convert the chemical energy contained in fuels directly into electricity [Kjeang *et al.* 2009, Lee *et al.* 2013], making these devices promising energy sources. Such devices are composed of a microfluidic channel that ensures rather good control of the hydrodynamic conditions. In the channel, two electrodes are embedded to enable an oxidation reaction at the anode and a reduction reaction at the cathode. Such MFC can be used both as fuel cell or electrolyzers, which makes this technology a promising candidate for energy conversion and storage. A wide variety of MFCs are present in the literature, and more details about them can be found in the following comprehensive reviews [Ibrahim *et al.* 2022, Zhou *et al.* 2021, Wang *et al.* 2021].

A schematic of a microfluidic electrolyzer is presented in Figure 3.6. In most systems, there are no porous layers in the microchannel making them easier to fabricate with the downside to make their performances highly dependant of the mass transport. To fully understand the relationship between mass transport and MFC performance, a deep look to the governing equation is necessary.

The main equations governing the performances of fuel cells and electrolyzers can be divided into three main kind:

- advection-diffusion of reactants in the microchannel:

$$\frac{\partial c}{\partial t} - \nabla \cdot (\vec{v}c + D\vec{\nabla}c) = 0 \quad (3.4)$$

where c is the reactant molar concentration, \vec{v} the velocity profile and D the mass diffusivity. This equation usually describes the transport in microchannel. Analytical expression of the velocity profile in microchannel can be found in [Bruus 2008].

- electrochemical reaction at the electrolyte/electrode interface

$$j(\vec{x}, t) = C_{DL} \frac{\partial \eta}{\partial t} + i_0 \frac{c}{c^{ref}} e^{-\eta(t)/b} \quad (3.5)$$

where j is the current density produced or consumed by the system, C_{DL} is the double layer capacity, η is the overpotential, i_0 and b are the parameters of the Tafel law modelling the electrochemical reaction. Using this equation assumes a plane catalyst layer working far from the Nernst potential.

- charge transport in the electrolyte

$$\nabla \cdot (-\sigma \vec{\nabla} \varphi) = 0, \quad (3.6)$$

where σ is the ionic conductivity and φ the electrolyte potential (different from the electrode potential). The ionic conductivity is usually a parameter which is barely known using theory but estimated for a range of operating conditions (temperature, concentration, humidity...).

These equations are usually solved in steady state along the channel [Braff *et al.* 2013] or in frequency domain to compute the electrochemical impedance since this latter is usually measured using classical EIS. Therefore, the performance of these electrochemical systems are investigated through the value of:

- the mass transfer parameters b and i_0 ;
- the mass transport D ;
- the electrochemical impedance $Z(\omega)$.

Associated with such model, imaging methods need to be developed to measure the concentration fields and therefore improving the parameter estimations. This is where the use of microfluidic has a great advantage since it enables the use of transmission spectroscopy from visible to IR as shown in chapter 2. Currently, IR imaging developments and its application for energy electrochemical system is hot topic [Sinton 2014], and I was able to bring two main contributions to this domain as described in the next sections.

3.2.2 Characterizing the kinetics at the electrode/electrolyte interface in MFC

The present study focuses on a coflow membraneless MFC [Choban *et al.* 2004] using formic acid (HCOOH) and potassium permanganate (KMnO₄). This system is relatively robust, is compatible with classical soft photolithography micro fabrication techniques, uses nonhazardous chemicals and is easy to operate [López-Montesinos *et al.* 2011, Salloum *et al.* 2008]. A schematic of this technology is presented in Figure 3.7.

A first theoretical study to establish the main equations governing the mass transfer was performed [Chevalier 2021]. In this work, I followed the same methodology used in heat transfers (and used during my PhD work): the solution was found in term of integral transform and a convolution product. Therefore, the concentration fields of a reactant, i.e. acid formic, in the microchannel of a MFC can be written as

$$\tilde{c}(\tilde{x}, \tilde{y}) = 1 + \tilde{j}(\tilde{x}) \otimes \mathcal{H}_j(\tilde{x}, \tilde{y}), \quad (3.7)$$

where $\tilde{j}(\tilde{x}) = j(\tilde{x})l_c/(n_e F D c_0)$ is the dimensionless current density distribution along the electrode, and \mathcal{H}_j is the impulse transfer function based on the distribution of the Dirac concentration flux, i.e. $d\tilde{c}/d\tilde{y}|_{\tilde{y}=0} = \delta(x)$. In the Laplace domain, this transfer function is defined as:

$$\hat{\mathcal{H}}_j(\tilde{p}, \tilde{y}) = \frac{2J_\alpha(\alpha e^{-\pi\gamma\tilde{y}/2})}{\sqrt{\tilde{p}}(J_{\alpha+1}(\alpha) - J_{\alpha-1}(\alpha))}, \quad (3.8)$$

and J_α is the Bessel function of the first kind and α th order. The mathematical details leading to this equation can be found in [Chevalier 2021]. This first result demonstrates the direct bridge that exists between the methods and tools developed to model heat and mass transfers. Using equation 3.7 enables in theory to estimate the current density field distribution from the measurement of the concentration by deconvolution method using the impulse response (a similar methods developed in the work of A. Aouali, see chapter 2). Equations 3.7 and 3.8 are here to illustrate the wide versatility of the analytical model developed during my works: from the mass transfers in MFC to heat transfers in semi-transparent media.

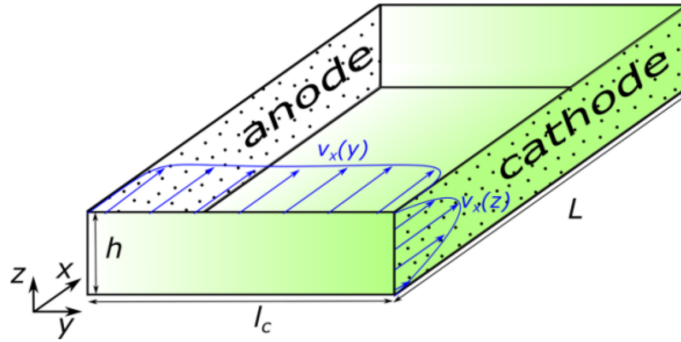
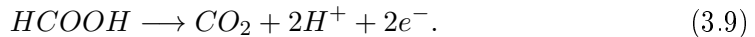


Figure 3.7: One example of a membraneless MFC with electrode deposited on side wall. Geometry used to develop mass transfer model in equation 3.8

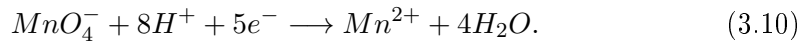
After modelling the main physical phenomena governing the MFC performances, a new setup was developed to measure the concentration profiles during the cell operation. This work was done during M. Garcia PhD thesis and led to the development of (i) a visible spectroscopic microscope (see Figure 3.8), and (ii) a MFC designed to image and model the concentration field. The expertise developed during my postdoctoral studies in fuel cell design and modelling was directly applied in this work.

As mentioned earlier, the reactants (formic acid and potassium permanganate) were chosen for their good performance [Kjeang *et al.* 2009] (few to hundreds mW/cm²). In addition, permanganate potassium has the advantage to have a clear light absorption at 540 nm in the visible range which allows the investigation of mass transport at the cathode. However, mass transport at the anode can not be studied since formic acid is transparent in the visible range. A specific study using IR was performed to image formic acid concentration, but it is not detailed in this manuscript, see ref [Garcia *et al.* 2023a].

Going deeper in MFC electrochemical reaction, formic acid oxidation at the anode is



Permanganate reduction at the cathode is



In equation 3.10, one can observe that when a current is produced, the permanganate ions (MnO_4^-) are transformed into manganese ions Mn^{2+} . Thus, the current applied through the MFC electrodes triggers a decrease in the permanganate concentration, which is measured by visible spectroscopy. It is also assumed that Mn^{2+} ions do not absorb light at the chosen wavelength, and that no CO_2 gas bubbles from the reaction are formed during the experiment. Such spectroscopic technique is similar to the ones used in X-rays or in

IRs, and the effect of current density production can be seen on concentration fields.

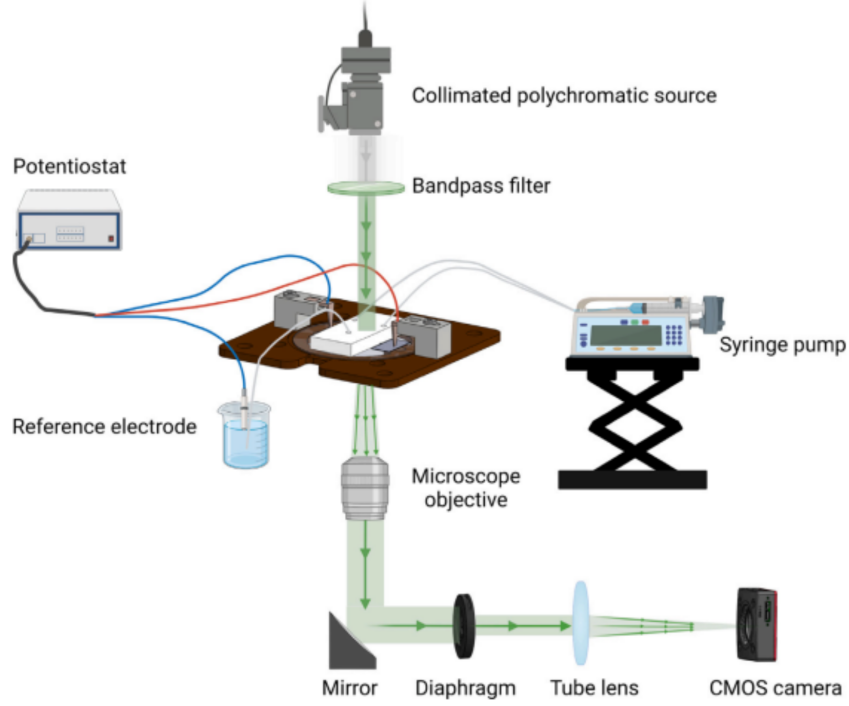


Figure 3.8: Schematic of the visible spectroscopy setup to image the concentration in MFC.

Two main results were obtained from this work. First, it was the first time that the molar concentration in an operating MFC was imaged around the electrodes: see Figure 3.9(a). It is worth mentioning that we were able to detect a concentration change of less than half mM using an house made microscope. An important work was done in image treatment (time and space averaging) and imaging setup optimization to achieve this goal.

The second main result obtained from this work was the quantitative estimation of the mass transfers properties in MFC: namely the mass diffusivity D and the reaction kinetic k_0 . The concentration field was modelled using a convolution product between the diffusive impulse response and the concentration at the electrode boundary, $y = e/2$, [Crank 1975] as

$$c(x, y) = \int_0^x c_e(x - x_0) \sqrt{\frac{\delta(y)}{\pi x_0^3}} \exp\left(-\frac{\delta(y)}{x_0}\right) dx_0, \forall y > e/2, \quad (3.11)$$

where $\delta = vy^2/(4D)$, e is the electrode width (in the y -direction), and $c_e(x) = c(x, y = e/2)$, is the concentration at the channel/electrode interface. This model is really fast to be solved (few ms) and enable to be used on the

3.2. Operando mass transport imaging in microfluidic electrochemical systems 49

large quantity of data collected through the images. After minimizing the norm of the difference between the data and the model, the parameter D and k were estimated for a range of operating current density (20 and 40 μA in Figures 3.9(b) and (c), respectively).

This first work has lifted numerous technological locks: the cell was entirely fabricated in house based on strong collaboration with chemist and physico-chemist from the neighbouring laboratory in Bordeaux. The acquisition chain was completely built from scratch and is now completely mastered. Therefore, this pioneer work open mainly opportunity to investigate different operating conditions (temperature, concentration, nature of reactants), catalysts (like Palladium) and microchannel designs.

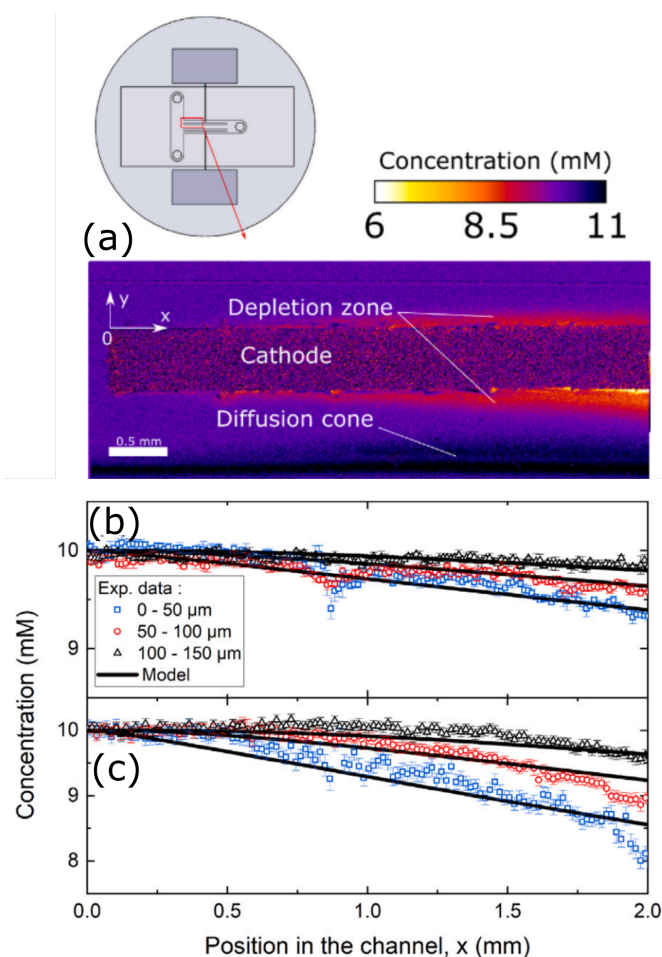


Figure 3.9: Operando concentration imaging in MFC. (a) Experimental concentration field of permanganate at the cathode. (b) and (c) Comparison between an analytical model and the experimental data after fitting the mass transfer parameters for two current density: 20 and 40 μA , respectively.

3.2.3 Probing the PEM hydration in microfluidic electrolyzers

In parallel to the development of the microfluidic platform, a collaboration with A. Bazylak's group (my former PI during my canadian postdoc) was initiated through the joint PhD program fund by the CNRS and the University of Toronto. The PhD thesis of K. Krause was at the heart of this collaborative work aiming at developing IR-based methods to image the charge transfer in microfluidic electrolyzers.

PEM electrolyzers are an attractive technology of energy storage when coupled with sustainable energy sources (e.g. solar and wind), as the excess electrical energy that is produced can be converted to chemical energy. However, the high material costs of PEM electrolyzers have significantly slowed their commercialization [Springer *et al.* 1991]. One solution to increase the commercial viability is higher current density operation, but this is accompanied with increased overpotentials and the risk of accelerating material degradation. Consequently, diagnosing the mechanisms that cause material degradation in the corrosive reaction environment will contribute to future optimizations and is essential towards realizing commercialization [Dai *et al.* 2009].

The PEM is the core component in water splitting electrolyzers, and utilizes perfluorosulfonate ionomers as a solid electrolyte to facilitate product separation (>99.95% product H₂ purity) and ion transport while being electrically insulative [Allen *et al.* 2015]. PEM research has also been focused on the inter-relations between its transport mechanisms, such as its water uptake (i.e. the number of water molecules per sulfonic acid site of the PEM), the electro-osmotic drag coefficient (i.e. the number of water molecules transported through the PEM per proton), and the protonic conductivity [Liso *et al.* 2015]. The comprehension and impact of such transport mechanisms have triggered extensive research efforts focused on characterizing the PEM in operating electrolyzers and fuel cells.

To answer this goal, a microfluidic PEM electrolyzer was developed specifically for membrane water content characterization. Membrane hydration is characterized via operando synchrotron FTIR spectroscopy in the through-plane direction relative to the membrane. The electrochemical performance and ohmic resistance of the electrolyzer are concurrently assessed over a range of temperature conditions and for two flow rates. The flow rates are intentionally selected to trigger cell failure through either ohmic or mass transport dominated losses.

Before to operate the electrolyzer using synchrotron FTIR spectroscopy, an important work was done during the fabrication of the IR transparent microfluidic electrolyzer. The choice of the material and the design was crucial to successfully probe liquid water through the PEM. As it can be seen in Figure 3.10(a) and (b) a chip made of silicon, PEM and PDMS was used with the channels side by side to let the beam crossing the PEM (see Figure 3.10(b)). The transmittance spectra of

3.2. Operando mass transport imaging in microfluidic electrochemical systems 51

each layer indicates that a fairly good transmission band can be found between 10.5 and 11.5 μm in the far IR range. This wavelength range corresponds to the far IR beamline from the Canadian Light Source in Canada. Beam time were asked and granted to this light source and a collaborative work was done with A. Bazylak's group and her students using this microfluidic electrolyzer.

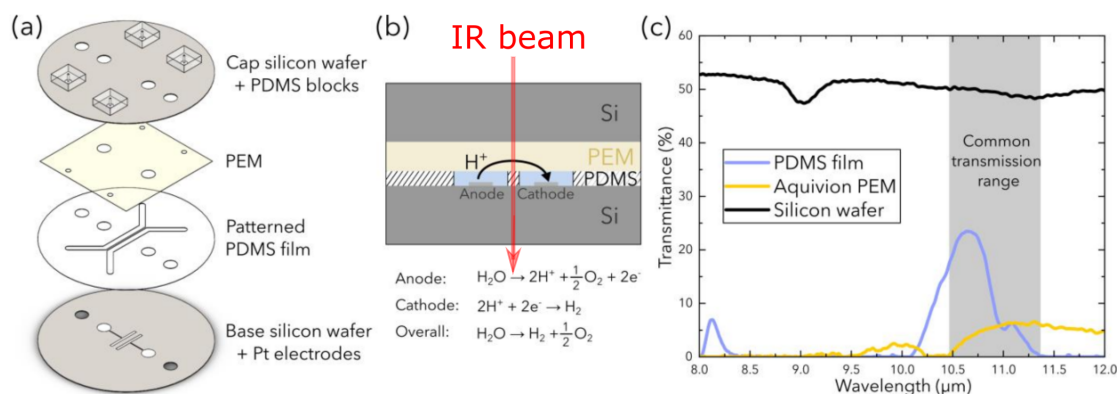


Figure 3.10: Microfluidic electrolyzers fabrication and properties. (a) Geometry. (b) Schematic of a slice. (c) Transmittance of the different layers.

The experimental setup built at the synchrotron far IR beamline is schemed in Figure 3.10(a). An IR beam from the synchrotron crossed the operating electrolyzer and the transmitted spectrum is obtained. The knowledge accumulated at I2M concerning the FTIR spectroscopy was of prime usefulness here to realise this experiment in a short period of time (144 h of beam time). A 2D view and a zoom on the beam location through the electrolyzer is proposed in Figure 3.10(b) and (c), respectively. In this case, only a local information in the middle of the PEM was probed.

The most interesting thing is this study is the change of IR beam signal in the 10-11 μm range induced by the membrane hydration. In Figure 3.10(d), one can observe that the increase of membrane water content results in a decrease of IR beam transmittance as liquid water absorbs more. Such signal is used in Beer-Lambert law to estimate the membrane water saturation as a function of different operating conditions: liquid water flow rates, temperature and current density (hydrogen production rate).

The main outcome of this study was to propose for the first time a direct probing of the membrane water content during the electrolyzer operation. From the first results obtained during the synchrotron campaign, it seems that the operating temperature has one of the greatest effects on the membrane water content. The water content increased with temperature from 20° C to 40° C, and then plateaued.

From the membrane hydration perspectives, it seems not necessary to increase the operating temperature above 50°C (see Figure 3.12(a) and(b)). The impact of operating flow rate was also visible in our measurement, but it was a bit less clear to establish general trend. More investigations need to be done to brought clearer conclusions.

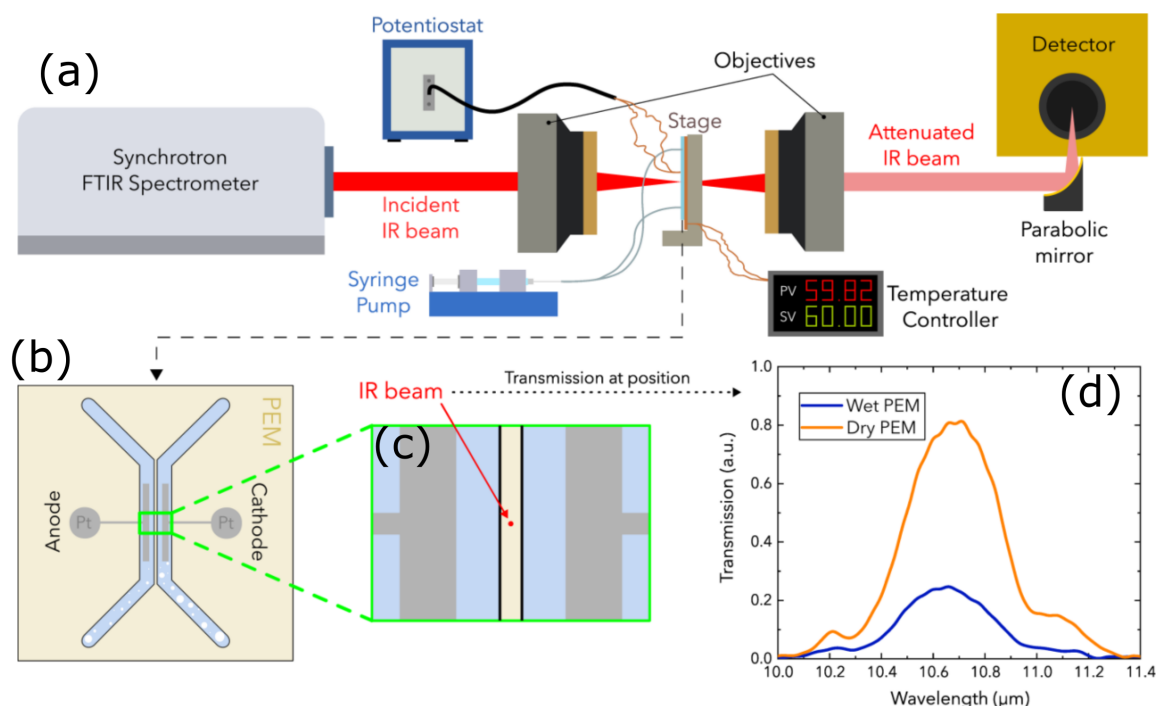


Figure 3.11: Synchrotron probing of the membrane hydration. (a) Experimental setup. (b) Top view of the electrolyzer. (c) Zoom in the area probed by the IR beam. (d) Typical signal recorded using FTIR synchrotron light through the membrane.

Despite the success of the electrolyzers fabrication and synchrotron campaign (done in December 2022), two downsides need to be mentioned as they will help to build the perspectives of this work. First, the particular cell geometry used imply a thick proton pathway from anode to cathode. It results that the electrolyzer ohmic resistance (measured by EIS) is ten times larger than the state of the art. Second, it appears that probing only one local information in the middle of the membrane hide the heterogeneities in the mass and charge transfer observed during the electrolyzer operation. In particular at low flow rate, where oxygen and hydrogen bubbles produced by the reaction get stuck in the channel, blocking locally the proton transport. Studying such heterogeneities would be of prime interest to be studied and to evaluate their impact on the local membrane water content. Therefore, the continuation of the synchrotron experiment using our IR imaging platform is the next goal.

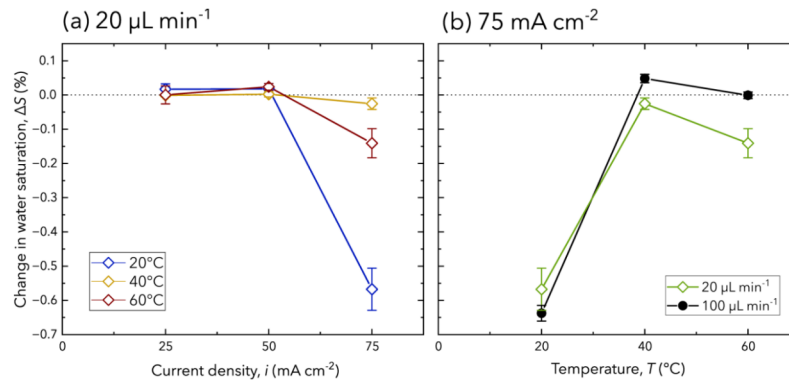


Figure 3.12: Results of the membrane water content measured in term of saturation. (a) For 3 operating temperatures. (b) For two liquid water flow rates.

3.3 Conclusions

In this chapter, the recent advances in imaging and modelling the mass transfer in fuel cell and MFCs were presented. From these last ten years of research on this topic, great achievements in term of imaging techniques and cell designs were achieved. In particular, it was demonstrated that it is possible to use IR imaging method to probe the mass transfer in PEM or visible light to image the concentration fields in MFCs. But at the cost important compromises on the cell design and choice of the reactants. From X-rays to IRs, microfluidic cells were always design to mimic the real technology but with the constrains to ensure good imaging of the heat and mass transfer fields. Such comprises are even stronger to find using IR light since it is much weaker compared to X-ray.

Once the engineering aspects in the cell design were solved, it was possible to obtain very promising results that would help to deepen our knowledge of the mass transfer in operando electrochemical systems. One can remember the liquid water probing in PEM and the concentration fields measurements in MFC. These works were quite original in the TIFC team, bringing a lot of new applications motivating fundamental research development in our IR imaging setups.

The two projects which have fund these research and K. Krause and M. Garcia PhD thesis end in early 2024, but many short term perspectives has already emerged. Concerning the molar concentration field imaging in MFC, the combination of EIS and visible spectroscopy is undergoing to perform lock-in spectroscopy. It is very similar to the method developed in C. Bourges PhD thesis where a current density modulation makes a concentration modulation which significantly increase the SNR. Concentration amplitude in the order of few μM were detected which opens a lot of perspectives to analyse the local current density distributions at the interface electrode/electrolyte. This aspect is detailed in the research project.

Another direct perspective concerning the electrolyzers work is, as mentioned, to make local measurement by using IR imaging spectroscopy. The tunable filter band setup described in chapter 2 will be used to investigate the membrane water content. The major change compared to the synchrotron campaign is that the electrolyzer transmittance is reduced in the 2 - 5 μm range of our setup. An important image treatment based on a lot of image averaging will have to be done to achieve a good SNR in the measurement. The first results obtained have shown that it will be possible to make it. The transient regime of the water diffusion through the PEM will also be investigated. Still using the inverse method inherited from the heat transfer, the mass diffusivity of liquid water through the PEM will be investigated for the first time for a large range of operating conditions (temperature and flow rate).

Finally, on the funding side, these two projects will be continued by hiring one post-doctoral candidate and one PhD candidate in the group. A Carnot ARTS funding from Arts et Métiers group fund a 18-month post-doctoral candidate to perform a PEM ageing study using our setup. Ageing model of the PEM needs to be integrated in a numerical twin to predict the fuel cell and electrolyzer rest of life. A second French-Japanese project will fund a PhD candidate to pursue the development of MFC using other organic reactants and a larger diversity of catalyst compounds. Here again, both IR and visible spectroscopic platforms will be used to quantitatively assess the performance of these new system. The starting collaboration with Minami's group in Tokyo will be of great help to improve the microfabrication of the cells.

Research project

Contents

4.1 Thermal tomography in solid heterogeneous media	56
4.1.1 Optothermal models in multilayer materials	56
4.1.2 Improved SNR by using laser sources	58
4.1.3 3D temperature measurements in heterogeneous media	58
4.2 Thermal super-resolution imaging	60
4.2.1 Temporal approach	61
4.2.2 Spatial approach	61
4.3 Applications	63
4.3.1 OptUseH2 project: PEM degradation assessment in microfluidic electrolyzers	63
4.3.2 SMARTBAT project: heat and mass transfer characterization in microfluidic redox flow batteries	64
4.4 Timeline	67

As it was summarized in the previous chapters, important milestones were reached with successful mass transport measurements in microfluidic electrolyser PEM using IR spectroscopy or bulk temperature measurements in dielectric materials at the microscale using thermotransmittance. The first proofs of concept toward 3D imaging were achieved yet any quantitative data were measured or reconstructed. However, my past research have reached now the needed maturity to move toward IR-based tomography at the microscale. This strong need is motivated by the latest developments of microfluidic electrochemical energy conversion devices started more than 20 years ago [Ibrahim *et al.* 2022] which need to be accompanied by more sensitive measurement techniques in 3D and at the microscale or beyond. The following research project aims at answering these goals.

In this frameworks, my future research will be focused on the following aspects :

1. how to measure 3D thermal fields at the microscale in heterogeneous semi-transparent media? A fundamental understanding on how the transmitted light is impacted by thermal and concentration gradients will be investigated at first, and inverse methods based on diffusion deconvolution and image processing will be developed.

2. how to image beyond the diffraction limit? The fundamental limitation of IR spatial resolution (i.e. 1 to 10 $\mu\text{m}/\text{px}$) will be overcome using a combination of laser-based imaging methods associated to inverse methods to reconstruct super resolution images.
3. how to apply the microscale thermal tomography to microfluidic electrochemical energy devices? A combination of specific microfluidic chip design engineering and analytical modelling will be derived to make heat and mass transport characterization in these devices.

A roadmap to answer these questions is proposed in this chapter with a main focus on two fundamental aspects: the development of thermal tomography, and image super resolution for IR imaging setups. Two applications of these fundamentals works for microscale energy conversion devices will be presented in the third section. Finally, a timeline is proposed in the last section.

4.1 Thermal tomography in solid heterogeneous media

Temperature measurements in semi-transparent media are still a hot topic. Many applications like flames, crystals, microfluidic, semi-conductors... require a deeper knowledge of their inner temperature to improve their operating conditions and/or design. Following this path, this part of my research project is a direct continuation of the works initiated in A. Aouali [Aouali 2022] and C. Bourges [Bourges 2023] PhD thesis. The idea here is to develop a methodology to reconstruct a 3D thermal fields at the microscale in a heterogeneous solid medium. Several funding sources, PhD thesis and post-doctoral candidates have been already secured to pursue in this direction at the short term (3/4 years).

4.1.1 Optothermal models in multilayer materials

The key to access temperature fields in semi-transparent media is the knowledge of the thermotransmittance coefficient κ . At first order, it links the light intensity variation $\Delta\Gamma$ to the average temperature of the medium as:

$$\frac{\Delta\Gamma}{\Gamma_0} = \kappa\Delta T. \quad (4.1)$$

However, as it was demonstrated in [Bourges 2023], this simple approach needs to be completed in the case of thick material with non uniform temperature distributions. In this case, it depends on both the light absorption and reflection as schemed on Figure 4.1.

Taken into account these phenomena have led to a first opto-thermal model

([Bourges 2023]) developed as

$$\frac{\Delta\Gamma(T)}{\Gamma_0} \approx - \underbrace{\frac{R_0\kappa_R}{1-R_0} [\Delta T_1 + \Delta T_2]}_{\text{reflectance}} - \underbrace{\alpha_0\kappa_\alpha \int_0^{L_z} \Delta T(z) dz}_{\text{absorbance}}, \quad (4.2)$$

where the absorption and reflection contributions of the light can be derived. This opto-thermal model brought the following key insights to develop a thermal tomography:

- the absorbance contribution depends on the temperature average along the beam path in the semitransparent media. This property is the key for 3D measurements as changing the beam path in the sample will change the absorbance measured and then inform on the 3D temperature fields.
- the reflection contribution at the interfaces must be taken into account in order to eliminate the bias in reflective materials.
- a coupling between interface temperature and average temperature over material thickness exists, enabling to extract an information on buried interface temperature (if this latter is reflective, see Figure 4.1) in multilayer materials.

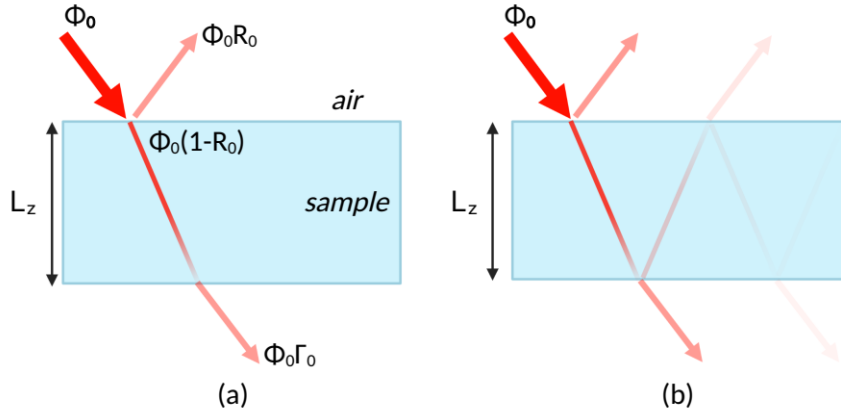


Figure 4.1: Beam path in a semi-transparent medium. (a) for a one reflection. (b) in the case of multiple reflections.

In our past works, samples were carefully chosen to neglect the contribution of reflection on the transmitted light [Bourges *et al.* 2023], but moving forward, new measurements are undergoing to discriminate the contribution of absorption and reflection in the transmitted light. This question needs to be answered to address the thermal tomography of thick of bilayer materials, comprising for example two semi-conductors.

4.1.2 Improved SNR by using laser sources

The second challenge to develop this technique is the improvement of the SNR during thermotransmittance measurements. The signal obtained is, as mentioned earlier, very low, i.e. $\kappa \sim 10^{-3} - 10^{-4} \text{ K}^{-1}$, and may be even decreased by adding a new layer of thick material. The weakness of the signal comes from the sample absorption, the localisation of the thermal sources and low optical power of the sources currently used in all our imaging setup: a heated globar (like silicon nitride globar) has monochromatic optical power ranging from 20 - 200 W/m². In our past works, see chapter 2, the weakness of the transmitted signal measured by IR cameras was compensated by using advanced signal processing techniques, such as in the case of lock-in thermotransmittance, but it is also possible to play with the heating or IR sources to improve the SNR.

Recent IR lasers and black body sources may help to gain one order of magnitude in terms of SNR. New laser sources [Rosas *et al.* 2023], enable to reach optical power around 10 kW/m². In addition, by selecting the appropriate wavelengths, such lasers can be used as buried thermal sources enabling a better heating of the materials and therefore increasing the light intensity variation. In the case of multiples substrate layers, which generally cover the sample like in microfluidic chips, selecting the laser wavelength can enable to heat specific area of the sample. On the side of the black body sources, new high-power IR emitters have proved a significant increase in multispectral IR sources (see Throlabs HPIR102). Thus, a close work with J. Maire (CNRS researcher) in our research team is undergoing to develop improve the capability of our experimental setup with the goal of improving by a factor of 10 the SNR.

Lasers and high-power IR emitters would also let more flexible source modulation, fast impulse excitation (down to the ns), and used more localised IR sources for the development of super resolution imaging (as developed in biological imaging by the group of [Betzig *et al.* 2006]). In particular, signal processing based on the double laser and black sources modulation is expected to facilitate and accelerate the measurements by making the mechanical chopper obsolete (see Figure 2.3). Such improvements in our setup would be one of the key to develop super resolution imaging, as it will be discussed in section 4.2.

4.1.3 3D temperature measurements in heterogeneous media

As seen in equation 4.2, the temperature average along the beam path in semitransparent media is the key for 3D measurements as changing the beam path in the sample will inform on the 3D temperature fields. Although, the physical principles to answer this goal have already been described by an optothermal model, several development in signal processing, inverse methods and modelling are still needed before reaching such 3D imaging.

In chapter 2, the proof of concept of thermal laminography obtained at the end of C. Bourgès PhD thesis [Bourges 2023] was established. 3D imaging measurements were obtained in terms of qualitative (or normalised) thermal fields. Similarly, the inverse methods used in my past works, such as inverse Radon transforms (in [Aouali 2022]) or retro projection methods in laminography, have lost the quantitative nature of the 2D fields. Usually, such tomographic techniques are used to create binary images, i.e. solid or void, and the signal processing community is more focused on the artefact elimination rather than the quantitative reconstruction of the fields.

Therefore, the next step is to move forward from qualitative topological reconstruction to quantitative fields reconstruction (temperature at first and concentration in the case of microfluidic applications). An important mathematical work concerning the definition of integral transforms (Fourier, Radon...) applied to images need to be done to achieve such goals. In the same way, quantitative data will require an accurate calibration of the multispectral thermotransmittance coefficients and all the laser sources (both in term of spatial distribution and intensity). Several solutions already exist in literature [Ozenne *et al.* 2023b], but they were never applied to IR spectroscopy for measuring 3D temperature fields. Far from the idea of reinventing the wheel on this topic, current reconstruction algorithms existing in the literature or public repository such as *Git-hub* will be used to target this goal.

Several routes are considered to be used in our case. Among them, stochastic algorithms based on Bayesian inferences will be proposed to reconstruct the most likely temperature fields from the projection [Venkatakrishnan *et al.* 2017], since the shape of the thermal fields is usually well-known based on modelling approaches (see the opto-thermal model developed in [Bourgès *et al.* 2023]). Such technique has already been used successfully to improve noisy time-resolved tomography [Myers *et al.* 2015]. Complementary, deterministic algorithms based on Fourier transforms are also under studies to keep the quantitative information of the 2D projections [Voropaev *et al.* 2016]. Such algorithms will be implemented in strong collaboration with CNRS researchers from the group, J. Maire and M.-M. Groz who have a greatest expertise in inverse problem and Bayesian inference [Groz *et al.* 2021]. A postdoctoral candidate co-supervised by this team is being hired.

Last but not least, to accompany the fundamental methodological works, technological developments regarding the rotation stage need to be done to have somewhat reliable stage for 2D and 3D measurements. This work is already undergoing and a new rotation stage is being fabricated within the next 6 months. A prototype was already designed as depicted in Figure 4.2. The budget for this rotation platform has already been secured.

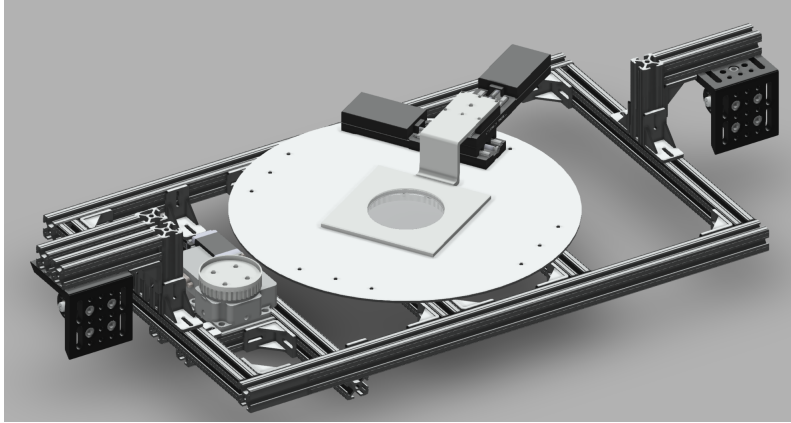


Figure 4.2: Design of the new rotating stage under fabrication for thermal laminography.

4.2 Thermal super-resolution imaging

Currently, the imaging setups used to characterize heat and mass transfers rely on IR cameras and sources using wavelengths from 2 to 10 μm . Such specification introduces an optical limit which is roughly $\lambda/2 \sim 1 - 5 \mu\text{m}/\text{px}$ when an objective with a large magnification is used. This means that even with the best optical setup, a pixel resolution lower than 1 μm would unlikely be reached without any specific signal processing. This physical limit of IR imaging hinders the use of our current imaging technique for biological tissues, thin membranes, or catalyst materials containing usually sub micrometer elements (cells, micro-pores, particles...).

The subject of thermal super-resolution has become a central topic in the research team (TIFC). Recent publications of the group have shown that at the microscale, nanoscale features in solid materials cannot be resolved (see [Mateos-Canseco *et al.* 2023]), or the thermal resolution in 3D medical imaging methods is still currently insufficient to well-resolved some human tissues [Ozenne *et al.* 2023a]. Another work in the group, [Groz *et al.* 2024], have shown that at the macroscale, small defects in large sample are usually not detected during NDT experiments. For all these reasons, the entire research group have started to collaborate to seek for new solutions to break down our instrumental spatial resolution limited either by optical systems or diffraction limit. A collaboration with other groups at I2M such as in acoustic department will also be done since they have similar issues using ultrasounds imaging [Burgholzer *et al.* 2017b].

4.2.1 Temporal approach

The first published work from our research group relies on the temporal resolution of the camera to improve the spatial resolution of the images. To enhance the resolution, a laser spot with a diameter smaller than a camera pixel was used and displaced on the sample surface [Groz *et al.* 2024, Batsale *et al.* 2023]. The key of the method stems from the algorithm used to process the sample thermal response. By analysing it with wavelet transform along with the laser position within the camera pixels, this method achieving thermal super-resolution. It was possible to detect defect twice smaller than the pixel size.

Such approach has the great advantage to use our classical thermographic setup on opaque materials. However, switching to semi-transparent material would necessitate to perform temperature measurements using thermotransmittance. Therefore, it makes the super resolution approach much closer to classical imaging methods using transmitted visible light. This aspect of the problem may be viewed as an advantage as most of the techniques already developed in optical imaging using visible light may be applied to thermal measurements using IR lighth. This aspect of the measurements was never treated in the literature and will be proposed in my research project.

4.2.2 Spatial approach

Going beyond the diffraction limits (or Abbe diffraction limits) in microscopy is an old trick. Plethora of papers describing hardware and data processing methods can be found in visible, electronic, or X-ray domain, mainly driven by the biomedical applications with important breakthroughs obtained in term of spatial resolution (see for example one of the last Nobel prize awarding this topic [Betzig *et al.* 2006]). Applied to IR domain, these methods were less developed, but recent publications on super resolution for chemical microscopy [Yeh *et al.* 2023, Tang *et al.* 2023] have shown the increase interest for such wavelengths. In particular, the development of IR lasers for thermal measurements [Lee *et al.* 2019, Gaverina *et al.* 2017], enable to produce very local heat source which are at the heart for super-resolution microscopy [Betzig *et al.* 2006].

A super-resolution problem can be written in general form as:

$$Im_M = (Im_R \cdot \rho) \otimes PSF + \varepsilon \quad (4.3)$$

where Im_M is the low resolution image obtained by our camera, Im_R is the super resolution image, ρ the illumination function, PSF is the image impulse response function (also called point spread function) and ε is the noise. Thus to reconstruct Im_R from Im_M imply to know or to identify ρ and PSF .

To achieve super-resolution imaging, the fundamental idea is to have objects (heat sources, light sources, chemical sources, structures) in the material

smaller than the pixel resolution, typically $< 1 \mu\text{m}$. Then multiple images are recorded where these sources are moved. The key idea behind this method is somehow to reconstruct the *PSF* by introducing high spatial frequencies (unit m^{-1}) in the signal. Such methods are based on localized heat source reconstruction using thermal impulse response or random illumination sources [Chen *et al.* 2023, Mudry *et al.* 2012], a topic well mastered in the team, such as in the last work of A. Aouali's PhD [Aouali *et al.* 2021]. Such impulse response can be either analytically computed or estimated from measurements [Battaglia *et al.* 2000]. Therefore, tackling this problem can be seen as an extension of the well know-how of the group in inverse methods and IR image processing. This work will be accompanied by all the task force from the TIFC team since it can be applied to all our applications.

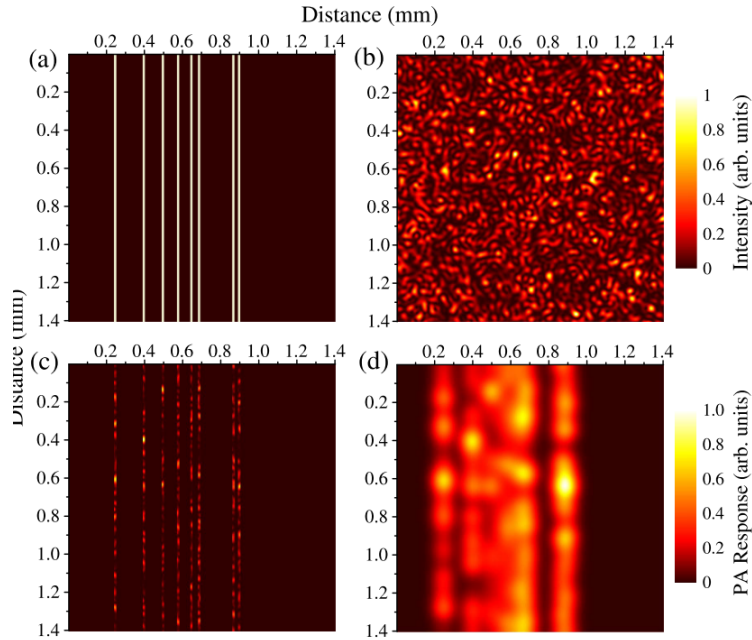


Figure 4.3: Super-resolution images based on speckles effect using IR lasers, from [Murray *et al.* 2017]. Top left: ideal image. Top Right: random illumination. Bottom left: super-resolution images. Bottom right: image obtained using no processing and uniform illumination.

In practice, a PhD student co-supervised by J. Maire and J.-L. Battaglia has started to implement a method using localized laser heat sources in a medium (generated by laser speckles or diffracting slits, [Burgholzer *et al.* 2017a]), and to record the images using our IR camera (spatial resolution of $15 \mu\text{m}/\text{px}$). A methodology similar to the one schemed in Figure 4.3 will be followed at first with an expected gain between 2 and 5 in spatial resolution. At the end, we hope to implement this technique with thermotransmittance in semi-transparent objects at the mi-

crosscale (such as in small supercapacitors or microelectronic devices studied by J. Maire [Sandell *et al.* 2020]). In the end, the combination of 3D quantitative reconstruction algorithms, super resolution processing will lead to a new microscopic tomography for temperature fields in semi-transparent media. Such new tool will find a direct application in microfluidic devices as described in the next sections.

4.3 Applications

4.3.1 OptUseH2 project: PEM degradation assessment in microfluidic electrolyzers

This long term project (5 years) is directly an application of the results obtained in K. Krause PhD with the development of microfluidic electrolyzers. They have been used as a seed to apply for funding at Carnot ARTS agency to build an ageing platform for hydrogen systems. In collaboration with five partners and laboratories from the Arts et Métiers group, the idea is to predict the ageing behaviour, degradation rate, and durability of several components of the hydrogen chain. The advantage of microfluidic is clearly visible in such long term operating studies. For instance, a classical fuel cell system of 1 kW operating over 1,000 h will consume around 60 kg of hydrogen¹. A single pressurised bottle contains 1 kg of hydrogen at a cost ranging from 30 to 50 €/bottle regarding the purity². Therefore, ageing a 1 kW PEMFC stack over 1,000 h will cost 60 bottles of hydrogen and between 1,500 and 2,500€. In contrast, by consuming only few mg of hydrogen, microfluidic technologies will significantly decrease these costs and makes the safety standard around the experimental benches easier to apply compared to the classical large scale fuel cell and electrolyzer systems.

An 18 months post-doctoral candidate will start in 2024/2025 to operate the microfluidic electrolyzers already built (see section 3.2.3) and study the performance degradations over time under several loading and thermal stresses (basically continuing K. Krause's work for long term monitoring). It is expected to focus on the study on the PEM degradation using our IR spectroscopic setup. Used in combination with the electrochemical characterisation based on EIS, changes in PEM chemistry, i.e. sulfonic group density, and water content will be followed over time and if possible quantified. Such results will follow current research on this topic from [Böhm *et al.* 2019], and crack apparition in PEM, see [Wei *et al.* 2023]. The degradation mechanisms will then be modelled using empirical law and integrated through a prognostic tool developed by our partners in Paris (the Procédés et Ingénierie en Mécanique et Matériaux (PIMM) and Laboratoire d'Ingénierie des Fluides Système Energétique (LIFSE) laboratories).

¹ $q_{H_2} = PM_{H_2} / (E_{cell} n_e F) \times t$ where $E_{cell} \approx 0.6 - 0.7$ corresponding to an electrochemical yield of around 50%

²based on the cost of compressed hydrogen in B50 bottle at 200 bar from Messer, given in December 2023.

At the end of it, it is expected to report the first ageing studies of PEM electrolyzers. During the two years of the project, the current IR spectroscopic setup will be used without any post-processing for super resolution, tomographic aspects nor thermal measurements based on thermotransmittance. Thus, the second step after would be to implement these new possibilities to measure and quantify the degradation mechanisms at the sub-micrometer scale. In particular, it would enable to study the degradations in catalyst layer. However, to reach this target, new PEM microfluidic fuel cell would have to be microfabricated which implies to solve numerous challenges in term of fabrication, like ensuring an hydrogen proof chip including carbon based catalyst layers. Therefore, both the effort in term of chip fabrication will have to be pursued, through tightened collaborative projects with physico-chemistry labs (Laboratoire du Futur (LOF), Institut de Chimie de la Matière Condensée de Bordeaux (ICMCB), Laboratory for Integrated Micro-Mechatronic Systems (LIMMS),...), and the development fundamental research for IR based imaging methods.

A last side effect in the development of such microfluidic platform is the link with my teaching activities. Arts et Métiers asked for more transverse projects between research and student training. Then, the proposed platform can be seen as one appropriate answer. It will be a unique tool for engineering student to practice basic electrochemical tests, energy assessments on small systems, and energy transfer imaging using state-of-art measurement methods. Such microfluidic and energy conversion lab class is particularly well suited since these experimental platforms are easy to maintain at relatively low cost. It is also in line with the "Hydrogen Program" supported by Arts et Métiers in which I am involved (I am in charge of the fuel cell course given to the fifth year Arts et Métiers students). Thus, this research activity will keep feeding my lectures through practical activities to train new generation of student on electrochemical energy conversion systems.

4.3.2 SMARTBAT project: heat and mass transfer characterization in microfluidic redox flow batteries

The SMARTBAT project is a direct continuation of M. Garcia PhD work. It is a collaborative work project funding by CNRS and Tokyo University in the framework of a joint PhD program. It consists in developing new redox flow batteries in which the concentration at small scale will be measured based on IR transmission spectroscopy and compared to the measurement carried out by extended-gate type organic transistors developed by Tokyo University. This collaboration, with two PhD students starting in early 2024, will establish lock-in IR spectroscopy as a new methods for microscale concentration measurements. It is also an opportunity to extend the thermal measurements based on thermotransmittance to microfluidic to measure the heat sources produce by the electrochemical reaction. These work and this project in particular will be followed by a research sabbatical year (2024/2025)

at LIMMS laboratory in Tokyo (research project submitted and under review when these lines have been written).

4.3.2.1 Lock-in concentration measurements

As mentioned in my past works in the last chapters, contactless methods to measure temperature and concentration fields in such applications require still more development. In particular, state-of-art methods using IR transmission to measure concentration fields are limited to concentration variations of few millimoles. Therefore, with the need for microsystems, heat and mass transfers at microscale require the development of methods measuring low concentration level (μmol) under thermally controlled environment using IR camera or FPA. Such work is completely similar to the thermotransmittance where it uses source modulation to be detect very small change in the signal.

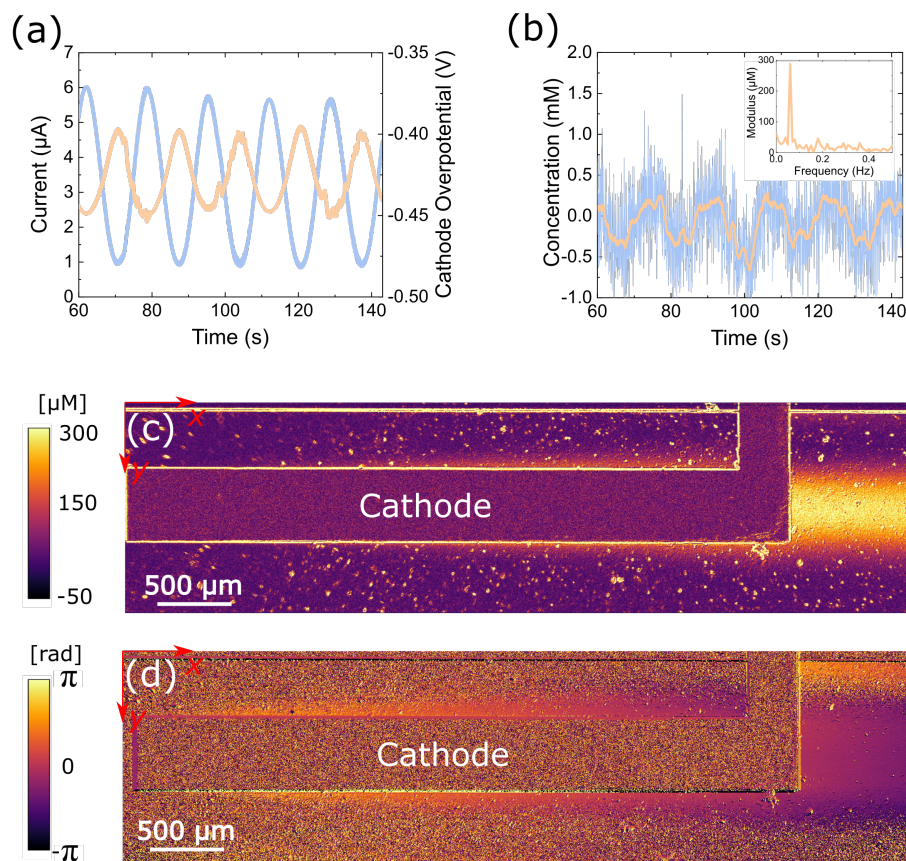


Figure 4.4: Proof of concept of the lock-in spectroscopy for micromolar concentration measurements. (a) modulated current and electrode voltage. (b) Resulting concentration variations through the microfluidic chip (signal averaged from 9 pixels of the camera) and the associated Fourier transform converted in the insert. (c) and (d) Modulus and phase, respectively, of the microscale concentration field around the electrode.

M. Garcia PhD works ended with the development of a new proof of concept to measure μmol variation of concentration in microfluidic chips. In her MFCs described in [Garcia *et al.* 2023b], it was shown that the molar flux at the electrodes surface is directly proportional to the electrochemical current drained, i.e. it is the well-known Faraday law. In lock-in concentration measurements, the concept is to impose a modulated current, i.e. $j(t) = j_0 + \delta j \cos(\omega t)$ to make the concentration field oscillating, i.e. $c(x, t) = c_0(x) + \delta c(x) \cos(\omega t + \Phi(x))$. By demodulating the concentration fields at the frequency $\omega/(2\pi)$, amplitude $\delta c(x)$ and phase lag $\Phi(x)$ in the concentration fields can be measured. As said, it is an exact measurement twin of lock-in thermography [Bourgès *et al.* 2023] applied for mass transfers. It shows how our fundamental methods can be applied to a wide range of application in heat and mass transfers.

The first numerical and experimental results obtained have shown our abilities to detect molar concentration variation in the order of tens μmol (see Figures 4.4), which is two order of magnitude lower than the classical measurements using spectroscopy. It is almost as sensitive as extended-gate type organic transistor [Didier *et al.* 2020] classically used for microsensing in biology and medical applications, but with the advantage to get a complete 2D fields. This methods will be extended to the new microfluidic redox flow batteries developed in collaboration with the Japanese team. Once well mastered in 2D, the super resolution processing and potentially the tomographic processing will be applied to extend the possibility of the methods to microscale systems.

4.3.2.2 Thermotransmittance measurements in fluids

Last but not least, thermotransmittance in fluids is the next step once the temperature fields measurement in heterogeneous solid will be mastered. Proof of concepts of fluid temperature measurement based on thermotransmittance have already been published in literature [Nguyen & Kakuta 2023], see Figure 4.5. Such method is very well suited in microfluidic technologies where contactless temperature measurements remain challenging. It depends on the same principles as explained before where the change of the medium optical indices with temperature is detected. However, transferring this technique from solid to fluid open new challenges. On the fundamental side, it has to be noticed that the change of transmitted signal varies with both temperature and concentration, as it can be seen from the definition of the absorption coefficient, μ , given by [Kakuta *et al.* 2016]:

$$d\mu = \left(\frac{\partial \mu}{\partial T} \right)_c dT + \left(\frac{\partial \mu}{\partial c} \right)_T dc. \quad (4.4)$$

In the case of multiple compounds in solution, a clear discrimination of the contribution of temperature and concentration on the transmitted signal has to be carried out. Analytical modelling of the heat and mass transfer in microfluidic

chip will help to solve this problem, as already developed through my ANR JCJC project: I2MPAC [Chevalier 2021]. In addition, careful thoughts need to be conducted to understand the how IR transmittance is affected by a heat field through multi-layered materials composed of solid and fluid. Thus, this implies to continue the development of opto-chemico-thermal model initiated previously to predict the signal response of light passing through the sample. Finally, the choice of heating sources will also be critical as it determines the measurement time and signal sensitivity.

All these fundamental questions will be tackled after the development of multi-layered solid thermotransmittance (see section 4.1.1), with the microfabrication of dedicated chips embedded heating elements and simple liquid water flow. It will serve as the first proof-of-concept in thermotransmittance measurements in microfluidic chip in our group. A tightened collaboration with the LOF laboratory is also considered to move forward on this topic, in particular with physico-chemist CNRS researchers with whom we have been collaborating on microscale mass transport [Lehtihet *et al.* 2021]. In the end, merging these skills with the super resolution tomographic measurement it will leverage the TIFC team to one of the most well known group for 3D small-scale heat and mass transfer measurements in microfluidic energy conversion devices.

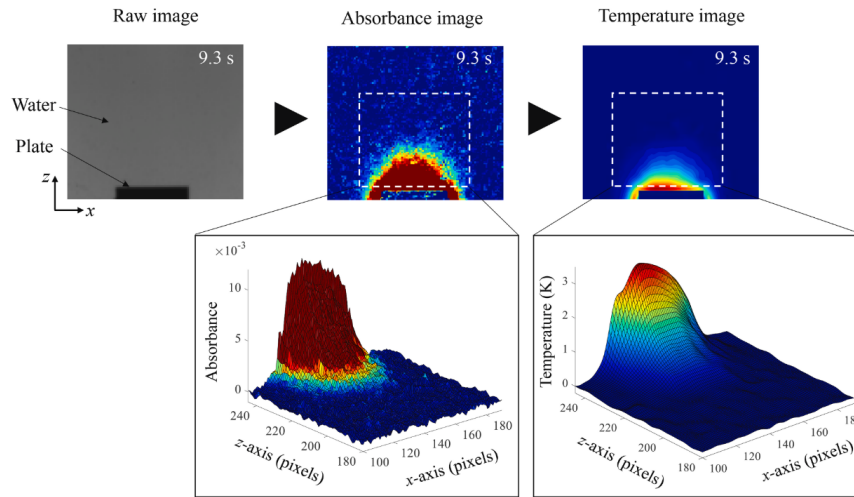


Figure 4.5: Proof of concept of the termotransmittance in water using IR imaging, from [Nguyen & Kakuta 2023]. The heat from the plate diffuses in liquid water.

4.4 Timeline

Answering these questions rely on experimental development at the microscale, data processing, and challenging energy transfers modelling at the confluence of

thermal, chemical, optical and signal processing sciences, applied to microfluidic technologies. The research project written for the next years was summarised through the timeline presented in Figure 4.6. It is mainly divided into 3 milestones at short (2/3 years), mid (5/6 years) and long term (7/8 years) where several tasks will have to be achieved.

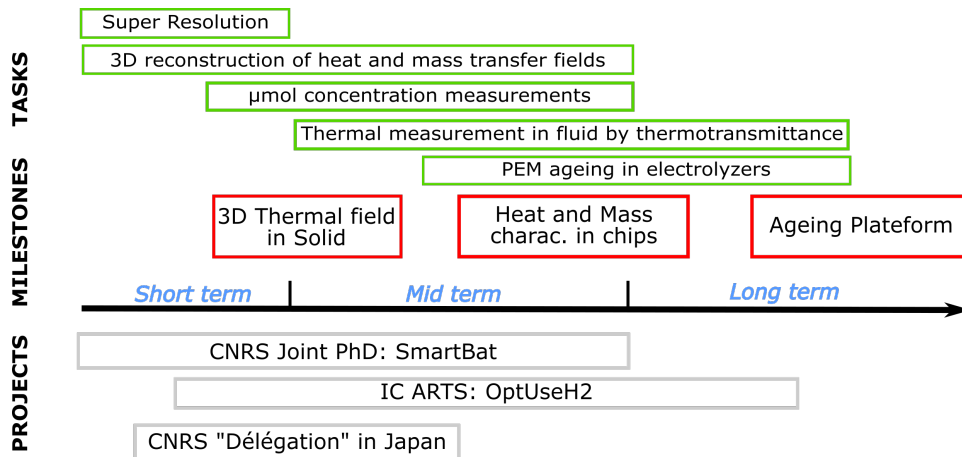


Figure 4.6: Summary of the research project with the different milestones, tasks and funding projects secured.

The work on super-resolution and imaging processing on for 3D reconstruction of thermal fields will start at first. Several actions have already begun on these topics. The 3D reconstruction of heat transfers should be achieved at short term in solid media, but more time will be required to extend this method to 3D concentration measurements in fluids based on FTIR spectroscopy with first results expected at minimum in mid-term. In parallel to these fundamental tasks, heat and mass transfer characterizations in microfluidic chips are expected to be conducted starting in 2 or 3 years, once the micromolar concentration and thermal measurements based on thermotransmittance will have started to be well mastered. Last but not least, the TIFC group should access to an ageing platform for hydrogen systems at the end of the OptUseH2 project including most of the new characterization techniques previously developed.

General conclusion & perspectives

The present manuscript is a tentative to summarize the last ten years of research I carried out in heat and mass transfers and their associate inverse methods and experimental developments. It proposes an original project for the next decade in the TIFC group and at Arts et Métiers.

First, important experimental developments were carried out based on spectroscopic imaging (from X-rays, visible to IR wavelength) dedicated to heat and mass transfers measurements in porous media, microfluidic chips and semi-transparent materials. The associated methods to convert the absorbance and thermotransmittance fields to concentration and thermal fields, respectively, were also developed. My main contributions can be seen through the improvement of imaging techniques to make them more sensitive and versatile. Such accomplishments were done through several research projects obtained since my appointment (ANR JCJC, CNRS, Nouvelle Aquitaine region's funding) for which I was principal investigators. During this time period (2018-2023), more than 30 papers were published, 7 master research students trained and 4 PhD student graduated. I was also able to establish or keep international collaborations: in Canada where I am still collaborating with my previous colleague A. Bazylak through K. Krause PhD, and new collaborations in Japan with Prof. Minami and Kakuta. Such accomplishments can also be credited to an increase of my international acknowledgement and my capacity to develop international relationships.

Second, an important part of my work have been focused on the development of energy characterisation methods for fuel cell systems and microfluidic applications. The development of original setups for fuel cell X-ray imaging, microfluidic fuel cells and PEM electrolyzers enabled to elucidate the heat and mass transfers in these technologies. A link between these fundamental processes and their electrochemical performances (power density, electrochemical impedances...) has always been established in order to propose guidelines for optimized design and operating conditions. These works are the continuation of more than 20 years of instrumental developments dedicated to microfluidic technologies in TIFC team. They correspond also to the expectations from the Arts et Métiers Hydrogen program to build experimental platform for these new technologies. Industrial partners from the electrochemical industry (Solvay or Automotive Cells Company (ACC)) were also involved in these works highlighting their interest in these research to serve industrial issues.

The research project proposed is in direct continuity with my past works. From the first proof of concept concerning the thermal tomography obtained during A. Aouali and C. Bourges PhD works, the idea is now to move toward a quantitative thermal tomography at the microscale. An important experimental works involving new IR laser sources and signal processing will be conducted to obtain the first thermotransmittance based laminography. A central topic for the TIFC group on super resolution imaging will also be tackled in this project to push IR imaging toward the microscale. These two objectives will largely rely on inverse methods and direct analytical modelling involving integral transforms to reconstruct heat and mass fields.

These fundamental developments belong to an ambitious but original project which is unique at international level. It is perfectly integrated to the TIFC group through multiple collaborations between researchers, in I2M with possible collaborations with other research teams (SIMFY) and department (APy). A lot of collaborations on Bordeaux Campus will keep going for the development on advanced microfluidic technologies and microsystems (ICMCB, LOF, Laboratoire Onde Matière d'Aquitaine (LOMA)), and the possibility for them to use our platform for advanced imaging characterization. Arts et Métiers call for advanced evolutive platforms to transform cutting edge research to teaching activities will also be answered in this project. My teaching activities on fuel cell systems and microtechnology for energy conversion course in third year will be fed from these new research developments.

Perspectives to this project concerns mainly new domains of application which can be reached by our thermal tomography. By developing more sensitive tools, it is possible to probe even smaller temperature variations (less than 100 mK) or concentration variations (less than 1 $\mu\text{mol/l}$). Such sensitivity improvements are the mandatory path toward biology applications (like in the case of neuronal activities sensing, see the NeuroTherm project in part II), and micro-sensing for medical application (see the work from Prof. Minami [Didier *et al.* 2020]). Improving the capability of our measurement techniques will accompany the miniaturisation of most technologies will be a great opportunity to develop new experimental platforms for industrial partners.

For the TIFC group, as it was said, such tomographic microscope development is one central subject (at least for the super resolution aspect) which can rally/federate the group. Skills of all researchers from the team in inverse methods, experimental developments with lasers, data processing, micro and nano scale measurements and fabrications will be involved. It is also a direct continuation of the microfluidic works started by the TIFC team more than 20 years ago and for which the group has gained a well-known acknowledgement locally (I2M is part of the Fédération de Microfluidique en Aquitaine (FAM) workshop and is member of the local organizing

committee of the 2025 microfluidic summer school in Oléron). Finally, the international relationship with partners in Japan and Canada will also be tightened with increased student exchanges at graduate and under-graduate level. As an example, Arts et Métiers Learning Abroad Program with University of Toronto was issued from my collaboration with prof. A. Bazylak in Canada. This is another side effect of all these collaborative work in developing close relationship with international organizations to strengthen the student mobility.

Part II

Personal records

Curriculum vitae

Stéphane CHEVALIER

36 years old

In common relationship, 2 children

Arts et Métiers Institute of Technology
 Institut de Mécanique et d'Ingénierie de Bordeaux
 CNRS UMR 5295 (I2M)
 Esplanade des Arts et Métiers
 F-33400 Talence France

phone: +33 (0)5 40 00 34 11

e-mail: stephane.chevalier@ensam.eu

h index 21 (Scopus), 21 (ResearchGate), 21 (Google Scholar)

ResearchGate profile: www.researchgate.net

Google Scholar profile: <https://scholar.google.fr>

Orcid profile: <https://orcid.org>

Personal webpage: <http://chevalierstephane.fr/>

6.1 Professional experience

- 2022-Present Head of SEM (*Systèmes Energétiques et Mécatroniques*) teaching department of Art et Métiers - Bordeaux Campus (7 professors + teaching assistants).
- 2021-Present Nominated member of the CORI (*Conseil des relations internationales*) board at the Arts et Métiers.
- 2019-Present Responsible of the program *Learning Abroad* for student exchanges between Arts et Métiers and University of Toronto.
[Link to the program](#)
- 2018-Present Associate Professor at Arts et Métiers (Bordeaux, France) and Institute of Mechanical Engineering of Bordeaux (I2M)
- 2016-2018 Incoming Marie Curie fellowship at Laboratoire de Thermique et Énergie de Nantes, Nantes Université, France
- Aug. 2015 Invited researcher (collaboration with R. Zeis) at Helmholtz Institute of Ulm, Germany
- 2014 - 2016 Postdoctoral fellow in Prof. A. Bazylak's group at Thermofluids for energy and advanced materials (TEAM) laboratory, University of Toronto, Canada

6.2 Education and training

- 2010-2013 PhD Candidate in Mechanical Engineering, supervised by M. Machmoum, D. Trichet & B. Auvity at Laboratoire de Thermique et Énergie de Nantes, Nantes Université, France. PhD title : *Multiphysics modelling of PEM fuel cell impedance applied to stack diagnosis by E.I.S.*
- 2007-2010 Engineering degree in Thermal and Energy Sciences at Polytech Nantes, Nantes Université, France
- 2005-2007 University Technology Diploma in *Mesures Physiques* at Poitiers University.

6.3 Pedagogic and administrative charges

- 2022-Present Member of the imaging working group at I2M. Advice the I2M executive comity to establish a shared imaging platform, open for all the I2M members and usable for the externals research projects.
- 2019-2023 In charge of the scientific communication of the research team TIFC at I2M (organization of internal seminars every two weeks with the PhD students and the research fellows of the group)
- 2018-Present Responsible for the Unités d'Enseignement (UE) Energétique Avancé (ENGA) (teaching advanced energy transfer in engines and power plant), 2A PGE
- 2016-2018 Elected member at the council of the Laboratoire de Thermique et Énergie de Nantes (LTEN)
- 2010-2013 Elected member of PhD students at the council of the graduate school ED STIM

6.4 International & national reputation

6.4.1 Scientific and organizing committees membership of national conferences

Conference organisation:

1. Member of the local organization committee of the summer school on Microfluidics in Oleron (France), 2025.
2. Member of organization committee of the second workshop Fédération Aquitaine de Microfluidique. June 10th 2023 in Bordeaux (France).
3. Organization of one lab class during advanced Autumn school on Thermal Measurement and Inverse Techniques. September 24-29th 2023 in Oleron (France). More than 80 participants.

4. Organization of the workshop Fédération Aquitaine de Microfluidique. May 13th 2022 in Bordeaux (France). More than 80 participants. Grant from I2M (800€) to help the organization

Conference Chairman:

1. Fédération Aquitaine de Microfluidique (FAM 2022), Bordeaux (France) in the second session.
2. Fundamentals & Development of Fuel Cells (FDFC2019), Nantes (France) in the Session 2b: PEM Fuel Cell : GDL I.
3. Colloque Interdisciplinaire en Instrumentation (C2I 2019), Bordeaux (France) in the session Instrumentation multi spectral, multi echelle.

6.4.2 Seminars at foreign Universities

1. Multiscale Heat and Mass Transfer Characterization in Fluids and Solids, Visiting scholar at Prof. Kakuta Lab, Tokyo Metropolitan University, Japan, 2022.
2. Multiscale Energy Transport Characterization in Fluids and Solids, Biomeg Symposium, University of Tokyo, Japan, 2022.
3. Caractérisation et visualisation du transport massique dans les piles à combustible hydrogène-air, UPR Solvay/LOF, Bordeaux, France, 2019.
4. Characterisation of the transport properties of gas diffusion layers in polymer electrolyte membrane fuel cells, Zentrum für Sonnenenergie- und Wasserstoff-Forschung, Ulm, Germany. 2015
5. Modélisation du transfert de masse dans les milieux poreux par réseau de pores, Laboratoire de Thermocinétique de Nantes, Nantes, France. 2014
6. Modeling of polymer electrolyte membrane fuel cell impedances, ETRERA seminar series, Messina, Italy. 2011

6.4.3 International mobility

1. November 2022 : visiting professor at the LIMMS laboratory (IIS, Tokyo University) for 2 weeks. Collaboration with Prof. Minami. Led to the funding of 1 collaborative projet (2 PhD scholarships)
2. August 2015 : Invited researcher at Helmholtz Institute of Ulm, Germany to work in collaboration with R. Zeis. Led to 1 common publication in 2017

6.5 Scientific collaborations

I have numerous scientific collaborations and students exchanges with many colleagues, especially in Europe, Canada and Japan. Here below, only the main collaborations are recalled for the sake of brevity. Further relevant collaborations are in progress in the framework of the activities related to the research projects summarised in Chapter 7.

National collaborations :

1. LOMA (Bordeaux University) : Prof S. Dilhaire. Co-supervision of C. Bourgès PhD thesis.
2. LOF (Bordeaux University): Dr. J.-B Salmon & J. Leng. Collaborative research on the mass diffusion in confined droplet.
3. ICMCB (Bordeaux University) : Dr. D. Michau. Collaboration on the micro-fabrication of microfluidic fuel cells (thin film deposition) and post mortem analysis.
4. LTEN (Nantes University) : Prof B. Auvity & C. Josset. Submission of a collaborative project to be funded at the ANR.
5. IREENA (Nantes University) : Prof J.-C. Olivier & F. Auger. Monitoring the PhD thesis of I. Ayoub.

International collaborations :

1. University of Toronto (Canada): Prof A. Bazylak & B. Hatton. Collaborative works to fabricate and image PEMFC material (few papers since 2018 act the collaboration)
2. Tokyo University (Japan): Prof. Minami. Inviting scholar for two weeks in 2022, and laureate of a collaborative CNRS project.
3. Tokyo Metropolitan University (Japan) : Prof. N. Kakuta. Inviting professor at I2M in 2020 and collaborative research in NIR spectroscopy.
4. Helmholtz Institute of Ulm (Germany) : Prof. R. Zeis. Inviting scholar in 2015 and submission of a collaborative research project to be funded at the ANR.
5. Baden-Württemberg Cooperative State University (Germany) : Prof. V. Schulz. Submission of a collaborative research project to be funded at the ANR.

6.6 Ph.D. thesis committees

6.6.1 Ph.D. monitoring thesis committee membership

1. Igourzal Ayoub: *Optimisation de chaines énergétiques hybrides pour navires* (2021-2024)

6.6.2 Ph.D. thesis defence committee membership

1. Examiner of Marie Lamard PhD thesis, *Approche multi-échelle de la marinisation des piles à combustible : effet du chlorure de sodium sur la dégradation de mono-cellules et stacks PEMFC*. On May 10th 2023 in Nantes.
2. Examiner of Mathieu Baudry PhD thesis, *Etude d'une pile à combustible à membrane échangeuse de protons haute température (HT-PEMFC) : caractérisation et modélisation*. On June 8th 2022 in Toulouse.

6.7 Peer review activity

28 papers reviewed between 2013 and 2023. They are sorted by journals in the table below :

International Journal of Hydrogen Energy	3
Electrochemistry communication	1
Journal of Applied Energy	2
Journal of Chemical Engineering Research and Design	1
Journal of Power Sources	9
Journal of Electrochemical Society	1
Electrochimica Acta	4
Experimental Thermal and Fluid Science	2
Chemical Engineering Journal	1
Review of Scientific Instrument	1
The Journal of Physical Chemistry	1
Energy Conversion and Management	1

I was also asked to review ANR PRC proposals : the project ENERGY for the French National Research Agency (ANR), 2019.

6.8 Scientific production

I am author and co-author of 62 publications published in refereed journal and conference proceedings. Co-supervised Trainees (Master and PhD students) underlined. 940 citations and h-index of 21 on Scopus, data extracted on 03/05/2023.

In the Table 6.8, I summarised all the communication published as author or co-author.

Type	Quantity
Paper published in international peer reviewed journal	49
Paper submitted to international peer reviewed journal	3
Plenary Lecture (as invited speaker)	6
International referenced conference proceedings	15
National referenced conference proceedings	5
National and international conference without proceedings	19
Total	98

Table 6.1: Summary of the all the communications as author and co-author.

The complete list of my communication, sorted by categories, is available in the appendix 9.

Students' supervision and research project granted

Contents

7.1 Undergraduated students	81
7.2 Master Students	82
7.3 PhD Students	82
7.4 Post-doctoral fellow	83
7.5 Research project granted	83
7.5.1 Project coordination	83
7.5.2 Work package leader	84
7.5.3 Industrial contracts	84

Within the last year I supervised 15 students in the framework of research project in the lab. They range from under graduate studies to PhD studies. Funding collected to support my research and the formation of the students is also detailed in this chapter.

7.1 Undergraduated students

Undergraduate students from two mains program were hired in the lab to conduct small research project.

The first program is the Learning Abroad Agreement between Arts et Métiers and the University of Toronto I am responsible of. The following students were hosted :

2. Adèle Crète Laurence (summer 2023): Developing a Distribution of Relaxing Times (DRT) tool for the characterization of microfluidic fuel cells
1. Steven Li (Summer 2023): Design and Fabrication of a rotating platform for infrared laminagraphy

The second program is the Mechanical Engineering Bachelor for Bordeaux University. In their second year, the students are invited to discover the lab activities through a small research project. Two students were hosted in the lab:

3. Victor Bugada-Jean (2023-2024): integrating under graduate program for research (development of a opto-thermal model for semi-transparent medium)
2. Victor Bugada-Jean (2022-2023): literature review on the DRT tool and development of a DRT algorithm under Python
1. Nino Chesne (2022-2023): literature review on the DRT tool and development of a DRT algorithm under Python

7.2 Master Students

In total I supervised 7 master 2 students for 6 months internship. Two of them were funded by an industrial (Solvay) to work in our lab. Half of them have pursued as PhD students.

6. Abel Netter (2024), Développement d'un banc d'imagerie thermique 3D pour les micro-batteries, student from Arts et Métiers Research Master, funded by BEST 4.0 program
5. Illian Bensana Tournier (2023), Development of a 3D thermal imaging bench for micro batteries, student from ENS Cachan
4. Cedric Palka (2022), Étude numérique du transport de charges dans des réacteurs électrochimiques (piles à combustibles), granted by Département TREFLE
3. Valentin Allard (2021), In situ characterization of polymer electrolyte membrane in microfluidic electrolyzer, granted by Solvay/LOF
2. Sami Mahmoud (2020), Etude et développement de méthodes inverses thermiques pour la reconstruction spatiale de sources, granted by ENSAM
1. Lucie Lindingre (2019), Couplage d'imagerie et de spectroscopie infrarouge : Caractérisation in-situ de milieux réactionnels, granted by Solvay/LOF

7.3 PhD Students

In total I supervised and I am supervising 6 PhD students. Among them, 4 have already defended their thesis.

6. Alisa Svirina, Energy optimization of microbatteries by 3D thermal microscopy, 2023-2026. Co-supervised (30%) with J. Maire and J.-C. Batsale
5. Florian Crouau, Super resolution thermal imaging for energy transfer optimization in microsystems, 2023-2026. Co-supervised (30%) with J. Maire and J.-L. Battaglia (I2M).

4. Marine Garcia, Caractérisation multiphysique des piles à combustible microfluidique par thermospectroscopie à détection synchrone, 2021-2024. Co-supervised (50%) with J.-C. Batsale (I2M), and A. Sommier (I2M)
3. Kevin Krause, Advanced PEM Electrolyzer Mass Transport Control using Infrared Thermal Imaging, 2021-2024. Co-director 50% with J.-L. Battaglia (I2M).
2. Coline Bourges, TomoThermoSpectroscopie InfraRouge pour l'étude des transferts de chaleur et de masse en milieu vivant, 2020-2023. Co-supervised 30% with C. Pradère (I2M) and S. Dilhaire (LOMA).
1. Abderezak Aouali, Tomographie thermo-spectroscopique pour l'étude des torches à plasma, 2019-2021. Co-supervised (50%) with C. Pradère (I2M)

7.4 Post-doctoral fellow

In total I am supervising 1 post-doctoral candidate.

1. Jonathan Letessier, Thermo-tomography of buried Interfaces in Micro-Supercapacitors, 2024-2026. Co-supervised (50%) with J. Maire

7.5 Research project granted

To support my research and hire PhD and Master students, I was able to collect almost 1 M€ (942 k€) over the last few years. I summarised in the following the main research projects as a project coordinator (5 projects in total), and the others where I work as partner or work package leader.

7.5.1 Project coordination

For all these project I was in charge of writing the proposal, hiring the students and performing a part or in totality the experiments planned, and writing the final reports.

6. 2023: SMARTBAT. Project coordinator. Grant from the Joint PhD Program between The University of Tokyo (Prof. Minani) and The Centre National de la Recherche Scientifique (CNRS). 2 PhD scholarships (246k€) and 30k€ for mobility and small consommables. Project related to XX PhD thesis.
5. 2022: Application as PI for beam time at the Canadian Light Source in Canada. Granted as principal investigator for 108 h of beam time in December 2022.

4. 2022: NeuroTherm. Project coordinator. Grant from the Centre National de la Recherche Scientifique (CNRS) in the framework of PEPS instrument. Project in collaboration with IMS. 20k€ for small equipment.
3. 2020: IMAGING. Project coordinator. Grant from the Joint PhD Program between The University of Toronto (U of T) and The Centre National de la Recherche Scientifique (CNRS). 1 PhD scholarship (123k€) and 15k€ for mobility. Project related to K. Krause PhD thesis.
2. 2020: I2MPAC. Project coordinator. Grant from the French National Research Agency (ANR) in the framework of JCJC instruments. A total of 238k€ for 1 PhD scholarship (123k€), 80k€ for equipment, 20k€ for mobility and publications, and 15k€ for teaching release. Project related to M. Garcia PhD thesis.
1. 2016 : Engineered gas diffusion layer structure with controlled transport properties for improved PEM fuel cell performance. Project coordinator. Grant from the European Union (Marie Curie fellowship) for a two-year postdoctoral scholarship (90 k€) at the Laboratoire de Thermique et Énergie de Nantes (LTEN).

7.5.2 Work package leader

3. 2022: OptUSEH2. Work package coordinator (WP1 & WP3). Grant from the Carnot Institute ART in the framework of the hydrogen program. Project in collaboration with three others academic partners. 120k€ for small equipments and an 18-month postdoc.
2. 2021: ITEM. Work package leader. Grant from the Region Nouvelle Aquitaine in the continuation of the project I2MPAC. 60 k€ of equipment are funded to acquire new cameras and optical sources. The total project funded by the Region Nouvelle Aquitaine is 200 k€.
1. 2015: Application as partner (postdoc) for beam time at the Canadian Light Source in Canada and BESSY II in Germany. Both granted.

7.5.3 Industrial contracts

A total of 54k€ of industrial contracts was earned over the last five years with mainly partners involved in the electrochemical industry for batteries and fuel cells.

3. 2023: Automotive Cells Company, 25k€. Project coordinator. Measurements of the impregnation kinetics of their electrolyte during the electrode batteries fabrication. It uses the flying spot and thermal flash techniques.

2. 2019-2021: Solvay, 20k€. Project coordinator. Grant for two Master 2 scholarships from Solvay to measure their PEM membrane permeability and develop the thermospectroscopic imaging setup.
1. 2018: Takazago, 9k€. Project coordinator. Development of an experimental protocol to measure vapor parfum diffusivity in air for Takasago Europe Perfumery.

Teaching activities at Arts et Métiers Institute of Technology (ENSAM)

Contents

8.1	Advanced energetic course	87
8.2	Heat transfer lab class	88
8.3	Hydrogen fundamental and technology course	88
8.4	Undergraduate student projects	89

In this chapter I summarised all my teaching activities within the last five years at Arts et Métiers. In particular, a focus is made on all the new courses I built since my nomination and the evolutions made of existing courses.

8.1 Advanced energetic course

Intended learning outcomes:

At the end of the course, the student will be able to:

1. classify different energy machines;
2. quantify energy transfer within machines and networks;
3. evaluate the occurrence of cavitation in machines and networks;
4. design machine blade pre-sizing;
5. determine the thermodynamic cycle of an energy machine and plant;
6. evaluate a real (polytropic) transformation in a component;

Number of students and academic level:

Approximatively 2×75 students at Master 1 level from the Programme Grande Ecole d'Arts et Métiers.

Involvement in the course:

Creation of the lectures and support of the tutorial class. Writing of a small 20-pages books dedicated to this course. Roughly 100 hours per year.

8.2 Heat transfer lab class

Intended learning outcomes:

At the end of the course, the student will be able to:

1. Measure the main thermal properties in solids media
2. Measure and classify the heat transfer by convection
3. Solve the heat transfer equation numerically in 2D
4. Evaluate defects in solid materials using infrared cameras.

Number of students and academic level:

Group of approximatively 12 students at License 3 level (equivalent to Bachelor).

Involvement in the course:

Preparation of Lab class, creation of one new practical exercises and annual update of all the lab class support in coordination with three other teachers. Roughly 60 hours per year.

8.3 Hydrogen fundamental and technology course

Intended learning outcomes:

At the end of the course, the student will be able to:

1. Classify the different fuel cell technologies
2. Understand the main physical phenomena occurring during the energy conversion
3. Do a basic modelling of the fuel cell polarization curve
4. Design an electrical chain powered by a fuel cell

Number of students and academic level:

Approximatively 30 students at Master 2 level (last year) from the Programme Grande Ecole d'Arts et Métiers.

Involvement in the course:

Entirely new course built from scratch for the hydrogen speciality in the last year of the Programme Grande Ecole. Writing of the course and tutorial activities. Roughly 10 hours per year.

8.4 Undergraduate student projects

Number of students and academic level:

Two groups of 4 students each every years.

Involvement in the course:

Small projects made over the second year of the Programme Grande Ecole d'Arts et Métiers. I am in charge to define the project and the objectives. I supervise the students over the year (one meeting every 2 weeks) and evaluate their accomplishments. Roughly 24 hours per year.

List of publications

Contents

9.1	Paper published in international peer reviewed journals . . .	91
9.2	Paper submitted to international peer reviewed journal . . .	96
9.3	Plenary Lecture (as invited speaker)	96
9.4	International referenced conference proceedings	97
9.5	National referenced conference proceedings	99
9.6	National and international conference without proceedings	99

9.1 Paper published in international peer reviewed journals

49. C. Bourges, **S. Chevalier**, J. Maire, A. Sommier, C. Pradere, S. Dilhaire, Mid-infrared spectroscopic thermotransmittance measurements in dielectric materials for thermal imaging, *Appl. Phys. Lett.* 124 (2024).
48. A. Aouali, **S. Chevalier**, A. Sommier, C. Pradere, Terahertz Constant Velocity Flying Spot for 3D Tomographic Imaging, *J. Imaging.* 9 (2023) 112.
47. A. Aouali, T. Lafargue-Tallet, **S. Chevalier**, A. Sommier, R. Peiffer, M. Tailandier, J. Batsale, C. Pradere, High power density laser estimation using quantitative thermal imaging method, *Quant. Infrared Thermogr. J.* 00 (2023) 1–14.
46. K. Krause, M. Garcia, D. Michau, G. Clisson, B. Billinghamurst, J. Battaglia, **S. Chevalier**, Probing membrane hydration in microfluidic polymer electrolyte membrane electrolyzers via operando synchrotron Fourier-transform infrared spectroscopy, *Lab Chip.* 23 (2023) 4002–4009.
45. M. Garcia, A. Sommier, T. Lafargue-Tallet, G. Clisson, J.-C. Batsale, **S. Chevalier**, Interdiffusion measurements in thermally controlled microchannel using infrared spectroscopic imaging, *Chem. Eng. Sci.* 282 (2023) 119136.
44. M. Garcia, A. Sommier, D. Michau, G. Clisson, J.-C. Batsale, **S. Chevalier**, Imaging concentration fields in microfluidic fuel cells as a mass transfer characterization platform, *Electrochim. Acta.* (2023).

43. C. Bourgès, **S. Chevalier**, J. Maire, A. Sommier, C. Pradère, S. Dilhaire, Infrared thermotransmittance-based temperature field measurements in semi-transparent media, *Rev. Sci. Instrum.* 94 (2023) 034905.
42. Y. Diab, F. Auger, E. Schaeffer, **S. Chevalier**, A. Allahham, Real-Time Estimation of PEMFC Parameters Using a Continuous-Discrete Extended Kalman Filter Derived from a Pseudo Two-Dimensional Model, *Energies.* 15 (2022) 2337.
41. **S. Chevalier**, Semianalytical modeling of the mass transfer in microfluidic electrochemical chips, *Phys. Rev. E.* 104 (2021) 035110.
40. A. Aouali, **S. Chevalier**, A. Sommier, M. Ayadi, J.-C. Batsale, D. Balageas, C. Pradere, Ultra-broadband contactless imaging power meter, *Appl. Opt.* 60 (2021) 7995.
39. **S. Chevalier**, J.-N. Tourvieille, A. Sommier, C. Pradère, Infrared thermospectroscopic imaging of heat and mass transfers in laminar microfluidic reactive flows, *Chem. Eng. J. Adv.* 8 (2021) 100166.
38. M.M. Groz, A. Sommier, E. Abisset-Chavanne, **S. Chevalier**, A. Meziane, J.C. Batsale, C. Pradere, Contactless thermal profilometry of carbon-resin materials by IR thermography, *Measurement.* 182 (2021) 109723.
37. A. Aouali, **S. Chevalier**, A. Sommier, E. Abisset-Chavanne, J.-C. Batsale, C. Pradere. 3D infrared thermospectroscopic imaging. *Sci. Rep. Nature Publishing Group UK*, (2021). 10(1): 22310.
36. **S. Chevalier**, J.-N. Tourvieille, A. Sommier, J.-C. Batsale, B. Beccard, C. Pradère, Thermal Camera-Based Fourier Transform Infrared Thermospectroscopic Imager. *Appl. Spectrosc.* 75 (4) (2021).
35. M. Lehtihet, E. Abisset, **S. Chevalier**, A. Sommier, C. Pradere, J. Leng, Thermospectroscopic infrared imaging of a confined drying process, *Chem. Eng. J.* 403 (2021) 126167.
34. M.M. Groz, A. Sommier, E. Abisset, **S. Chevalier**, J.L. Battaglia, J.C. Batsale, C. Pradere, Thermal resistance field estimations from IR thermography using multiscale Bayesian inference, *Quant. Infrared Thermogr. J.* (2020) 1–12.
33. M.-M. Groz, M. Bensalem, A. Sommier, E. Abisset-Chavanne, **S. Chevalier**, A. Chulkov, J.-L. Battaglia, J.-C. Batsale, C. Pradere, Estimation of Thermal Resistance Field in Layered Materials by Analytical Asymptotic Method, *Appl. Sci.* 10 (2020) 2351.
32. J.-L. Battaglia, E. Ruffio, A. Kusiak, C. Pradere, E. Abisset, **S. Chevalier**, A. Sommier, J.-C. Batsale, The periodic pulse photothermal radiometry technique within the front face configuration, *Measurement.* 158 (2020) 107691.

31. N. Ge, **S. Chevalier**, D. Muirhead, R. Banerjee, J. Lee, H. Liu, P. Shrestha, K. Fahy, C. H. Lee, T. Aoki, Y. Tabushi, and A. Bazylak, Detecting cathode corrosion in polymer electrolyte membrane fuel cells in dead-ended anode mode via alternating current impedance, *J. Power Sources* 439 (2019).
30. **S. Chevalier**, J.-C. Oliver, C. Josset, and B. Auvity, Polymer Electrolyte Membrane Fuel Cell Operating in Stoichiometric Regime, *J. Power Sources* 440 (2019).
29. **S. Chevalier**, J. Hinebaugh, A. Bazylak, Establishing accuracy of watershed-derived pore network extraction for characterizing in-plane effective diffusivity in thin porous layers. *J. Electrochem. Soc.* 166 (7) (2019), F3246-F3254.
28. J. Lee, H. Liu, M.G. George, R. Banerjee, N Ge, **S. Chevalier**, T. Kotaka, Y. Tabuchi, A. Bazylak, Microporous layer to carbon fibre substrate interface impact on polymer electrolyte membrane fuel cell performance, *J. Power Sources* 422 (2019) 113–121.
27. **S. Chevalier**, C. Josset, and B. Auvity, Analytical solution for the low frequency polymer electrolyte membrane fuel cell impedance, *J. Power Sources* 147 (2018) 123-131.
26. **S. Chevalier**, C. Josset, and B. Auvity, Analytical solutions and dimensional analysis of pseudo 2D current density distribution model in PEM fuel cells, *Renewable Energy* 125 (2018) 738-746.
25. H. Liu, J. Hinebaugh, **S. Chevalier**, R. Banerjee, C. Lee, and A. Bazylak, Modeling the effect of fibre surface roughness on the liquid water transport in polymer electrolyte membrane fuel cell gas diffusion layers, *Transp Porous Med* 121 (2018) 437-458.
24. D. Muirhead, R. Banerjee, J. Lee, M.G. George, N. Ge, H. Liu, **S. Chevalier**, J. Hinebaugh, K. Han, and A. Bazylak, Simultaneous characterization of oxygen transport resistance and spatially resolved liquid water saturation at high-current density of PEM fuel cells with varied cathode relative humidity, *Int. J. Hydrogen Energy* 42 (2017) 29472-29483.
23. **S. Chevalier**, C. Josset, and B. Auvity, Fluid dynamic breakthrough in two-connected capillaries: from stationnary to oscillating state, *Physics of Fluids* 29 (2017) 102102.
22. J.-C. Olivier, G. Wasselynck, **S. Chevalier**, B. Auvity, C. Josset, D. Trichet, G. Squadrito, N. Bernard, Multiphysics Modeling and Optimization of the Driving Strategy of a Light Duty Fuel Cell Vehicle, *J. Hydrogen Energy* 42 (2017) 29472-29483.
21. R. Banerjee, **S. Chevalier**, H. Liu, J. Lee, R. Yip, K. Han, B.K. Hong, and A. Bazylak, A comparison of felt-type and paper-type gas diffusion layers for

- polymer electrolyte membrane fuel cell applications using X-ray techniques, Accepted in *J. Electrochem. En. Conv. Stor.* 15(11) (2017) E3215-E3224 (Invited Paper for Special Issue: Emerging Investigators in Electrochemical Energy Conversion and Storage 2017.).
20. J. Lee, R. Banerjee, M.G. George, D. Muirhead, P. Shrestha, H. Liu, N. Ge, **S. Chevalier**, and A. Bazylak, Multiwall carbon nanotube-based microporous layers for polymer electrolyte membrane fuel cells, *J. Electrochem. Soc.* 164(12) (2017) F1149-F1157
 19. N. Ge, M.G. George, J. Lee, D. Muirhead, **S. Chevalier**, R. Banerjee, H. Liu, T.W. Wysokinski, G. Belev, M.A. Webb, N. Zhu, and A. Bazylak, Considering Photon Scattering and Harmonics for Synchrotron X-ray Radiographic Imaging of Polymer Electrolyte Membrane Fuel cells, *J. Electrochem. Soc.* 164(11) (2017) E3215-E3224.
 18. M.G. George, H. Liu, D. Muirhead, R. Banerjee, N. Ge., P. Shrestha, J. Lee, **S. Chevalier**, J. Hinebaugh, M. Messerschmidt, R. Zeis, J. Scholta, A. Bazylak, Accelerated Degradation of Polymer Electrolyte Membrane Fuel Cell Gas Diffusion Layers Part 3: Mass Transport Resistance and Liquid Water Accumulation at Limiting Current Density with in operando Synchrotron X-ray Radiography, *J. Electrochem. Soc.* 164(7) (2017) F714-F721.
 17. H. Liu, M.G. George, R. Banerjee, N. Ge, J. Lee, D. Muirhead, P. Shrestha, **S. Chevalier**, J. Hinebaugh, R. Zeis, M. Messerschmidt, J. Scholta, A. Bazylak, Accelerated Degradation of Polymer Electrolyte Membrane Fuel Cell Gas Diffusion Layers: Part 2 – Steady State Liquid Water Distributions with in Operando Synchrotron X-ray Radiography, *J. Electrochem. Soc.* 164(7) (2017) F704-F713.
 16. J. Lee, **S. Chevalier**, R. Banerjee, P. Antonacci, N. Ge, R. Yip, T. Kotaka, Y. Tabuchi, A. Bazylak Investigating the effects of gas diffusion layer substrate thickness on polymer electrolyte membrane fuel cell performance via synchrotron X-ray radiography, *Electrochim. Acta* 236 (2017) 161–170.
 15. **S. Chevalier**, N. Lavielle, B.D. Hatton, and A. Bazylak, Novel electrospun gas diffusion layers for polymer electrolyte membrane fuel cells: Part I. Fabrication, morphological characterization, and in situ performance, *J. Power Sources* 352 (2017) 272–280.
 14. **S. Chevalier**, N. Ge, J. Lee, M.G. George, H. Liu, P. Shrestha, D. Muirhead, N. Lavielle, B.D. Hatton, and A. Bazylak, Novel electrospun gas diffusion layers for polymer electrolyte membrane fuel cells: Part II. In operando synchrotron imaging for microscale liquid water transport characterization, *J. Power Sources* 352 (2017) 281-290.

13. R. Banerjee, N. Ge, J. Lee, M.G. George, **S. Chevalier**, H. Liu, P. Shrestha, D. Muirhead, A. Bazylak, Transient liquid water distributions in polymer electrolyte membrane fuel cell gas diffusion layers observed through in-operando synchrotron X-ray radiography, *J. Electrochem Soc.* 164(2) (2017) F154-F162.
12. **S. Chevalier**, N. Ge, J. Lee, R. Banerjee, H. Liu, M. George, P. Shrestha, D. Muirhead, J. Hinebaugh, Y. Tabuchi, T. Kotaka, and A. Bazylak, Synchrotron X-ray radiography as a highly precise and accurate method for measuring the spatial distribution of liquid water in operating PEM fuel cells, *J. Electrochem. Soc.* 164(2) (2017) F107-F114.
11. N. Ge, **S. Chevalier**, J. Lee, P., M. George, H. Liu, R. Banerjee, C. Lee, M. Fazeli, R. Yip, T. Kotaka², Y. Tabuchi, and A. Bazylak, Non-isothermal two-phase transport in a polymer electrolyte membrane fuel cell crack-free microporous layer, *Int. J Heat and Mass Transfer* 107 (2017) 418-431.
10. C. Lee, J. Hinebaugh, R. Banerjee, **S. Chevalier**, R. Abouatallah, R. Wang, A. Bazylak, Influence of limiting throat and flow regime on oxygen bubble saturation of polymer electrolyte membrane electrolyzer porous transport layers, *Int. J. Hydrogen Energy* 42 (2017) 2724-2735.
9. **S. Chevalier**, M. Fazeli, F. Mack, S. Galbiati, I. Manke, A. Bazylak, and R. Zeis, Role of the microporous layer in the redistribution of phosphoric acid in high temperature PEM fuel cell gas diffusion electrodes, *Electrochim. Acta* 212 (2016) 187-194.
8. **S. Chevalier**, J. Lee, N. Ge, Y. Ronnie, P. Antonacci, Y. Tabuchi, T. Kotaka, and A. Bazylak, In operando measurements of liquid water saturation distributions and effective diffusivities of polymer electrolyte membrane fuel cell gas diffusion layers, *Electrochim. Acta* 210 (2016) 792-803.
7. **S. Chevalier**, C. Josset, A. Bazylak, and B. Auvity, Measurements of Air Velocities in Polymer Electrolyte Membrane Fuel Cell Channels Using Electrochemical Impedance Spectroscopy, *J. Electrochem. Soc.* 163(8) (2016) F816-F823.
6. N. Ge, **S. Chevalier**, J. Hinebaugh, R. Yip, J. Lee, P. Antonacci, T. Kotaka, Y. Tabuchi and A. Bazylak. Correcting sample movement during synchrotron X-ray radiographic imaging of polymer electrolyte membrane fuel cells, *J. Synchrotron Radiat.* 23 (2016) 550-599.
5. P. Antonacci, **S. Chevalier**, J. Lee, N. Ge, R. Yip, J. Hinebaugh, Y. Tabuchi, T. Kotaka and A. Bazylak, Balancing mass transport resistance and membrane resistance when tailoring MPL thickness for polymer electrolyte membrane fuel cells operating at high current densities, *Electrochim. Acta* 188 (2016) 888-897.

4. P. Antonacci, **S. Chevalier**, J. Lee, R. Yip, N. Ge and A. Bazylak, Feasibility of combining electrochemical impedance spectroscopy and synchrotron X-ray radiography for determining the influence of liquid water on polymer electrolyte membrane fuel cell performance. *Int. J. Hydrogen Energy* 40 (2015) 16494-16502.
3. **S. Chevalier**, N. Ge, J. Lee, P. Antonacci, R. Yip, M.G. George, H. Liu, R. Banerjee, M. Fazeli and A. Bazylak, In situ analysis of voltage degradation in a polymer electrolyte membrane fuel cell with a dead-ended anode. *Electrochem. Commun.* 59 (2015) 16-19.
2. **S. Chevalier**, B. Auvity, J.-C. Olivier, C. Josset, D. Trichet and M. Machmoum, Detection of cells state-of-health in PEMFC Stack using EIS Measurements coupled with Multiphysics Modelling. *Fuel Cells* 14 (2014) 416–429.
1. **S. Chevalier**, D. Trichet, B. Auvity, J.-C. Olivier, C. Josset and M. Machmoum, Multiphysics DC and AC models of a PEMFC for the detection of degraded cell parameters. *Int. J. Hydrogen Energy* 38 (2013) 11609–11618.

9.2 Paper submitted to international peer reviewed journal

4. K. Krause, C. Palka, M. Garcia, A. Erriguible, S. Glockner, J.-L. Battaglia and **S. Chevalier**, Heat and mass transfer visualization of an exothermic acid-base microfluidic reactor using infrared thermospectroscopy, submitted to QIRT journal.
3. C. Bourgès, J.Maire, A. Sommier, **S. Chevalier**, C. Pradère, S. Dilhaire, Contribution of surface and average volume temperature in semitransparent media based on multi-spectral thermotransmittance, submitted to Heat and Mass transfer Journal
2. M. Garcia, A. Sommier, J.-C. Batsale, **S. Chevalier** Micromole concentration imaging in microfluidic fuel cell by lock-in spectroscopy, submitted to ACS Energy Letters
1. K. Krause, A. Crete, D. Michaud, J.L. Battaglia, **S. Chevalier**, Mass transfer imaging in microfluidic electrolyzers using IR spectroscopy submitted to Journal of Power Sources.

9.3 Plenary Lecture (as invited speaker)

6. Multiscale Heat and Mass Transfer Characterization in Fluids and Solids, Visiting scholar at Prof. Kakuta Lab, Tokyo Metropolitan University, Japan, 2022.

5. Multiscale Energy Transport Characterization in Fluids and Solids, Biomeg Symposium, University of Tokyo, Japan, 2022.
4. Caractérisation et visualisation du transport massique dans les piles à combustible hydrogène-air, UPR Solvay/LOF, Bordeaux, France, 2019.
3. Characterisation of the transport properties of gas diffusion layers in polymer electrolyte membrane fuel cells, Zentrum für Sonnenenergie- und Wasserstoff-Forschung, Ulm, Germany. 2015
2. Modélisation du transfert de masse dans les milieux poreux par réseau de pores, Laboratoire de Thermocinétique de Nantes, Nantes, France. 2014
1. Modeling of polymer electrolyte membrane fuel cell impedances, ETRERA seminar series, Messina, Italy. 2011

9.4 International referenced conference proceedings

16. J.-C. Batsale, E. Abisset, F. Achchaq, A. Aouali, **S. Chevalier**, M.-M. Groz, J. Maire, A. Sommier, Multiscale aspects of the response of a temperature field to a pulsed laser or a periodic laser spot: some applications for IR thermography for non destructive evaluation, terahertz tomography, super-resolution, and microscale heat transfer, in: N.P. Avdelidis (Ed.), *Thermosense Therm. Infrared Appl. XLV*, SPIE, 2023: p. 9.
15. M. Garcia, A. Sommier, K.Krause, J-C. Batsale and **S Chevalier**. Measurements of mass transfer in a microchannel using infrared spectroscopy imaging in QIRT 2022 (Paris, France)
14. K. Krause, C. Palka, M. Garcia, A. Erriguible, S. Glockner, C. Pradère and **S. Chevalier**. Krause Heat and mass transfer visualization of an exothermic acid-base microfluidic reactor using infrared thermospectroscopy in QIRT 2022 (Paris, France)
13. A. Aouali, **S. Chevalier**, A Sommier, Jean-Christophe Batsale, Christophe Pradere, Inverse Method based on Cosine Integral Transforms to Estimate 2-D Heat Flux and Thermal Diffusivity in QIRT 2022 (Paris, France)
12. **S. Chevalier**, J.-N. Tourvieille, A. Sommier, J.-C. Batsale, & C. Pradere, Microfluidic microcalorimetry of Acid/Base reaction using FTIR Thermospectroscopy imaging. In QIRT 2020 (Porto, Portugal)
11. **S. Chevalier**, J.-C. Olivier, C. Josset, and B. Auvity, Polymer Electrolyte Membrane Fuel Cell Characterisation Based on Current Distribution Measurements, *ECS Trans.* 86 (2018) 211-220.

10. **S. Chevalier**, C. Josset, and B. Auvity, Change of Preferential Liquid Break-through Pathways in PEMFC Gas Diffusion Layers: Evidence of Pressure-Induced Dynamic Transport, *ECS Trans.* 86 (2018) 119-126.
9. M.G. George, H. Liu, R. Banerjee, N. Ge, P. Shrestha, D. Muirhead, J. Lee, **S. Chevalier**, J. Hinebaugh, M. Messerschmidt, R. Zeis, J. Scholta, A. Bazylak, Accelerated Degradation of Polymer Electrolyte Membrane Fuel Cell Gas Diffusion Layers: Mass Transport Resistance and Liquid Water Accumulation at Limiting Current Density with in operando Synchrotron X-ray Radiography, *ECS Trans.* 75 (2016) 89-100.
8. R. Banerjee, N. Ge, J. Lee, M. G. George, H. Liu, D. Muirhead, P. Shrestha, **S. Chevalier**, J. Hinebaugh and A. Bazylak, Determining the Impact of Dynamic Load Conditions on Interfacial Liquid Water Accumulation in Polymer Electrolyte Membrane Fuel Cell Gas Diffusion Layers Using Synchrotron X-Ray Radiography, *ECS Trans.* 75 (2016) 251–259.
7. N. Ge, **S. Chevalier**, J. Hinebaugh, M.G. George, J. Lee, R. Banerjee, H. Liu, D. Muirhead, P. Shrestha, A. Bazylak, Roles of Photon Scattering in Synchrotron X-ray Radiography of In Operando Visualizations of the Polymer Electrolyte Membrane Fuel Cell, *ECS Trans.* 75 (2016) 261–274.
6. H. Liu, M.G. George, N. Ge, R. Banerjee, **S. Chevalier**, J. Lee, P. Shrestha, D. Muirhead, J. Hinebaugh, R. Zeis, M. Messerschmidt, J. Scholta, A. Bazylak, Accelerated Degradation of Polymer Electrolyte Membrane Fuel Cell Gas Diffusion Layers: Performance Degradation and Steady State Liquid Water Distributions with in Operando Synchrotron X-ray Radiography, *ECS Trans.* 75 (2016) 289–300.
5. J. Lee, R. Banerjee, N. Ge, **S. Chevalier**, M.G. George, H. Liu, P. Shrestha, D. Muirhead, J. Hinebaugh, A. Bazylak, Performance Benefits of Multiwall Carbon Nanotubes in the Polymer Electrolyte Membrane Fuel Cell Gas Diffusion Layer, *ECS Trans.* 75 (2016) 237–244.
4. **S. Chevalier**, R. Banerjee, J. Lee, N. Ge, C. Lee, T. W. Wysokinski, G. Belev, A. Webb, D. Miller, N. Zhu, Y. Tabuchi, T. Kotaka and A. Bazylak. 2015. In situ Liquid Water Visualization in Polymer Electrolyte Membrane Fuel Cells with High Resolution Synchrotron X-ray Radiography. SRI 2015 (New York, USA), published in American Institute of Physics Conference Proceedings.
3. J.-C. Olivier, G. Wasselynck, D. Trichet, N. Bernard, S. Hmam, **S. Chevalier**, C. Josset, B. Auvity and G. Squadrito. 2015. Optimization of the Driving Strategy of a Low Consumption Urban Concept Vehicle. IEEE VPPC 2015 (Montreal, Canada). Published in VPPC2015.
2. **S. Chevalier**, C. Josset, J.-C. Olivier, B. Auvity, D. Trichet and M. Machmoum. 2013. Experimental Validation of an Identification Procedure of

PEMFC Stack State of Health Using EIS Combined with a Physical Impedance Modelling. IEEE PHM 2013 (Milano, Italy), published in Chemical Engineering Transactions, volume 33, pp. 1015–1020.

1. D. Trichet, **S. Chevalier**, G. Wasselynck, J.-C. Olivier, B. Auvity, C. Josset and M. Machmoum. 2011. Global Energy Optimization of a Light-Duty Fuel-Cell Vehicle. 2011 IEEE Vehicle Power and Propulsion Conference, published in VPPC 2011 art. no. 6043180.

9.5 National referenced conference proceedings

5. C. Bourges, **S. Chevalier**, J. Maire, C. Pradere, S. Dilhaire, Mesure de température dans des milieux semi-transparents à l'infrarouge à l'échelle micrométrique, in Ann. Du Congrès Annu. La Société Française Therm. 2023, Reims, 2023: p. 8
4. M. Garcia, A. Sommier, J.-C. Batsale, **S. Chevalier**, In operando mass transport imaging in microfluidic fuel cells, in: CFM 2022, Nantes, France.
3. A. Aouali, **S. Chevalier**, A. Sommier, J.-C. Batsale, C. Pradere, Développement d'un fluxmètre imageur hyperspectral sans contact par thermographie infrarouge, in: Ann. Du Congrès Annu. La Société Française Therm. 2021, Belfort, 2021: p. 8.
2. C. Bourges, **S. Chevalier**, A. Sommier, C. Pradere, Mesure transitoire et sans contact de champ de température par thermotransmittance dans des milieux semi-transparents à l'infrarouge, in: Ann. Du Congrès Annu. La Société Française Therm. 2021, Belfort, 2021: p. 8.
1. A. Aouali, **S. Chevalier**, A. Sommier, J.-C. Batsale, C. Pradere, Mesure de Champs de Températures dans des Flamme par Imagerie-Spectroscopique InfraRouge, in: Ann. Du Congrès Annu. La Société Française Therm. 2020, Belfort, 2020: p. 8.

9.6 National and international conference without proceedings

19. A. Aouali, **S. Chevalier**, A. Sommier, J.-C. Batsale, C. Pradere, Tomographie thermo-spectroscopique 3D par "Flying Spot" en utilisant un thermoconvertisseur hyperspectral couplée à une caméra infrarouge, in: Ann. Du Congrès Annu. La Société Française Therm. 2022, Valenciennes (France)
18. K. Krause, **S. Chevalier**, Mesure des champs de température et de concentration dans un réacteur microfluidique par thermospectroscopie infrarouge. In La Société Française Therm. 2022, Valenciennes (France)

17. C. Bourges, **S. Chevalier**, J. Maire, S. Dilhaire, Étude de la thermotransmittance dans des milieux semi-transparents à l'infrarouge pour la mesure de température. In La Société Française Therm. 2022, Valenciennes (France)
16. **S. Chevalier**, A. Sommier, M.M. Groz, E. Abisset-Chavanne J.-C. Batsale, & C. Pradere, Mesure du flux thermique à l'interface buse/polymère dans le procédé de fabrication additive par dépôt de fil fondu. In La Société Française Therm. 2021, Belfort (France)
15. **S. Chevalier**, J.-N. Tourvielle, A. Aouali, A. Sommier, C. Pradere and J.-C. Batsale, Imageur 4D ultrarapide basé sur la thermospectroscopie infrarouge à transformée de Fourier, in SFT 2020 (Belfort, France)
14. **S. Chevalier**, J.-C. Olivier, C. Josset, and B. Auvity. Multiscale Characterization of Polymer Electrolyte Membrane Fuel Cell Operating in Stoichiometric Regime. In FDFC 2019 (Nantes, France).
13. **S. Chevalier**, C. Josset, and B. Auvity. Novel single channel PEM fuel cell to investigate the channel impedance. In Hypothesis XII (Syracuse, Italy).
12. **S. Chevalier**, C. Josset, and B. Auvity. Water management in the Gas Diffusion Layer of PEM fuel cells: Dynamic breakthrough effects on porous media liquid water saturation. In Next Generation PEM Fuel Cells conference: Strategic Partnerships for Tackling Multiscale Challenges (Physikzentrum Bad Honnef, Germany).
11. **S. Chevalier**, C. Josset, A. Bazylak, and B. Auvity. "Novel methodology to diagnose fuel cell air channel velocities based on EIS measurements." In FDFC 2017 (Stuttgart, Germany).
10. **S. Chevalier**, C. Josset, B. Auvity, Using the channel impedance to measure air velocities in polymer electrolyte membrane fuel cells, In IDHEA 2016 (Nantes, France).
9. M. George, H. Liu, N. Ge, R. Banerjee, J. Lee, **S. Chevalier**, D. Muirhead, P. Shrestha, R. Zeis, M. Messerschmidt, J. Scholta, and A. Bazylak. In Situ Synchrotron Radiography of Artificially Degraded Gas Diffusion Layers: Limiting Current Study As a Function of Relative Humidity. In PRIME 2016 230th ECS Meeting (Honolulu, Hawaii).
8. D. Muirhead, R. Banerjee, **S. Chevalier**, N. Ge, M. George, J. Hinebaugh, J. Lee, H. Liu, P. Shrestha, and A. Bazylak Impact of Liquid Water on Oxygen Transport Resistance in a PEMFC Cathode Via Limiting Current Methods and Concurrent Synchrotron X-Ray Radiography. In PRIME 2016 230th ECS Meeting (Honolulu, Hawaii).
7. N. Ge, **S. Chevalier**, J. Lee, J. Hinebaugh, R. Banerjee, M. George, H. Liu, D. Muirhead, P. Shrestha, and A. Bazylak. Quantifying Synchrotron x-Ray

Harmonics and Scattering for Informed in Operando Visualizations of Polymer Electrolyte Membrane Fuel Cells. In PRIME 2016 230th ECS Meeting (Honolulu, Hawaii).

6. H. Liu, M. George, N. Ge, J. Lee, R. Banerjee, **S. Chevalier**, P. Shrestha, D. Muirhead, R. Zeis, M. Messerschmidt, J. Scholta, and A. Bazylak. Synchrotron X-Ray Radiographic Imaging of Liquid Water Transport Dynamics in Aged Polymer Electrolyte Membrane Fuel Cell Gas Diffusion Layers. In PRIME 2016 230th ECS Meeting (Honolulu, Hawaii).
5. **S. Chevalier** and A. Bazylak. Microcomputed tomography based pore network modelling. In FDFC 2015 (Toulouse, France).
4. **S. Chevalier** and A. Bazylak. In-Situ characterisation of gas diffusion layers of polymer electrolyte fuel cell. In FDFC 2015 (Toulouse, France)
3. D. Trichet, **S. Chevalier**, B. Auvity, C. Josset, J.-C. Olivier and M. Machmoum. Water Management and Thermal Effects on PEMFC Accessories Consumption. In International Discussion on Hydrogen Energy and Applications IDHEA 2014 (Nantes, France)
2. **S. Chevalier**, C. Josset, J.-C. Olivier, B. Auvity, D. Trichet and M. Machmoum. Numerical simulation of localized impedance along a segmented PEM fuel cell. In FDFC 2013 (Karlsruhe, Germany)
1. **S. Chevalier**, C. Josset, J.-C. Olivier, D. Trichet, B. Auvity and M. Machmoum. Physical modeling of the electrochemical impedance of PEMFC. In EMHYTEC 2012 (Hammamet, Tunisia)

Bibliography

- [Allen *et al.* 2015] Frances I. Allen, Luis R. Comolli, Ahmet Kusoglu, Miguel A. Modestino, Andrew M. Minor and Adam Z. Weber. *Morphology of Hydrated As-Cast Nafion Revealed through Cryo Electron Tomography*. ACS Macro Letters, vol. 4, no. 1, pages 1–5, jan 2015. (Cited on page 50.)
- [Aouali *et al.* 2020] A Aouali, S Chevalier, A Sommier, E. Abisset-Chavanne, J.-C. Batsale and C Pradere. *3D infrared thermospectroscopic imaging*. Scientific Reports, vol. 10, no. 1, page 22310, dec 2020. (Cited on page 23.)
- [Aouali *et al.* 2021] A. Aouali, S. Chevalier, A. Sommier, M. Ayadi, J.-C. Batsale, Daniel Balageas and C. Pradere. *Ultra-broadband contactless imaging power meter*. Applied Optics, vol. 60, no. 26, page 7995, sep 2021. (Cited on pages 27 and 62.)
- [Aouali *et al.* 2023a] Abderezak Aouali, Stéphane Chevalier, Alain Sommier and Christophe Pradere. *Terahertz Constant Velocity Flying Spot for 3D Tomographic Imaging*. Journal of Imaging, vol. 9, no. 6, page 112, may 2023. (Cited on pages 26 and 27.)
- [Aouali *et al.* 2023b] Abderezak Aouali, Thomas Lafargue-Tallet, Stéphane Chevalier, Alain Sommier, Raymond Peiffer, Maximilian Taillandier, Jean-christophe Batsale and Christophe Pradere. *High power density laser estimation using quantitative thermal imaging method*. Quantitative InfraRed Thermography Journal, vol. 00, no. 00, pages 1–14, jul 2023. (Cited on page 27.)
- [Aouali 2022] Abderezak Aouali. *Tomographie thermo-spectroscopique par imagerie 3D pour l'étude des torches à plasma*. PhD thesis, 2022. (Cited on pages 56 and 59.)
- [Ayvazyan 2012] Vigen Ayvazyan. *Etude de champs de température séparables avec une double décomposition en valeurs singulières: quelques applications à la caractérisation des propriétés thermophysiques des matériaux et au contrôle non destructif*. PhD thesis, Bordeaux 1, 2012. (Cited on page 26.)
- [Barbir *et al.* 2005] F Barbir, H Gorgun and X Wang. *Relationship between pressure drop and cell resistance as a diagnostic tool for PEM fuel cells*. Journal of Power Sources, vol. 141, no. 1, pages 96–101, February 2005. (Cited on page 37.)
- [Batsale *et al.* 2023] Jean-Christophe Batsale, Emmanuelle Abisset, Fouzia Achchaq, Abderezak Aouali, Stéphane Chevalier, Marie-Marthe Groz, Jeremie Maire and Alain Sommier. *Multiscale aspects of the response of a*

- temperature field to a pulsed laser or a periodic laser spot: some applications for IR thermography for non destructive evaluation, terahertz tomography, super-resolution, and microscale heat transfer.* In Nicolas P. Avdelidis, editor, *Thermosense: Thermal Infrared Applications XLV*, page 9. SPIE, jun 2023. (Cited on page 61.)
- [Battaglia *et al.* 2000] Jean-Luc Battaglia, Ludovic Le Lay, Jean-Christophe Batsale, Alain Oustaloup and Olivier Cois. *Utilisation de modèles d'identification non entiers pour la résolution de problèmes inverses en conduction.* International Journal of Thermal Sciences, vol. 39, no. 3, pages 374–389, mar 2000. (Cited on page 62.)
- [Bazylak 2009] A. Bazylak. *Liquid water visualization in PEM fuel cells: A review.* International Journal of Hydrogen Energy, vol. 34, no. 9, pages 3845–3857, May 2009. (Cited on page 37.)
- [Bernardi & Verbrugge 1991] D. Bernardi and M. Verbrugge. *MATHEMATICAL MODEL OF GAS DIFFUSION ELECTRODE BONDED TO A POLYMER ELECTROLYTE.* AIChE Journal, vol. 37, no. 8, page 1151/1163, 1991. (Cited on page 37.)
- [Betzig *et al.* 2006] Eric Betzig, George H. Patterson, Rachid Sougrat, O. Wolf Lindwasser, Scott Olenych, Juan S. Bonifacino, Michael W. Davidson, Jennifer Lippincott-Schwartz and Harald F. Hess. *Imaging intracellular fluorescent proteins at nanometer resolution.* Science, vol. 313, no. 5793, pages 1642–1645, sep 2006. (Cited on pages 58 and 61.)
- [Bhargava *et al.* 2003] Rohit Bhargava, Shi-Qing Wang and Jack L. Koenig. *FTIR Microspectroscopy of Polymeric Systems.* In *Advances in Polymer Science*, volume 163, pages 137–191, aug 2003. (Cited on page 8.)
- [Böhm *et al.* 2019] Thomas Böhm, Riko Moroni, Matthias Breitwieser, Simon Thiele and Severin Vierrath. *Spatially Resolved Quantification of Ionomer Degradation in Fuel Cells by Confocal Raman Microscopy.* Journal of The Electrochemical Society, vol. 166, no. 7, pages F3044–F3051, 2019. (Cited on page 63.)
- [Bourgès *et al.* 2023] C. Bourgès, Stephane Chevalier, Jeremie Maire, Alain Sommier, C. Pradère and Stefan Dilhaire. *Infrared thermotransmittance-based temperature field measurements in semitransparent media.* Review of Scientific Instruments, vol. 94, no. 3, page 034905, mar 2023. (Cited on pages 28, 57, 59 and 66.)
- [Bourges 2023] Coline Bourges. *Thermographie dans des milieux semi-transparents à l'infrarouge par thermotransmittance.* PhD thesis, 2023. (Cited on pages 15, 31, 56, 57 and 59.)

- [Braff *et al.* 2013] William A. Braff, Cullen R. Buie and Martin Z. Bazant. *Boundary Layer Analysis of Membraneless Electrochemical Cells*. Journal of The Electrochemical Society, vol. 160, no. 11, pages A2056–A2063, sep 2013. (Cited on page 45.)
- [Brereton 2000] Richard G. Brereton. *Introduction to multivariate calibration in analytical chemistry*. The Analyst, vol. 125, no. 11, pages 2125–2154, 2000. (Cited on pages 14 and 20.)
- [Bruus 2008] Henrik Bruus. Theoretical microfluidics. Oxford university press, 2008. (Cited on page 45.)
- [Burgholzer *et al.* 2017a] Peter Burgholzer, Thomas Berer, Jürgen Gruber and Günther Mayr. *Super-resolution thermographic imaging using blind structured illumination*. Applied Physics Letters, vol. 111, no. 3, page 31908, 2017. (Cited on page 62.)
- [Burgholzer *et al.* 2017b] Peter Burgholzer, Michael Thor, Jürgen Gruber and Günther Mayr. *Three-dimensional thermographic imaging using a virtual wave concept*. Journal of Applied Physics, vol. 121, no. 10, page 105102, mar 2017. (Cited on pages 25, 26 and 60.)
- [Busse *et al.* 1992] G. Busse, D. Wu and W. Karpen. *Thermal wave imaging with phase sensitive modulated thermography*. Journal of Applied Physics, vol. 71, no. 8, pages 3962–3965, apr 1992. (Cited on page 29.)
- [Butler *et al.* 2019] Holly J. Butler, Paul M. Brennan, James M. Cameron, Duncan Finlayson, Mark G. Hegarty, Michael D. Jenkinson, David S. Palmer, Benjamin R. Smith and Matthew J. Baker. *Development of high-throughput ATR-FTIR technology for rapid triage of brain cancer*. Nature Communications, vol. 10, no. 1, page 4501, dec 2019. (Cited on page 14.)
- [Cahill 1990] David G Cahill. *Thermal conductivity measurement from 30 to 750 K: the 3ω method*. Review of Scientific Instruments, vol. 61, no. 2, pages 802–808, feb 1990. (Cited on page 29.)
- [Chan & Kazarian 2012] K. L. Andrew Chan and Sergei G. Kazarian. *FT-IR Spectroscopic Imaging of Reactions in Multiphase Flow in Microfluidic Channels*. Analytical Chemistry, vol. 84, no. 9, pages 4052–4056, may 2012. (Cited on page 8.)
- [Chapuis *et al.* 2008] O. Chapuis, M. Prat, M. Quintard, E. Chane-Kane, O. Guillot and N. Mayer. *Two-phase flow and evaporation in model fibrous media*. Journal of Power Sources, vol. 178, no. 1, pages 258–268, March 2008. (Cited on page 37.)

- [Chen *et al.* 2023] Xin Chen, Suyi Zhong, Yiwei Hou, Ruijie Cao, Wenyi Wang, Dong Li, Qionghai Dai, Donghyun Kim and Peng Xi. *Superresolution structured illumination microscopy reconstruction algorithms: a review*. Light: Science & Applications, vol. 12, no. 1, page 172, jul 2023. (Cited on page 62.)
- [Chevalier *et al.* 2016a] Stéphane Chevalier, R. Banerjee, J. Lee, Nan Ge, C. Lee, Tomasz W. Wysokinski, G. Belev, A. Webb, D. Miller, N. Zhu, Y. Tabuchi, T. Kotaka and A. Bazylak. *In situ liquid water visualization in polymer electrolyte membrane fuel cells with high resolution synchrotron x-ray radiography*. In SRI 2015, page 050006, New York, USA, 2016. AIP Publishing. (Cited on page 38.)
- [Chevalier *et al.* 2016b] Stéphane Chevalier, Christophe Josset, Aimy Bazylak and Bruno Auvity. *Measurements of Air Velocities in Polymer Electrolyte Membrane Fuel Cell Channels Using Electrochemical Impedance Spectroscopy*. Journal of The Electrochemical Society, vol. 163, no. 8, pages F816–F823, may 2016. (Cited on pages 38 and 42.)
- [Chevalier *et al.* 2017a] Stéphane Chevalier, Nan Ge, Jongmin Lee, M.G. George, Hang Liu, Pranay Shrestha, Dan Muirhead, Nicolas Lavielle, B.D. Hatton and Aimy Bazylak. *Novel electrospun gas diffusion layers for polymer electrolyte membrane fuel cells: Part II. In operando synchrotron imaging for microscale liquid water transport characterization*. Journal of Power Sources, vol. 352, pages 281–290, jun 2017. (Cited on page 40.)
- [Chevalier *et al.* 2017b] Stéphane Chevalier, Nicolas Lavielle, B.D. Hatton and Aimy Bazylak. *Novel electrospun gas diffusion layers for polymer electrolyte membrane fuel cells: Part I. Fabrication, morphological characterization, and in situ performance*. Journal of Power Sources, vol. 352, pages 272–280, jun 2017. (Cited on page 40.)
- [Chevalier *et al.* 2018] S. Chevalier, C. Josset and B. Auvity. *Analytical solution for the low frequency polymer electrolyte membrane fuel cell impedance*. Journal of Power Sources, vol. 407, pages 123–131, dec 2018. (Cited on page 42.)
- [Chevalier *et al.* 2019] S. Chevalier, J. Hinebaugh and A. Bazylak. *Establishing Accuracy of Watershed-Derived Pore Network Extraction for Characterizing In-Plane Effective Diffusivity in Thin Porous Layers*. Journal of The Electrochemical Society, vol. 166, no. 7, pages F3246–F3254, may 2019. (Cited on page 40.)
- [Chevalier *et al.* 2021] S. Chevalier, J.-N. Tourvieille, A. Sommier and C. Pradère. *Infrared thermospectroscopic imaging of heat and mass transfers in laminar microfluidic reactive flows*. Chemical Engineering Journal Advances, vol. 8, page 100166, nov 2021. (Cited on page 20.)

- [Chevalier 2021] Stéphane Chevalier. *Semianalytical modeling of the mass transfer in microfluidic electrochemical chips*. Physical Review E, vol. 104, no. 3, page 035110, sep 2021. (Cited on pages 11, 12, 17, 18, 46 and 67.)
- [Choban *et al.* 2004] Eric R. Choban, Larry J. Markoski, Andrzej Wieckowski and Paul J.A. Kenis. *Microfluidic fuel cell based on laminar flow*. Journal of Power Sources, vol. 128, no. 1, pages 54–60, mar 2004. (Cited on page 46.)
- [Colinart 2008] Thibaut Colinart. *Gestion de l'eau et performances électriques d'une pile à combustible : des pores de la membrane à la cellule*. PhD thesis, Institut National Polytechnique de Lorraine, 2008. (Cited on page 37.)
- [Crank 1975] J. Crank. *The Mathematics of Diffusion*. Oxford university press, London, second edi édition, 1975. (Cited on page 48.)
- [Dai *et al.* 2009] Wei Dai, Haijiang Wang, Xiao-Zi Yuan, Jonathan J. Martin, Daijun Yang, Jinli Qiao and Jianxin Ma. *A review on water balance in the membrane electrode assembly of proton exchange membrane fuel cells*. International Journal of Hydrogen Energy, vol. 34, no. 23, pages 9461–9478, dec 2009. (Cited on page 50.)
- [Dawadi *et al.* 2015] Mahesh B. Dawadi, Sylvestre Twagirayezu, David S. Perry and Brant E. Billingham. *High-resolution Fourier transform infrared synchrotron spectroscopy of the NO₂ in-plane rock band of nitromethane*. Journal of Molecular Spectroscopy, vol. 315, pages 10–15, 2015. Spectroscopy with Synchrotron Radiation. (Cited on page 9.)
- [Didier *et al.* 2020] Pierre Didier, Nicolas Lobato-Dauzier, Nicolas Clément, Anthony J. Genot, Yui Sasaki, Éric Leclerc, Tsukuru Minamiki, Yasuyuki Sakai, Teruo Fujii and Tsuyoshi Minami. *Microfluidic System with Extended-Gate-Type Organic Transistor for Real-Time Glucose Monitoring*. ChemElectroChem, vol. 7, no. 6, pages 1332–1336, mar 2020. (Cited on pages 66 and 70.)
- [Ding *et al.* 2013] Yulong Ding, Ryan Anderson, Lifeng Zhang, Xiaotao Bi and David P. Wilkinson. *Simulations of two-phase flow distribution in communicating parallel channels for a PEM fuel cell*. International Journal of Multiphase Flow, vol. 52, pages 35–45, June 2013. (Cited on page 37.)
- [Eikerling 2006] M. Eikerling. *Water Management in Cathode Catalyst Layers of PEM Fuel Cells*. Journal of The Electrochemical Society, vol. 153, no. 3, page E58, 2006. (Cited on page 37.)
- [Garcia *et al.* 2023a] Marine Garcia, Alain Sommier, Thomas Lafargue-Taller, Gérard Clisson, Jean-Christophe Batsale and Stéphane Chevalier. *Inter-diffusion measurements in thermally controlled microchannel using infrared spectroscopic imaging*. Chemical Engineering Science, page 119136, 2023. (Cited on pages 17, 18 and 47.)

- [Garcia *et al.* 2023b] Marine Garcia, Alain Sommier, Dominique Michau, Gérald Clisson, Jean-Christophe Batsale and Stéphane Chevalier. *Imaging concentration fields in microfluidic fuel cells as a mass transfer characterization platform*. *Electrochimica Acta*, vol. 460, page 142489, aug 2023. (Cited on pages 17, 43 and 66.)
- [Gaverina *et al.* 2017] L. Gaverina, J. C. Batsale, A. Sommier and C. Pradere. *Pulsed flying spot with the logarithmic parabolas method for the estimation of in-plane thermal diffusivity fields on heterogeneous and anisotropic materials*. *Journal of Applied Physics*, vol. 121, no. 11, page 115105, mar 2017. (Cited on pages 25 and 61.)
- [Ghosh *et al.* 2016] Ayanjeet Ghosh, Arnaldo L. Serrano, Tracey A. Oudenhoven, Joshua S. Ostrander, Elliot C. Eklund, Alexander F. Blair and Martin T. Zanni. *Experimental implementations of 2D IR spectroscopy through a horizontal pulse shaper design and a focal plane array detector*. *Opt. Lett.*, vol. 41, no. 3, pages 524–527, Feb 2016. (Cited on page 10.)
- [Groz *et al.* 2021] M.M. Groz, A. Sommier, E. Abisset-Chavanne, S. Chevalier, A. Meziane, J.C. Batsale and C. Pradere. *Contactless thermal profilometry of carbon-resin materials by IR thermography*. *Measurement*, vol. 182, page 109723, sep 2021. (Cited on pages 25 and 59.)
- [Groz *et al.* 2024] M.M. Groz, E. Abisset-Chavanne, J.C. Batsale and A Sommier. *Active thermal super-resolution based on laser flying spot technique coupled with IR thermography and wavelet transform*. *Quantitative InfraRed Thermography Journal*, vol. 0, no. 0, pages 1–24, jan 2024. (Cited on pages 60 and 61.)
- [H. Hashemi *et al.* 2015] S. Mohammad H. Hashemi, Miguel A. Modestino and Demetri Psaltis. *A membrane-less electrolyzer for hydrogen production across the pH scale*. *Energy & Environmental Science*, vol. 8, no. 7, pages 2003–2009, 2015. (Cited on page 44.)
- [Hadamard 1902] Jacques Hadamard. *Sur les problèmes aux dérivées partielles et leur signification physique*. In *Princeton University Bulletin*, pages 49–52, 1902. (Cited on page 26.)
- [Hale & Querry 1973] George M. Hale and Marvin R. Querry. *Optical Constants of Water in the 200-nm to 200- μ m Wavelength Region*. *Applied Optics*, vol. 12, no. 3, page 555, 1973. (Cited on page 14.)
- [Huck *et al.* 2016] Christian Huck, Yukihiro Ozaki and Verena Huck-Pezzei. *Critical Review Upon the Role and Potential of Fluorescence and Near-Infrared Imaging and Absorption Spectroscopy in Cancer Related Cells, Serum, Saliva, Urine and Tissue Analysis*. *Current Medicinal Chemistry*, vol. 23, no. 27, pages 3052–3077, sep 2016. (Cited on page 10.)

- [Ibrahim *et al.* 2022] Omar A. Ibrahim, Marina Navarro-Segarra, Pardis Sadeghi, Neus Sabaté, Juan Pablo Esquivel and Erik Kjeang. *Microfluidics for Electrochemical Energy Conversion*. Chemical Reviews, page acs.chemrev.1c00499, jan 2022. (Cited on pages 44 and 55.)
- [Kakuta *et al.* 2011] Naoto Kakuta, Yuko Fukuhara, Katsuya Kondo, Hidenobu Arimoto and Yukio Yamada. *Temperature imaging of water in a microchannel using thermal sensitivity of near-infrared absorption*. Lab on a Chip, vol. 11, no. 20, page 3479, 2011. (Cited on page 15.)
- [Kakuta *et al.* 2016] Naoto Kakuta, Hiroki Yamashita, Daisuke Kawashima, Katsuya Kondo, Hidenobu Arimoto and Yukio Yamada. *Simultaneous imaging of temperature and concentration of ethanol–water mixtures in microchannel using near-infrared dual-wavelength absorption technique*. Measurement Science and Technology, vol. 27, no. 11, page 115401, nov 2016. (Cited on pages 11, 14, 15 and 66.)
- [Kempfert *et al.* 2001] Kenneth D Kempfert, Eric Y Jiang, Sherwin Oas and John Coffin. *Detectors for Fourier transform spectroscopy*. AN-00125, 2001. (Cited on page 9.)
- [Kirchner *et al.* 2018] Sara Kirchner, Sebastien Narinsamy, Alain Sommier, Marta Romano, Meguya Ryu, Junko Morikawa, Jacques Leng, Jean-Christophe Batsale and Christophe Pradère. *Calibration Procedure for Attenuation Coefficient Measurements in Highly Opaque Media Using Infrared Focal Plane Array (IRFPA) Spectroscopy*. Applied Spectroscopy, vol. 72, no. 2, pages 177–187, feb 2018. (Cited on page 11.)
- [Kittel 1986] C. Kittel. Introduction to solid state physics. Play; 9. Wiley, 1986. (Cited on page 15.)
- [Kjeang *et al.* 2009] Erik Kjeang, Ned Djilali and David Sinton. *Microfluidic fuel cells: A review*. Journal of Power Sources, vol. 186, no. 2, pages 353–369, jan 2009. (Cited on pages 44 and 47.)
- [Krafft *et al.* 2008] Christoph Krafft, Daniela Codrich, Gloria Pelizzo and Valter Sergio. *Raman mapping and FTIR imaging of lung tissue: Congenital cystic adenomatoid malformation*. Analyst, vol. 133, no. 3, pages 361–371, 2008. (Cited on page 8.)
- [Krause *et al.* 2023] Kevin Krause, Marine Garcia, Dominique Michau, Gérald Clisson, Brant Billinghamurst, Jean-luc Battaglia and Stéphane Chevalier. *Probing membrane hydration in microfluidic polymer electrolyte membrane electrolyzers via operando synchrotron Fourier-transform infrared spectroscopy*. Lab on a Chip, 2023. (Cited on pages 17 and 43.)
- [Lamy 2016] Claude Lamy. *From hydrogen production by water electrolysis to its utilization in a PEM fuel cell or in a SO fuel cell: Some considerations on*

- the energy efficiencies*. International Journal of Hydrogen Energy, vol. 41, no. 34, pages 15415–15425, sep 2016. (Cited on page 36.)
- [Lee & Bae 2012] Dongryul Lee and Joongmyeon Bae. *Visualization of flooding in a single cell and stacks by using a newly-designed transparent PEMFC*. International Journal of Hydrogen Energy, vol. 37, no. 1, pages 422–435, January 2012. (Cited on page 37.)
- [Lee *et al.* 2013] Jin Wook Lee, Marc-Antoni Goulet and Erik Kjeang. *Microfluidic redox battery*. Lab on a Chip, vol. 13, no. 13, page 2504, 2013. (Cited on page 44.)
- [Lee *et al.* 2019] Seok Hwan Lee, Seongchong Park, Joohyun Lee and Woong Kang. *Practical methodology for in situ measurement of micro flow rates using laser diode absorption sensors*. Metrologia, vol. 56, no. 4, page 045010, aug 2019. (Cited on page 61.)
- [Lehmkuhl *et al.* 2015] Brynson Lehmkuhl, Scott D. Noblitt, Amber T. Krummel and Charles S. Henry. *Fabrication of IR-transparent microfluidic devices by anisotropic etching of channels in CaF₂*. Lab on a Chip, vol. 15, no. 22, pages 4364–4368, 2015. (Cited on page 14.)
- [Lehtihet *et al.* 2021] M Lehtihet, E. Abisset, S. Chevalier, A. Sommier, C. Pradere and J. Leng. *Thermospectroscopic infrared imaging of a confined drying process*. Chemical Engineering Journal, vol. 403, no. July, page 126167, jan 2021. (Cited on pages 14 and 67.)
- [Lewis *et al.* 1995] E. Neil. Lewis, Patrick J. Treado, Robert C. Reeder, Gloria M. Story, Anthony E. Dowrey, Curtis. Marcott and Ira W. Levin. *Fourier Transform Spectroscopic Imaging Using an Infrared Focal-Plane Array Detector*. Analytical Chemistry, vol. 67, no. 19, pages 3377–3381, oct 1995. (Cited on pages 8 and 10.)
- [Liso *et al.* 2015] Vincenzo Liso, Samuel Simon Araya, Anders Christian Olesen, Mads Pagh Nielsen and Søren Knudsen Kær. *Modeling and experimental validation of water mass balance in a PEM fuel cell stack*. International Journal of Hydrogen Energy, vol. 41, no. 4, pages 3079–3092, nov 2015. (Cited on page 50.)
- [Litster *et al.* 2006] S. Litster, D. Sinton and N. Djilali. *Ex situ visualization of liquid water transport in PEM fuel cell gas diffusion layers*. Journal of Power Sources, vol. 154, no. 1, pages 95–105, March 2006. (Cited on page 37.)
- [Liu *et al.* 2006] Zhixiang Liu, Zongqiang Mao and Cheng Wang. *A two dimensional partial flooding model for PEMFC*. Journal of Power Sources, vol. 158, no. August 2005, pages 1229–1239, 2006. (Cited on page 37.)

- [López-Montesinos *et al.* 2011] P. O. López-Montesinos, N. Yossakda, A. Schmidt, F. R. Brushett, W. E. Pelton and P. J.A. Kenis. *Design, fabrication, and characterization of a planar, silicon-based, monolithically integrated micro laminar flow fuel cell with a bridge-shaped microchannel cross-section*. Journal of Power Sources, vol. 196, no. 10, pages 4638–4645, 2011. (Cited on page 46.)
- [Maillet *et al.* 2000] Denis Maillet, Stéphane André, Jean-Christophe Batsale, Alain Degiovanni and Christian Moyne. *Thermal Quadrupoles: Solving the Heat Equation through Integral Transforms*. Wiley, 2000. (Cited on page 27.)
- [Maldague 1993] Xavier P. V. Maldague. *Nondestructive Evaluation of Materials by Infrared Thermography*. Springer London, London, 1993. (Cited on page 25.)
- [Maldague 2012] Xavier PV Maldague. *Nondestructive evaluation of materials by infrared thermography*. Springer Science & Business Media, 2012. (Cited on page 15.)
- [Mateos-Canseco *et al.* 2023] Alejandro Mateos-Canseco, Andrzej Kusiak and Jean-Luc Battaglia. *Thermal imaging by scanning photothermal radiometry*. Review of Scientific Instruments, vol. 94, no. 10, page 104902, oct 2023. (Cited on page 60.)
- [Modestino *et al.* 2016] M. A. Modestino, D. Fernandez Rivas, S. M. H. Hashemi, J. G. E. Gardeniers and D. Psaltis. *The potential for microfluidics in electrochemical energy systems*. Energy & Environmental Science, vol. 9, no. 11, pages 3381–3391, 2016. (Cited on page 1.)
- [Mudry *et al.* 2012] E Mudry, K Belkebir, J Girard, J Savatier, E Le Moal, C Nicoletti, M Allain and A Sentenac. *Structured illumination microscopy using unknown speckle patterns*. Nature Photonics, vol. 6, no. 5, pages 312–315, 2012. (Cited on page 62.)
- [Murray *et al.* 2017] Todd W Murray, Markus Haltmeier, Thomas Berer, Elisabeth Leiss-Holzinger and Peter Burgholzer. *Super-resolution photoacoustic microscopy using blind structured illumination*. Optica, vol. 4, no. 1, page 17, 2017. (Cited on page 62.)
- [Myers *et al.* 2015] Glenn R Myers, Matthew Geleta, Andrew M Kingston, Benoit Recur and Adrian P Sheppard. *Bayesian approach to time-resolved tomography*. Optics express, vol. 23, no. 15, pages 20062–20074, 2015. (Cited on page 59.)
- [Nguyen & Kakuta 2023] The-Anh Nguyen and Naoto Kakuta. *Experimental study on the initial thermal plumes produced by small heating plates in water*. Experimental Thermal and Fluid Science, vol. 142, no. October 2022, page 110803, apr 2023. (Cited on pages 15, 16, 66 and 67.)

- [Ozenne *et al.* 2023a] Valéry Ozenne, Pierre Bour, Baudouin Denis de Senneville and Bruno Quesson. *3D motion strategy for online volumetric thermometry using simultaneous multi-slice EPI at 1.5T: an evaluation study*. International Journal of Hyperthermia, vol. 40, no. 1, dec 2023. (Cited on page 60.)
- [Ozenne *et al.* 2023b] Valéry Ozenne, Pierre Bour, Baudouin Denis de Senneville and Bruno Quesson. *3D motion strategy for online volumetric thermometry using simultaneous multi-slice EPI at 1.5T: an evaluation study*. International Journal of Hyperthermia, vol. 40, no. 1, page 2194595, 2023. PMID: 37080550. (Cited on page 59.)
- [Perro *et al.* 2016] Adeline Perro, Gwenaëlle Lebourdon, Sarah Henry, Sophie Lecomte, Laurent Servant and Samuel Marre. *Combining microfluidics and FT-IR spectroscopy: towards spatially resolved information on chemical processes*. Reaction Chemistry and Engineering, vol. 1, no. 6, pages 577–594, 2016. (Cited on page 14.)
- [Pharoah *et al.* 2006] J G Pharoah, K Karan and W Sun. *On effective transport coefficients in PEM fuel cell electrodes : Anisotropy of the porous transport layers*. Journal of Power Sources, vol. 161, pages 214–224, 2006. (Cited on page 37.)
- [Polshin *et al.* 2014] Evgeny Polshin, Bert Verbruggen, Daan Witters, Bert Sels, Dirk De Vos, Bart Nicolaï and Jeroen Lammertyn. *Integration of microfluidics and FT-IR microscopy for label-free study of enzyme kinetics*. Sensors and Actuators B: Chemical, vol. 196, pages 175–182, jun 2014. (Cited on page 14.)
- [Pradere *et al.* 2011] C. Pradere, L. Clerjaud, J. C. Batsale and S. Dilhaire. *High speed heterodyne infrared thermography applied to thermal diffusivity identification*. Review of Scientific Instruments, vol. 82, no. 5, page 054901, may 2011. (Cited on page 12.)
- [Pradere *et al.* 2017] C. Pradere, M. Ryu, A. Sommier, M. Romano, A. Kusiak, J. L. Battaglia, J. C. Batsale and J. Morikawa. *Non-contact temperature field measurement of solids by infrared multispectral thermotransmittance*. Journal of Applied Physics, vol. 121, no. 8, page 085102, feb 2017. (Cited on page 15.)
- [Rao *et al.* 2007] R. Madhusudana Rao, D. Bhattacharyya, R. Rengaswamy and S.R. Choudhury. *A two-dimensional steady state model including the effect of liquid water for a PEM fuel cell cathode*. Journal of Power Sources, vol. 173, no. 1, pages 375–393, November 2007. (Cited on page 37.)
- [Rashed *et al.* 2007] A. Rashed, D. P. Almond, D. A. S. Rees, S. Burrows and S. Dixon. *Crack Detection by Laser Spot Imaging Thermography*. AIP Conference Proceedings, vol. 894, no. 1, pages 500–506, 03 2007. (Cited on page 25.)

- [Romano *et al.* 2015] M. Romano, C. Ndiaye, A. Duphil, A. Sommier, J. Morikawa, J. Mascetti, J.C. Batsale, L. Servant and C. Pradere. *Fast infrared imaging spectroscopy technique (FIIST)*. *Infrared Physics & Technology*, vol. 68, pages 152–158, jan 2015. (Cited on page 11.)
- [Rosas *et al.* 2023] Samir Rosas, Keegan A. Schoeller, Edward Chang, Hongyan Mei, Mikhail A. Kats, Kevin W. Eliceiri, Xinyu Zhao and Filiz Yesilkoy. *Metasurface-Enhanced Mid-Infrared Spectrochemical Imaging of Tissues*. *Advanced Materials*, may 2023. (Cited on pages 11 and 58.)
- [Ryu *et al.* 2017] M. Ryu, J.A. Kimber, T. Sato, R. Nakatani, T. Hayakawa, M. Romano, C. Pradere, A.A. Hovhannisyanyan, S.G. Kazarian and J. Morikawa. *Infrared thermo-spectroscopic imaging of styrene radical polymerization in microfluidics*. *Chemical Engineering Journal*, vol. 324, pages 259–265, sep 2017. (Cited on pages 11 and 13.)
- [Salazar *et al.* 2020] Agustín Salazar, Arantza Mendioroz and Alberto Oleaga. *Flying spot thermography: Quantitative assessment of thermal diffusivity and crack width*. *Journal of Applied Physics*, vol. 127, no. 13, 04 2020. 131101. (Cited on page 25.)
- [Salloum *et al.* 2008] Kamil S. Salloum, Joel R. Hayes, Cody A. Friesen and Jonathan D. Posner. *Sequential flow membraneless microfluidic fuel cell with porous electrodes*. *Journal of Power Sources*, vol. 180, no. 1, pages 243–252, may 2008. (Cited on page 46.)
- [Salmon *et al.* 2005] Jean-Baptiste Salmon, Armand Ajdari, Patrick Tabeling, Laurent Servant, David Talaga and Mathieu Joanicot. *In situ Raman imaging of interdiffusion in a microchannel*. *Applied Physics Letters*, vol. 86, no. 9, page 094106, feb 2005. (Cited on pages 17 and 19.)
- [Sandell *et al.* 2020] Susanne Sandell, Emigdio Chávez-Ángel, Alexandros El Sachat, Jianying He, Clivia M. Sotomayor Torres and Jeremie Maire. *Thermoreflectance techniques and Raman thermometry for thermal property characterization of nanostructures*. *Journal of Applied Physics*, vol. 128, no. 13, oct 2020. (Cited on page 63.)
- [Schleeger *et al.* 2009] Michael Schleeger, Christoph Wagner, Michiel J. Vellekoop, Bernhard Lendl and Joachim Heberle. *Time-resolved flow-flash FT-IR difference spectroscopy: the kinetics of CO photodissociation from myoglobin revisited*. *Analytical and Bioanalytical Chemistry*, vol. 394, no. 7, pages 1869–1877, aug 2009. (Cited on pages 8 and 11.)
- [Shrestha & Bazylak 2023] Pranay Shrestha and Aimy Bazylak. *Pursuit of next-generation electrochemical energy devices*. *Electrochimica Acta*, page 142810, jul 2023. (Cited on page 38.)

- [Siegel *et al.* 2004] N.P. Siegel, M.W. Ellis, D.J. Nelson and M.R. von Spakovsky. *A two-dimensional computational model of a PEMFC with liquid water transport*. Journal of Power Sources, vol. 128, no. 2, pages 173–184, April 2004. (Cited on page 37.)
- [Sinton 2014] David Sinton. *Energy: the microfluidic frontier*. Lab Chip, vol. 14, no. 17, pages 3127–3134, 2014. (Cited on page 45.)
- [Springer *et al.* 1991] T. E. Springer, T A Zawodzinski and S Gottesfeld. *Polymer Electrolyte Fuel Cell Model*. Journal of The Electrochemical Society, vol. 138, no. 8, pages 2334–2342, 1991. (Cited on pages 37 and 50.)
- [Steiner & Koch 2009] Gerald Steiner and Edmund Koch. *Trends in Fourier transform infrared spectroscopic imaging*. Analytical and Bioanalytical Chemistry, vol. 394, no. 3, pages 671–678, jun 2009. (Cited on page 8.)
- [Tang *et al.* 2023] Mingwei Tang, Yubing Han, Danchen Jia, Qing Yang and Ji-Xin Cheng. *Far-field super-resolution chemical microscopy*. Light: Science & Applications, vol. 12, no. 1, page 137, jun 2023. (Cited on page 61.)
- [Uema *et al.* 2021] Takato Uema, Toshiya Ohata, Yutaka Washizuka, Ryo Nakanishi, Daisuke Kawashima and Naoto Kakuta. *Near-infrared imaging in a microfluidic channel of aqueous acid–base reactions*. Chemical Engineering Journal, vol. 403, no. April 2020, page 126338, jan 2021. (Cited on page 11.)
- [Venkatakrisnan *et al.* 2017] S. V. Venkatakrisnan, Ercan Cakmak, Hassina Billheux, Philip Bingham and Richard K. Archibald. *Model-based iterative reconstruction for neutron laminography*. In 2017 51st Asilomar Conference on Signals, Systems, and Computers, volume 2017-Octob, pages 1864–1869. IEEE, oct 2017. (Cited on page 59.)
- [Voropaev *et al.* 2016] Alexey Voropaev, Anton Myagotin, Lukas Helfen and Tilo Baumbach. *Direct Fourier Inversion Reconstruction Algorithm for Computed Laminography*. IEEE Transactions on Image Processing, vol. 25, no. 5, pages 2368–2378, may 2016. (Cited on page 59.)
- [Wang *et al.* 2021] Yifei Wang, Shijing Luo, Holly Y.H. Kwok, Wending Pan, Yingguang Zhang, Xiaolong Zhao and Dennis Y.C. Leung. *Microfluidic fuel cells with different types of fuels: A prospective review*. Renewable and Sustainable Energy Reviews, vol. 141, no. January, page 110806, may 2021. (Cited on page 44.)
- [Weber & Newman 2004a] Adam Z. Weber and John Newman. *Transport in Polymer-Electrolyte Membranes II. Mathematical Model*. Journal of The Electrochemical Society, vol. 151, no. 2, page A311, 2004. (Cited on page 37.)

- [Weber & Newman 2004b] Adam Z. Weber and John Newman. *Transport in Polymer-Electrolyte Membranes III. Model Validation*. pages 326–339, 2004. (Cited on page 37.)
- [Wei *et al.* 2023] Xiaoran Wei, Kun Zhou, Shaowu Feng, Shouwen Shi, Qiang Lin, Gang Chen, Kai Song and Xu Chen. *Exploring fast-inferring in transformer backbone model for fatigue crack detection and propagation tracking for proton exchange membrane*. Journal of Power Sources, vol. 573, no. May, page 233129, 2023. (Cited on page 63.)
- [Woodbury *et al.* 2023] Keith A. Woodbury, Najafi Hamidreza, Filippo de Monte and James V. Beck. *Inverse Heat Conduction Problems*. In Inverse Heat Conduction, pages 1–23. Wiley, mar 2023. (Cited on page 26.)
- [Woodbury 1999] Keith A. Woodbury. *Sequential Function Estimation - “Beck’s Method”*. In 3rd Int. Conf Inverse Problems in Engineering, 1999. (Cited on page 26.)
- [Yeh *et al.* 2023] Kevin Yeh, Ishaan Sharma, Kianoush Falahkheirkhah, Matthew P. Confer, Andres C. Orr, Yen-Ting Liu, Yamuna Phal, Ruo-Jing Ho, Manu Mehta, Ankita Bhargava, Wenyan Mei, Georgina Cheng, John C. Cheville and Rohit Bhargava. *Infrared spectroscopic laser scanning confocal microscopy for whole-slide chemical imaging*. Nature Communications, vol. 14, no. 1, page 5215, aug 2023. (Cited on page 61.)
- [Zawodzinski *et al.* 1993] Thomas a. Zawodzinski, C. Derouin, S. Radzinski, R. J. Sherman, T. Smith, T. E. Springer and S Gottesfeld. *Water Uptake by and Transport Through Nafion® 117 Membranes*. Journal of The Electrochemical Society, vol. 140, no. 4, page 1041, 1993. (Cited on page 37.)
- [Zawodzinski 1993] Thomas a. Zawodzinski. *A Comparative Study of Water Uptake By and Transport Through Ionomeric Fuel Cell Membranes*. Journal of The Electrochemical Society, vol. 140, no. 7, page 1981, 1993. (Cited on page 37.)
- [Zhou *et al.* 2021] Yuan Zhou, Xun Zhu, Yang Yang, Dingding Ye, Rong Chen and Qiang Liao. *Route towards high-performance microfluidic fuel cells: a review*. Sustainable Energy and Fuels, vol. 5, no. 11, pages 2840–2859, 2021. (Cited on page 44.)

Thermal tomography for microscale energy conversion devices

Abstract:

The main objective of this thesis is to provide energy conversion devices with three-dimensional (3D) heat and mass transfer characterization carried out at microscale, i.e. achieving a spatial resolution of 1 μm per voxel.

Microscale energy conversion devices embed both microfluidic electrochemical chips (fuel cells, electrolyzers, redox flow batteries), micro batteries or super capacitors among others. Regardless their growing use in our current energy mix, many fundamental questions remain open, hindering either their performances and lifetime. In particular, the knowledge of heat transfers is used to inform on many physical processes such as diffusion, kinetics, current density distributions, double capacity layers, contact resistances and so on.

To achieve this goal, new contactless methods based on thermospectroscopy imaging, thermotransmittance imaging and analytical modelling of heat and mass transfers in microfluidic energy conversion devices has been developed over the five last years. Important milestones were reached with successful mass transport loss measurements in microfluidic electrolyser membrane using infrared (IR) spectroscopy and bulk temperature measurements in dielectric materials at the microscale. All these imaging techniques have reached the needed maturity to move toward IR-based tomography at the microscale.

The approach proposed in this thesis to achieve 3D fields is based on laminographic technique to transform a set of images captured by an IR camera with different angle of projection to depth coordinates. This method requires the use of thermotransmittance in semi-transparent media and can only be achieved (i) by increasing our camera signal to noise by a factor one thousand and (ii) by designing specific energy conversion devices compatible with IR transmission. To meet these challenges a combination of advanced inverse methods using integral transforms, deconvolution algorithm of diffusion equations and superresolution imaging is proposed along with the development of a new instrumentation based on modulated high power density IR lasers. Energy characterization in some microfluidic energy conversion devices using this new thermal tomography is also proposed at the end of this thesis.

Keywords: Infrared imaging, Tomography, Spectroscopy, Microfluidic, Heat transfer, Mass transfer, Energy conversion.
